Experimental Study on Flame Behaviour of LPG-Air Flame in Mini Scale Combustor

THESIS SUBMITTED IN PARTIAL FULFILMENT OF
THE REQUIREMENT FOR THE DEGREE OF

MASTER OF MECHANICAL ENGINEERING

BY

KOUSHIK SAMANTA

Registration Number- **144502** of **2018-2019**

Exam Roll Number – M4MEC24006

UNDER THE GUIDANCE OF

PROF. Swarnendu Sen

&

Dr. Sourav Sarkar

DEPARTMENT OF MECHANICAL ENGINEERING
JADAVPUR UNIVERSITY
KOLKATA-32

DEPARTMENT OF MECHANICAL ENGINEERING
FACULTY OF ENGINEERING AND TECHNOLOGY
JADAVPUR UNIVERSITY
KOLKATA 700032
MAY 2024

DECLARATION OF ORIGINALITY AND COMPLIANCE OF ACADEMIC ETHICS

I hereby declare that the thesis entitled "**Experimental Study on Flame Behaviour of LPG-Air Flame in Mini Scale Combustor**" contains literature survey and original research work by the undersigned candidate, as a part of his *MASTER OF ENGINEERING IN MECHANICAL ENGINEERING* studies during academic session 2022-2024.

All information in this document have been obtained and presented in accordance with the academic rules and ethical conduct.

I also declare that, as required by these rules of conduct, I have fully cited and referenced all the material and results that are not original to this work.

Name: **KOUSHIK SAMANTA**

Class Roll Number: **002211202012**

Exam Roll Number: **M4MEC24006**

University Registration No: **144502 of 2018-2019**

Thesis Title: **Experimental Study on Flame Behaviour of LPG-Air Flame in Mini Scale Combustor**

Date:

SIGNATURE:

Faculty of Engineering and Technology

DEPARTMENT OF MECHANICAL ENGINEERING

JADAVPUR UNIVERSITY

KOLKATA-32

CERTIFICATE OF RECOMMENDATION

This is to certify that the thesis entitled ‘‘**Experimental Study on Flame Behaviour of LPG-Air Flame in Mini Scale Combustor**’’ is a bonafide work carried out by KOUSHIK SAMANTA under our supervision and guidance in partial fulfilment of the requirements for awarding the degree of Master of Engineering in Mechanical Engineering under Department of Mechanical Engineering, Jadavpur University during the academic session 2018-2020.

THESIS SUPERVISOR

Prof. (Dr.) Swarnendu Sen

Professor

Department of Mechanical Engineering

Jadavpur University, Kolkata

THESIS CO-SUPERVISOR

Dr. Sourav Sarkar

Assistant Professor

Department of Mechanical Engineering

Jadavpur University, Kolkata

Prof. Swarnendu Sen

Head of Department

Department of Mechanical Engineering

Jadavpur University, Kolkata

Prof. Dipak Laha

Dean

Faculty of Engineering and Technology

Jadavpur University, Kolkata

Faculty of Engineering and Technology

DEPARTMENT OF MECHANICAL ENGINEERING

JADAVPUR UNIVERSITY

KOLKATA-32

CERTIFICATE OF APPROVAL

This foregoing thesis titled "**Experimental Study on Flame Behaviour of LPG-Air Combustion in Mini Scale Combustor**'' is hereby approved as a credible study of Mechanical Engineering subject carried out and presented in a manner satisfactorily to warrant its acceptance as a pre-requisite to the degree for which it has been submitted. It is understood that by this approval the undersigned, do not endorse or approve any statement made or opinion expressed or conclusion drawn therein, but approve the thesis only for purpose for which it has been submitted.

Committee of final evaluation of Thesis

_____

(External Investigator)

_____

(Thesis Supervisor)

_____

(Thesis Co-Supervisor)

ACKNOWLEDGEMENTS

Though the thesis work has been done by myself for Master in Mechanical Engineering degree but there are many other people without whom the thesis would not been possible. I would like to extend my sincere gratitude to all of them.

First and foremost, I would like to express my deepest gratitude to my thesis guide Prof. Swarnendu Sen, Professor, Department of Mechanical Engineering and thesis co-guide Dr. Sourav Sarkar, Assistant Professor, Department of Mechanical Engineering whose expertise, understanding, and patience added considerably to my graduate experience. I appreciate your vast knowledge and skill in many areas, and your assistance in writing reports and this thesis) was invaluable.

I am profoundly grateful to all my professors for their invaluable guidance, supervision, and unwavering support throughout the development of this thesis. Their insightful advice and provision of essential resources have been instrumental in the successful completion of my master's thesis. The expertise and encouragement provided by the esteemed faculty members of mechanical engineering department have been indispensable to my academic journey and the realization of this work.

I would like to thank Arindam Mandal, Sabyasachi Mandal, Phd scholars of Neptune Lab for helping in the experimental setup process and sharing many insights about experimental process throughout the thesis.

I would also like to thank Soumendra Nath Mishra and Manish Manna, Phd scholars of Neptune Lab for helping me in learning several software such as origin and Microsoft office so that I can complete my thesis.

I would also thank senior research scholars in Neptune Lab for their unconditional support and encouragement

I thank Arijit Bhattacharya, ex research scholar of Neptune Lab for giving me his valuable time and guiding me carefully about operating spectroscope.

I would like to thank undergraduate students of Jadavpur University Anshuman Mandal, Arnab Kapri, Sujan Banerjee, Biraj Barua, Anupam Majhi, Bhimesh Murmu for assisting me in the during the experiment.

I would like to express my gratitude towards my friends who always stood by my side and supported me in completion of my master's thesis.

Last but certainly not least, I would like to thank my family. To my parents, for their unwavering support and love, and to my friends, who provided both emotional support and encouragement when it was most required. Your belief in me has been my driving force.

Koushik Samanta

M.M.E. 2nd Year, Final Semester

Department of Mechanical Engineering

Jadavpur University, Kolkata-32

TABLE OF CONTENTS

LIST OF FIGURES

LIST OF TABLES

CHAPTER 1: INTRODUCTION

The total energy consumption in the world for year 2022 is 604 exajoules [1], this is around 1.1% more than that of 2021 when net consumption of energy was 597 exajoules [1]. In the last 10 years the energy consumption has only increased expect for year 2020 when it decreased due to the covid 19 pandemic worldwide as the factories etc. was closed [2,3]. This energy demand will increase over the period. For India in 2022 the energy consumption was 10123.44 Twh [4]. According to a report by BP [5] the total energy consumption in India by 2040 will be 1921 Mtoe (million tons of oil equivalent) by 2040. Currently India is 4th in total energy consumption worldwide after USA, China and EU [6]. But in 2040 India will be just behind China and USA in terms of total energy consumption per year. The graph showing energy consumption from 1965 to 2022 and its percentage increase per year is shown below for both the world as well as India. Total energy consumption and change of energy consumption has been shown in Fig. 1.

To meet the demand for energy the energy is mainly produced by the fossil's fuels. Worldwide about 92% and for India 94% of total energy is produced by the fossils fuel [1]. A pie chart containing information of the total amount of energy produced fuel wise is given in figure 2. For world oil in the most used at 31.57% followed by coal 26.73% and natural gas at 23.49% for India coal is major contributor for energy production at over 50% of total energy produced followed by oil and natural gas.

As the world majorly runs on the fossils fuel so therefore even in years to come to replace the fosssils fuels as primary fuel will be very much difficult as it take a time to introduce and popularize a power source. However the poratability doesnot come with the use of fossils fuel. For the poratable device people majorly depends on battery as energy storing device.

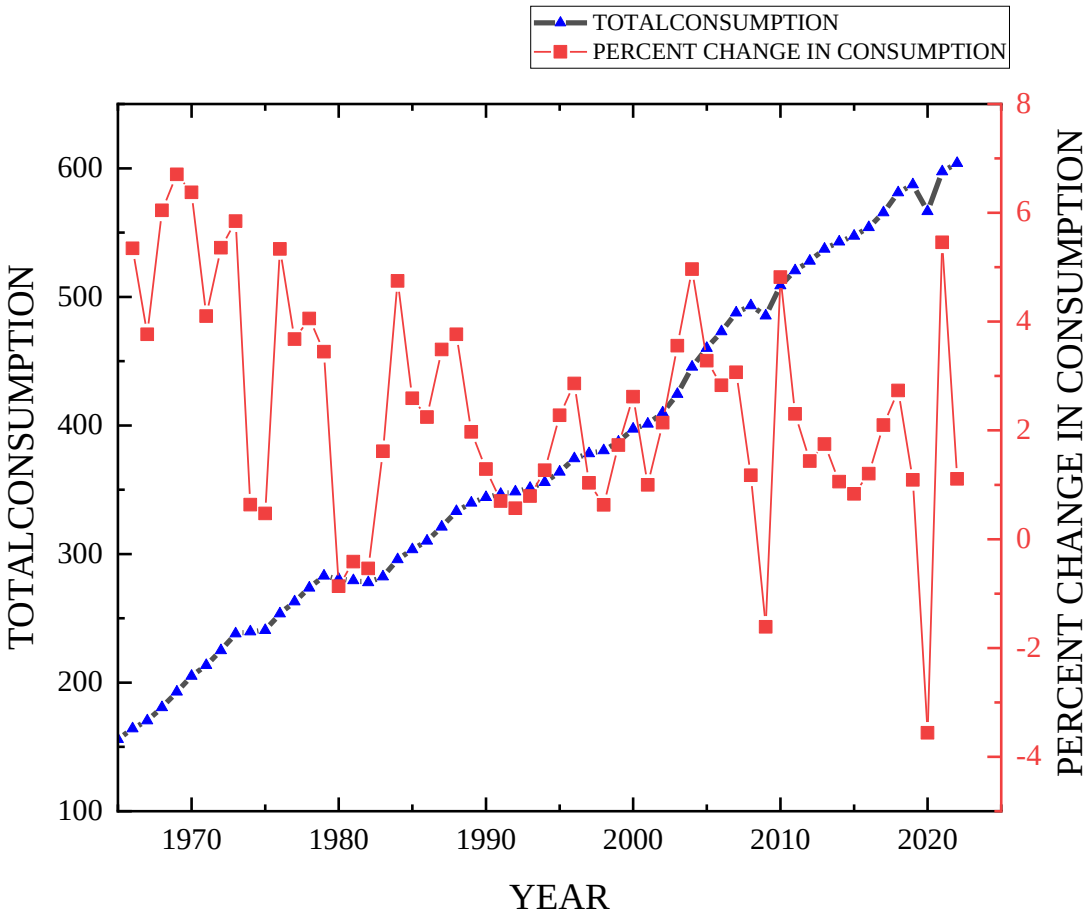

Figure 1: Total energy consumptions and increase in energy demand year wise

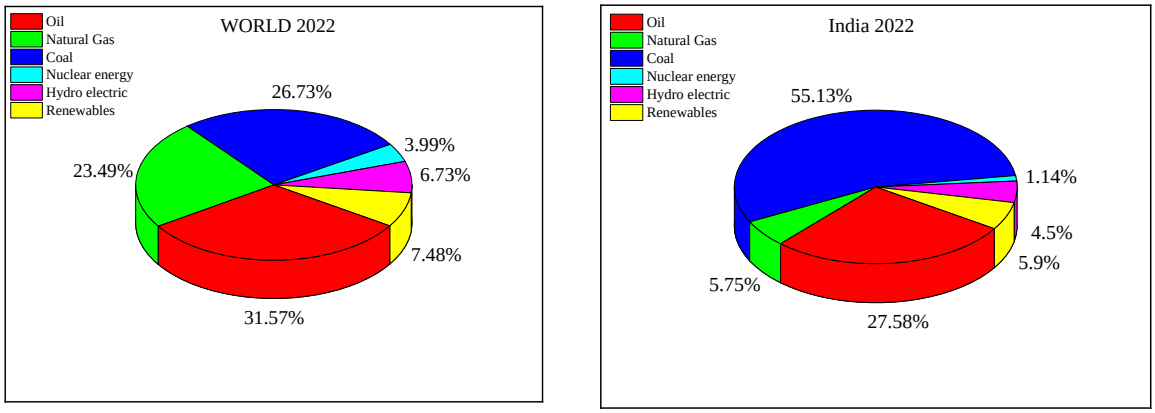

Figure 2: Energy consumption by fuel in year 2022 (worldwide and India)

Energy storage is a problem that is faced by civilisation. Most simple trick of storing energy is storing water at an high altitude so that energy can be stored as potential energy. It means using

pump to take water to uphill into reserviour and then when power production is needed then allow the water to flow downhill and use turbine to produce electricity[7].

Now,why the energy storage is such an important thing! It is vital in high-tech production because a steady frequency, uninterruptible power supply is necessary. According to reports, U.S. business loses over $80 billion annually [8] as a result of mostly brief interruptions in electricity. At the same time the reduction and multifunctionalities of micromechanical, portable, communicative devices has accelerated dramatically due to the recent advancements in nano and microfabrication technology. These gadgets will need to be small in size, have a long lifespan, and recharge extremely quickly. Rechargeable batteries are now a major component of many portable electronics, including computers, torches, mobile phones, etc. The battery market was valued at US $62 billion in 2014 [9], and by 2019 it had grown to US $120 billion [10]. The increasing use of UPS devices in healthcare, oil, gas, chemical industry sectors will play a vital role increasing demands of batteries in future. The size of the worldwide battery market was estimated at USD 104.31 billion in 2022, and between 2023 and 2030, it is projected to increase at a compound annual growth rate (CAGR) of 15.8% [11]. Rechargeable and non-rechargeable batteries are also the source to power devices such as laptop, torch, mobile phone, wall clock, wrist watch, smartphone, iPad, tablets etc. without the advancement in batteries these portable devices would not have advanced as these have progressed [12]. But the batteries also come with its short comings. The main problem of battery is its low energy density. Even advanced Li-ion batteries has energy density of 0.20 kWh/kg.[13].

To put this energy density of advanced batteries it can last up to few hours for modern computers, mobiles etc. Batteries has limited no of rechargeable cycle before it gets wasted also to charge battery it takes several hours to get fully charged to 100%.

Furthermore, the disposals of batteries created several environmental issues. Therefore, due to all these the advancement of micromechanical devices is greatly reduced by the non-availability of compact, robust, efficient, light weight instantaneously rechargeable portable power source.

In addition to using a microreactor, micro-sensing and chemical analysis devices offer novel ways to quickly and effectively test tiny amounts of chemicals for security and safety [14]. an effective micro-combustor is required for the supply of chemical species, species analysis, and sensor actuation on a microchip chemical analyzer. This micro-combustor must be able to boost reaction temperature, give partial oxidation, and deliver electrical power. Obviously, a battery's low density makes it an inappropriate choice.

For a prolonged operating time of years, micro-satellite thrusters for station maintaining require a modest thrust (1-1000 mN) and a high specific impulse (250-450 s) with a small impulse bit (~1e5 Ns) [15]. Propellers with a high energy density (~4 kWh/kg for solid propellants) and precise thrust control are thus necessary for an effective micro-thruster. However, a battery-powered thruster has a relatively poor thrust to weight ratio and cannot provide such a precise impulse.

Examining the energy densities of the fuels and the energy conversion systems is necessary to extend a power device's operating lifespan. Energy density of different batteries such as Li ion batteries, Lead acid batteries, Nickel cadmium (NiCad) batteries, Lithium sulfur batteries, and conventional fuels like gasoline, diesel, octane, butane, propane as well as energy densities of renewable resource such as ethanol, methanol, hydrogen are all compared in terms of energy densities in Fig. 3 [18]. The most cutting-edge lithium-ion batteries now on the market have an energy density of y 0.61 MJ/kg [16,17], which is about one-sixtieth that of hydrocarbon fuels (such as diesel and methane). Furthermore, a lithium battery's energy density is one-twentieth that of a diesel engine (200 kW with 450 kg of engine weight).

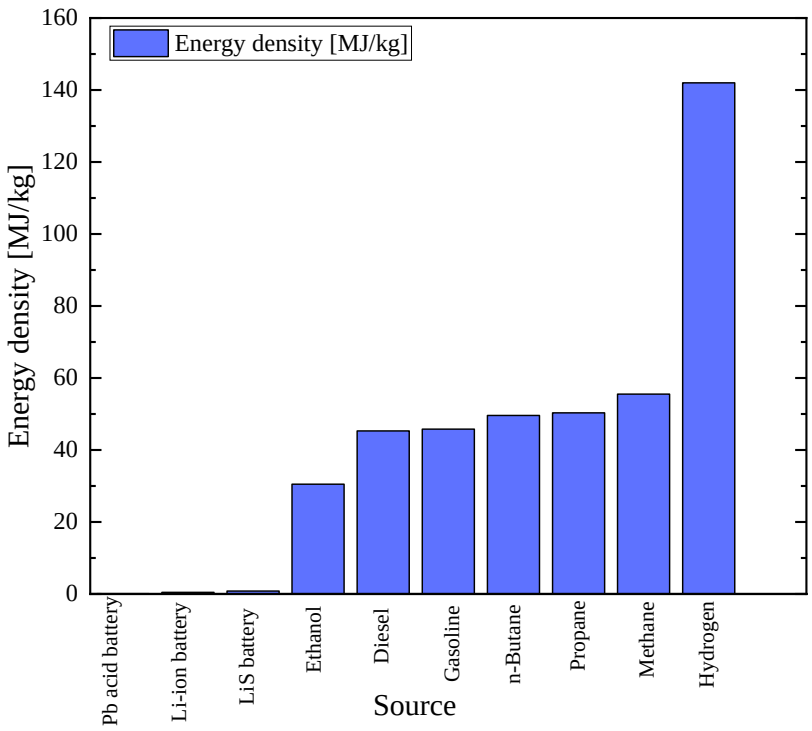

Figure : 3: Energy densities of different sources. The energy density of combustion-based sources is based on complete combustion to carbon dioxide and liquid water, at 298 K and 1 atm.

From the above discussions the need for portable power source is understandable. Also, with the problems of batteries as energy storing unit for portable devices. Therefore, there is a need for micro scale or mini scale combustor which runs on fuels with much higher energy density compared to battery.

CHAPTER 2: LITERATURE REVIEW:

2.1 Length Scale for Micro and Meso Scale:

Over the last few years, several micro-engines [19,26,27], micro-thrusters [20,22-25], and micro-reactors [21,20] have been constructed. The term "micro-scale combustion" can be misleading and even mistaken with "mesoscale combustion" due to arbitrary reference length scales. Therefore, defined length scale is necessary for micro combustion research.

Previous research has utilized three length ranges to define "micro-scale" combustion (see Table 1).

Table 1: *Length ranges for meso and micro combustors*

Combustor type	Length scale	Definition base
Micro scale	Smaller than conventional device size	Device size
Meso scale Micro scale	1-10 millimeter 1-1000 micrometer	Physical length
Meso scale Micro scale	~flame quenching diameter	Flame quenching diameter

The physical dimension of the combustor is a commonly used length scale for distinguishing "micro-scale" and "meso-scale" combustion. Mesoscale combustion occurs when the physical length scale exceeds 1 mm but falls within the range of 1 cm. Micro-combustion occurs when the combustor's physical length is less than 1 mm. This definition is commonly used in the development of micro-engines [19]. The second definition involves using a flame reference length scale, known as the quenching diameter [28]. The combustion is considered micro-scale (mesoscale) when the combustor size is less than the quenching diameter. Researchers choose this terminology for studying micro-combustion because it better reflects physical flame

regimes. Quantifying the border between micro and meso combustion is challenging due to the variable quenching diameter, which depends on mixture composition and wall parameters such as temperature and surface reactivity. Meso and micro-scale combustion can also be defined by comparing a device's length to that of larger devices used for comparable purposes. A micro-combustor for a satellite does not always indicate a micro-scale combustor [29]. The combustor is used for a micro-satellite weighing between 10 and 100 kg, which is considered "micro" in comparison to a conventional commercial satellite weighing over 1000 kg. Researchers apply this concept while developing micro-thrusters for specific purposes.

2.2 Challenges of Microscale Combustion

When burner length scale is very less or burner size is comparable to flame quenching diameter micro combustion occurs. Small burner size makes it difficult for the charge to burn inside the combustor completely due to small volume of the burner for reaction as well as very high reaction rate [30]. By reducing the combustor characteristic size, the surface area-to-volume ratio increases, which leads to heat loss at the combustor walls resulting unstable combustion. The flame becomes extinct due to heat loss in combustor walls. The homogenous combustion stops when the heat and radicals created by the reactions quickly exhaust themselves on the wall [31].

For micro burner the internal volume of the burner is lesser compared to traditional burners. The ratio of internal volume of the burner and the volume of the mixture inflow is proportional to the residence time of the burner. As the volume of the burner is low therefore the residence time for micro burner will also be low. Due to this short period of residence time the mixture will be blown out before it burns completely sometimes even before burning. This will cause incomplete combustion due to which the efficiency will be lower. At the same time incomplete combustion also cause the creation of pollutants such as NOx, carbon monoxide etc. Therefore, due to shorter period of residence time sustaining a stable combustion for micro and meso scale combustion is very much challenging [32].

As the size of the combustor is reduced therefore sustaining a stable flame is becoming more difficult [33]. Numerous different flame shapes were seen in micro combustors [34]. Relatively tiny combustors have been reported to exhibit pulsing flames and flashbacks [35, 36]. Rotation and spinning are examples of unsteady flame propagation that have been seen [37]. Micro combustors frequently experienced localized re-extinction and re-igniting of flames (local RERI) and flames with repetitive extinction and ignition (FREI) [38,39]. The instability of the

flame is only part of the problem with achieving stable micro combustion. Another issue is inefficient and incomplete combustion due to a residence time that is too short, equating to the time of chemical reaction. Therefore, increasing flame stability, extending fuel residence time, or shortening chemical reaction time are all crucial for ensuring the reliability of micro combustion.

2.3 Flame Dynamics

There are two different types of combustion one is premixed where fuel and air is mixed with each other before entering into the burner another is non premixed when fuel and air is not mixed before entering the burner. Compared to traditional methods premixed combustion ensures more efficient combustion and more uniform fuel distribution among the air fuel mixture. Therefore, premixed combustion is more suitable for power MEMS [40].For micro and meso scale combustor many different types of flame regime have been observed by previous studies. The different behaviours of flame depend on many factors such as premixed flame or non-premixed flame, fuel type, burner geometry, equivalence ratio, flow velocity, Reynold's no, thermal conductivity of combustor walls etc. Here different types of flame behaviours are studied previously will be discussed one by one.

2.3.1 Stable Flame

A stable flame is such a flame where the flame remains stable or constant without flickering. after starting combustion process the flame might move upstream or downstream and then stabilizes at a certain location. It is observed experimentally by Maruta et al. [41] in the year 2005. The flame whether stable or unstable depends on several parameters such as flow velocity, fuel type, wall preheating etc. Schematic representation of a stable micro-flame is given in Fig. 4.

Numerical simulations by Ghaeini et al. [42] for two dimensions were utilized to examine the stable flame region for ammonia/hydrogen, NOx emission, and combustion efficiency in micro-combustors. An analysis was conducted to determine how the fuel's hydrogen percentage and entrance flow velocity affected the temperature distribution and combustion properties. It has been discovered in the study that an unstable flame cannot occur when the input velocity

is either too high in relation to wall heating or too low in relation to flame speed. Moreover, when the fuel's hydrogen content is less than 60%, a steady flame does not form.

A work by Cinieri et al. [43] presents the results of a numerical study in which they used Ansys Fluent for simulation for a Y-shaped micro combustor to investigate aspects of non-premixed NH_3/air and H_2/air combustion in micro-scale combustors. The results show how the various fuels affect the species produced, emissions, and micro combustor efficiency. Even at lower equivalency ratios, steady flames are observed by H_2 combustion. For H_2 fuel, a flame is present when the Φ is greater than 0.5. On the other hand, for NH_3 fuel, the minimum Φ required for flame ignition is 0.7. Furthermore, H_2 in the flame often produces twice as many pollutants as NH_3. Under NH_3 circumstances, the micro combustor's total efficiency is twice as high as under H_2 conditions.

Di Stazio et al. [44] made a new experimental device to conduct study on micro combustion which is made of micro tubular channel with an external heating provided by three hydrogen/oxygen flames positioned at the downstream side of the tube. The study carried out for equivalence ration 0.5 to 1.5. Stable flame has been observed in this study for high flow velocity along with few instable flame regions such as FREI at middle flow velocity and weal flame at low flow velocity.

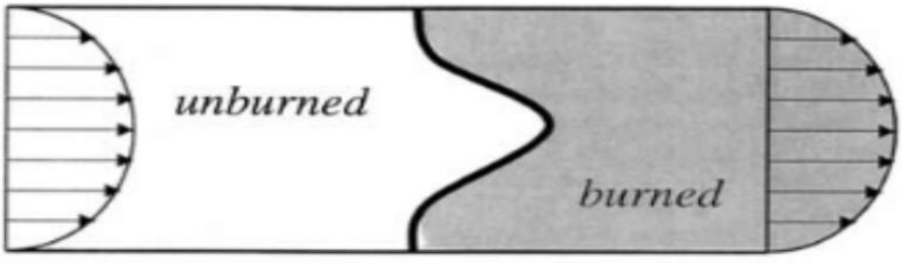

Figure :4 Schematic representation of a stable micro-flame [35]

An elliptic two-dimensional computational fluid dynamics model was used to investigate the combustion properties of micro burners such as conductivity and wall thickness [45]. It has been accomplished by the study that the conductivity and thickness of the wall play a crucial role in determining the upstream heat transfer required for flame stability and ignition. It is observed that a micro burner can sustain combustion within a limited range of flow velocities. Additionally, Significant differences in propagation velocities were caused by different velocity profiles, and the flame structures observed.

Research conducted by Sai et al. [46] where a numerical modelling has been used to study the steady propagation of a premixed flame exposed to the Poiseuille flow in an isothermal duct. Also, how flame symmetry behaves in relation to input velocity profile intensity, duct width, duct shape, and gravity along the duct has been studied. According to the study, a flame that is continuously spreading in ducts that are opposite to the Poiseuille flow can have one of two unique shapes: an asymmetrical slant form or a symmetric mushroom shape. For instance, only an asymmetrical slant-shaped flame may be discovered in a bigger duct, while a symmetric mushroom-shaped flame can be found in a smaller one. Instead of the asymmetric slant-shaped flame, the tulip-shaped flame appears when the symmetric flow assumption is taken.

For non-fuel ultra-lean conditions, Cai et al. [47] developed stable flame dynamics of CH_4–air within a micro-combustor with a flame holder and preheating channels. This study shows the importance to preheat the incoming unburnt mixture. The findings show that when there was a stable flame, the rising Reynolds and equivalency ratios forced the flame downstream, which resulted in a notable rise in flame height and an amazing anchoring impact of the flow recirculation.

2.3.2 Flashback, Lift Off and Blowout

Depending on flame propagation downstream or upstream flashback and blowout can be defined.

For flames when the flame velocity is higher than the mixture velocity then flame propagates towards the unburnt mixture or into the combustor this phenomenon of the flame is known as flashback. In case of flashback, it not only disturbs the combustion process but also it causes safety problem. As the flame moves upstream therefore large volume of unburnt mixture is exposed to the flame. Therefore, the unburnt mixture can catch fire and explode. Because flashback happens when the flame spreads into the unburned mixture, the flame propagation velocity exceeds the local flow velocity. As a result, mixes with high flame speeds are more likely to flashback.

Lift-off occurs when the flame detaches and flows downstream from the burner. Lift-off stabilizes flames above the burner, resulting in a raised flame. Lifted flames can be unsuitable in practical applications for many reasons. After stabilizing the flame away from the burner, some fuel may still remain unburned. Stabilizing the flame in a specific spot might lead to inefficient heat transmission. These flames can be loud and sensitive to environmental factors. Flame lift-off happens when the flame moves in the direction of fluid motion. In certain cases, the local flow velocity surpasses the flame speed.

Increased flow velocity at the burner output causes the flame to move further away from the burner. After a certain distance, the flame loses stability and blows out altogether. This occurrence is referred to as blowout. Blowouts can cause shutdowns and tragic accidents, making them an unwanted event. Flame velocity reduces when the operational zone is moved towards rich or lean mixture from stoichiometry. Therefore, on both the lean and richer side of stoichiometry blowout can be observed. Lean mixture zone is generally operated for low

emission therefore it is always at the risk of blowout. This type of blowout is known as lean blowout.

Fruzza et al. [48] studied the flashback of various H_2/CH_4 mixes at an equivalency ratio of 0.8 and proposed a numerical model to estimate the critical flashback velocity for laminar premixed flames. The model accounts for conjugate heat transfer between the gas phase and the burner plate. Two flashback regimes are recognized based on the H_2 content. The findings indicate that employing laminar flame speed alone is insufficient for planning the safe functioning of realistic premixed burners.

This study is then also extended by Fruzza et al. [49]. This study looks at the effects of operating and geometrical factors on flashback phenomena in multi-slit burners fed with hydrogen methane-air mixtures. Transient numerical simulations that account for conjugate heat transport between the fluid and solid walls are used in conjunction with a stochastic sensitivity analysis based on Generalized Polynomial Chaos. complete maps of flashback velocities and burner temperatures within the parameter space of hydrogen concentration, equivalency ratio, and slit width has been created by using a small number of numerical simulations. Furthermore, the study investigates the effects of several characteristics such as burner geometry, adiabatic flame temperature, flame thickness and their relationships on flashback propensity. The ranges the study carried out include highly H_2-enriched lean mixes (80% to 100% H_2 by volume) with equivalence ratios ranging from 0.5 to 1.0. These findings show promise for driving the design and optimization of perforated burners, allowing them to operate safely and efficiently in actual end-user applications.

The impact of Lewis number on the blow-off and stability of laminar lean limit premixed flames has been investigated both numerically and experimentally by F.H. Vance et al. [50]. Distinct Lewis numbers result in distinct forms, structures, and anchoring phenomena in flames. Le > 1 flames anchor just at the boundary of the low velocity recirculation zone,

become locally lean in the recirculation zone, and lose heat to the unburned side. It is explained that the reason the Le > 1 flame blows off is that it is no longer able to stabilize in the low velocity recirculation zone.

Vance et al. [51] found that flame can adjust its speed by moving to different locations near the flame holder in a complicated manner by adjusting the contributions from stretch, heat transfer with the flame holder and preferential diffusion which broadened the blow off or flashback limit noticeably.

Experimental research is conducted on the laminar flame dynamics of the premixed combination of methane and air in a preheated micro combustor equipped with a flame holder that serves as both a micro source of heat and a micro source of power by Cai et al. [47]. The findings show that the premixed flame is stable far in advance of flame extinction. Through experimentation, the anomalous blow-off is discovered within the micro combustion chamber for the first time, and the associated underlying processes are also disclosed. The center of the flame in the vertical direction is observed to have a constricted shape in this anomalous blow-off dynamic. Additionally, blowoff dynamics changing with different flow characteristic also observed. When the Reynolds number is greater than 240, the blow-off dynamics are significantly different from those with a Reynolds number of less than 180. The oscillating flame initially occurs when the Reynolds number is less than 180. Over time, the flame gets smaller and weaker until finally going out entirely close to the flame tip. The flame with local extinction and periodic re-ignition happens initially when the Reynolds number exceeds 240. The remaining flame then shrinks upstream and eventually extinguishes directly behind the holder.

Wan et al. [52] studied using an experimental setup the blow-off modes of methane/air flame in a combustor equipped with preheating channels and a plate flame holder. Both the typical and anomalous blow-off phenomena—which are initially seen for the flame of Le 1.0—exist

in fuel-lean conditions. The study reported the discovery of a novel blow-off mode, called low speed blow-off, for fuel rich situations in addition to the equivalent normal and anomalous blow-off under fuel lean settings. Furthermore, the results show that, for moderate and high Reynolds numbers, the ratio of the flammable range between fuel-rich and lean situations essentially stays the same, but that, with a drop in Reynolds number, the difference in the flammable range between fuel-rich and lean conditions grows dramatically.

2.3.3 Flames with Repetitive Extinction and Ignition (FREI)

Flame repetitive extinction and ignition (FREI) are referred to an instable flame observed commonly of meso and micro combustor for various fuels and flow condition. FREI is basically the combustion events that occur cyclically inside meso or micro scale combustor. These flames display periodic repeating extinction, in which the flame extinguishes, and ignition, in which it ignites again. Complex interplay involving heat transfer, chemical reactions, and fluid dynamics cause the phenomena. As for meso and microscale combustor the flame repetitive extinction and ignition regime is often found out therefore it is very crucial to understand the phenomenon happening in this regime to build a portable power device with micro or meso combustor with higher performance and higher stability.

Maruta et al. [53] observed flame repetitive extinction and ignition regime experimentally. This study found out some observation like extinction will happen upstream if the wall temperature there is lowered or if the upstream channel width is less than the quenching diameter of the typical propagating flame. When the mixture after flame extinction reaches a position where the wall temperature is higher than the ignition temperature, auto-ignition will happen once again since the downstream wall is still heated (Fig. 5). This process is repeated in cyclic manner which generates flame repetitive extinction and ignition regime.

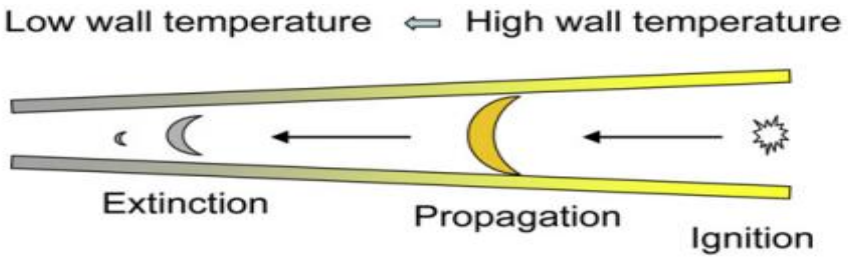

Figure 5: Schematic diagram of FREI in meso scale combustion

Additionally, the study found out that for lower flow rate the FREI occurring while for higher flow rate the stable flame is observed. Because of the reason high flow rate balances the flame speed with a high wall temperature, a stable flame is observed for higher flow rate. Comparison of still images of stable flame vs FREI is shown in Fig. 6.

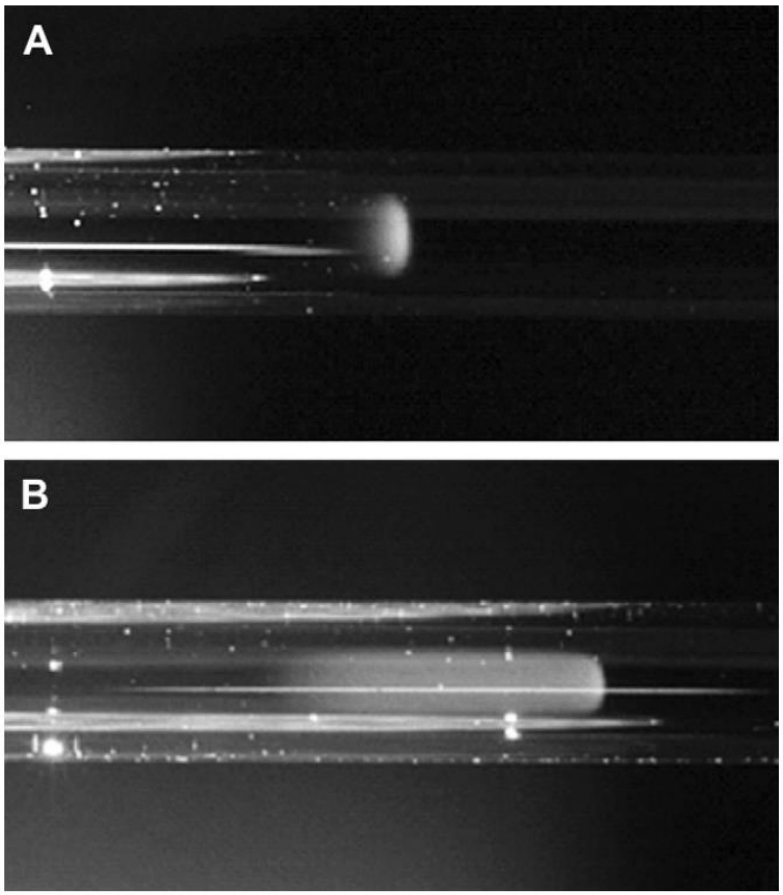

Figure :6 Comparison of still images of stable flame and FREI [53]

Kyritsis et al. [54] carried out experiment for curved mesoscale ducts and found out for constant boundary conditions, a steady flame oscillation with extinction/re-ignition phenomena may be created in "mesoscale" tubes. When the right circumstances are met, these oscillations cause sound to be emitted in the 50–350 Hz range.

For fuel-rich methane-oxygen and propane-oxygen mixtures, another research by Kyritsis et al. [55] aimed to identify the mode of oscillation as a function of equivalency ratio and flow speed. The oscillating flames were detected in small circular ducts. Premixed fuel and oxygen were burnt in an optically accessible straight quartz tube with an inner diameter of a few millimetres, one end of which was exposed to the environment, in order to investigate flame stability in narrow ducts with diameters on the order of the quenching diameter. Different oscillating and stable flame forms were noticed, and the methane-oxygen and propane-oxygen flames were analysed. The boundaries between behavioural regimes for methane were found to be almost exclusively dependent on equivalence ratio, with boundary equivalence ratio values staying relatively constant for varying Reynolds numbers; in the case of propane, however, the boundaries were dependent on both equivalency ratio and Reynolds number, with limit equivalence ratio values declining as Reynolds number increased. Experiments with tubes measuring 35, 70, and 210 mm in length were also conducted to investigate the impact of tube length on oscillatory behavior and stability. Lengthening the tube reduced oscillation stability for both fuels, albeit the impact on propane was less severe. Furthermore, it was noted that oscillations were only established in low conductivity material mesoscale ducts; the significance of this finding was explained in terms of the Biot and Fourier numbers.

By putting out a one-dimensional nonlinear evolutionary equation of the flame front that takes flame front acceleration and rate of flame temperature fluctuation into account, the non-stationary flame behaviors are analytically explained [4].

Three groups of people have modeled numerically oscillating flames in small-scale combustion engines: Norton et al. [56], Jackson et al. [57]. The temperature evolution as a function of time and the limit cycle of self-sustained oscillations [58] in situations when the micro-scale catalyst has a large heat loss. The findings demonstrated that in situations with significant heat loss, the stationary flames became unstable. The frequency of the limit cycle is around 1000 Hz. Frequent flame oscillations were seen, along with recurring instability caused by quenching and reignition.

The intricacies of the repeated ignition/extinction phenomenon were effectively captured by a two-dimensional direct numerical simulation with detailed chemistry and transport for fuel lean (φ= 0.5) hydrogen/air flames in planar microchannels with regulated wall temperature [59, 60]. At a specific downstream point, the hot walls heat the incoming new mixture, causing it to ignite. The contained flame then spreads horizontally in both the upstream and downstream directions. The flame that is spreading upstream becomes almost flat in shape before extinguishing in the upstream. In the residual fresh mixture, the downstream spreading flame maintains its original configuration until ultimately going out. Upon increasing the input mixture velocity from 0.8 to 0.9 cm/s, the weak flame transitioned to a periodic firing/extinction state.

More thorough research is done [61] utilizing a quartz microchannel that is rectangular and heated by an infrared light. In addition, PLIF measurements for CH* and OH* are carried out, along with the observation of extinction and reignition processes. For the first time, the movements of these ecstatic species during extinction and reignition have been successfully recorded.

Alipoor et al. [62] investigated flames in microchannels with widths ranging from 0.4 to 1 mm, with equivalency ratios ranging from 0.5 to the stoichiometric condition of ϕ = 1. The cumulative results showed that while the frequency of the FREI phenomena decreased, its

amplitude rose as the equivalency ratio and burner width were raised. Moreover, our analysis revealed that the occurrence causes flame bifurcation and fluid recirculation zones because of the heavier species present. These species have a higher capacity to absorb heat, which lowers the temperature.

Gamezo and Oran [63] modelled a closed end flame acceleration in a mesoscale channel. The results demonstrated that when the flame spread from the end wall toward the end with an open exit, the boundary layer effect caused the flame surfaces to considerably grow. A powerful flame self-acceleration resulted from the flame surface area rapidly increasing.

The study by Alipoor et al. [64] uses numerical modelling to derive flame dynamics for the combustion of premixed lean hydrogen-air in a heated microchannel. In this simulation, low Mach number formulation and careful examination of chemical kinetics in detail are used to formulate the Navier-Stokes equations as well as the equations for the conservation of energy and species. Three dynamics—periodic repeated ignition-extinction, stable symmetric flame, and steady asymmetric flame—are shown in the microchannel under various settings. The impacts of several factors on the flame dynamics are examined, including channel width, equivalency ratio, and input velocity. When traveling at low speeds, one may notice the periodic repeating ignition-extinction dynamics in proximity to the lower flammability limit. A constant symmetric flame is visible in the channel when the input velocity is increased and the response time and fluid residence time are balanced.

Further computer studies have also been carried out to further our understanding of the FREI phenomena across various fuel types. Air mixes and CH_4 were the subject of analyses conducted by Nakamura et al. [65], Tsuboi et al. [66], and Miyata et al. [67]. They used a one-dimensional model at first, which they then verified against the results of their experiments. They therefore only used direct numerical simulations to examine how boundary parameters, including wall temperature gradients and intake temperatures, affected the

dynamics of the flame. Yamamoto et al. [68] conducted an experimental and numerical investigation of the n-heptane–air combustion properties, noting the occurrence of FREI dynamics.

2.3.4 Spinning Flame

Spinning flame for a meso scale combustor was first observed experimentally by Ju et al. [69]. They carried out experiment on premixed methane air and propane air mixture for a divergent channel. The focus was on how the flame-wall interaction and variable cross-section area affected the flame's transition between regimes and the beginning of flame instability. The spinning flame was found for a wide range of equivalency ratios in both lean and rich methane and propane–air mixes (Fig. 7). With equal probability, the spinning flames revolved in a clockwise or counter clockwise way. This equal probability for both direction of spin can conclude that the spinning flame is caused by thermal diffusion rather than flow motion. The findings demonstrated the existence of a threshold flow rate, over which flames begin to spin, for a certain equivalency ratio. The flame speed and the spin frequency were about proportionate. Additionally, it was discovered that the spinning flame appeared while the transition of fast to slow flow regime. Frequencies of methane air and propane air flame spinning flame is given in Fig. 8.

Thermal interaction between the flame and the wall enhances enthalpy transfer by indirect heat recirculation, resulting in multi-dimensional spinning instability in mesoscale combustion. Variations in flame-wall coupling, such as cooling or heating, can regulate the transition from spinning to stable planar flames. Cooling the wall can cause a spinning flame to stabilize. So, if the burner walls are at room temperature, then there might be stable flame instead of spinning flame. This discovery confirms that flame instability is regulated by thermal interaction between the flame and the wall. Furthermore, the spinning flame was confirmed in tubes with only one divergent portion and observed when the tube was positioned horizontally or upside

down. The spinning flame is caused by thermal interaction between the flame and the wall, rather than buoyancy.

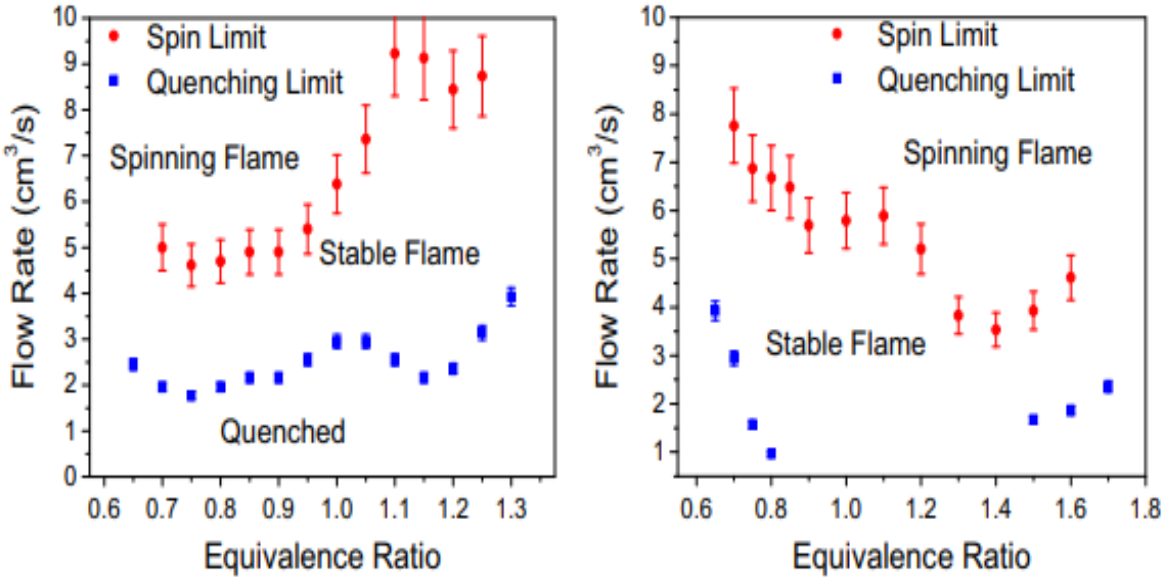

Figure 7: Flame regime diagram for different flow rates equivalence ratios. (Left: Methane-air mixture; Right: Propane-air mixtures) [69]

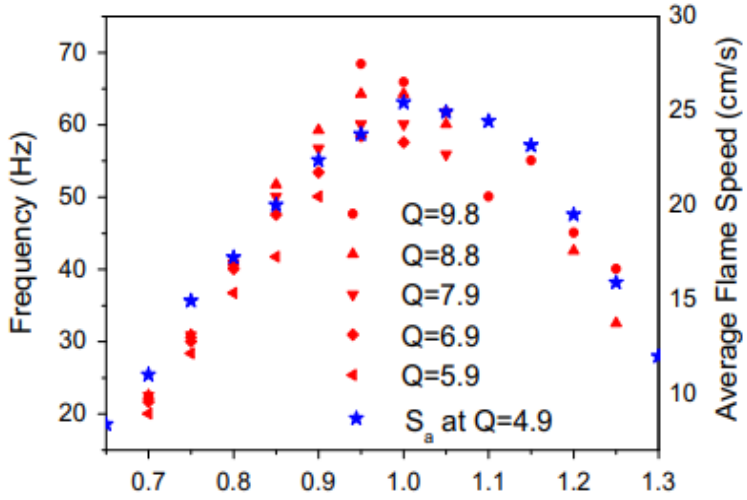

Figure 8: Frequencies of methane and propane spin flames at different equivalence ratios for methane-air flames [69]

Pizza et al. [70] studied the dynamics of fuel-lean (equivalence ratio φ = 0.5) premixed hydrogen/air atmospheric pressure flames in open cylindrical tubes with diameters of 1.0 and 1.5 mm using three-dimensional numerical simulations. This study is carried out by taking hydrogen as fuel. Here the researchers also observed the spinning flame regime.

Experiments carried out on premixed fuel air mixtures in stepped tube micro combustors [71] found that thermal wall coupling causes both stable and unsteady spinning flame propagation modes across different flow rates and mixture ratios. For the first time, spinning flames of very high frequency (~150 Hz) were detected with diverse fuel-air mixes. These flames whirl almost twice as fast as those recorded in previous studies. Spinning flames were detected in both lean and rich methane air, LPG air, and propane air mixes. The creation of spinning flames in a micro combustor is determined by the mixture flow rate, equivalency ratio, and number of steps in the combustor.

2.3.5 Spiral Flame Patterns

Spiral and other patterns, which are typically found in excitable media, have been documented in combustion systems [72-74]. Repetitive extinction and ignition instability in a straight tube with an external heat source result in a variety of instability and oscillatory phenomena, including regular cyclic oscillation, pulsation, and other chaotic oscillations. While these events happened in a spatially one-dimensional geometry, current research on two-dimensional radial-flow systems has shown further rich types of chaotic instabilities and pattern generation (Fig. 9). Such phenomena found in radial micro-channels [75-77] and rectangular channels between two parallel plates [78,79], both with external heat sources, are discussed.

Flame patterns may be changed by adjusting parameters such mixture flow rate, equivalence ratio, and spacing between plates, as seen in Fig. [184].

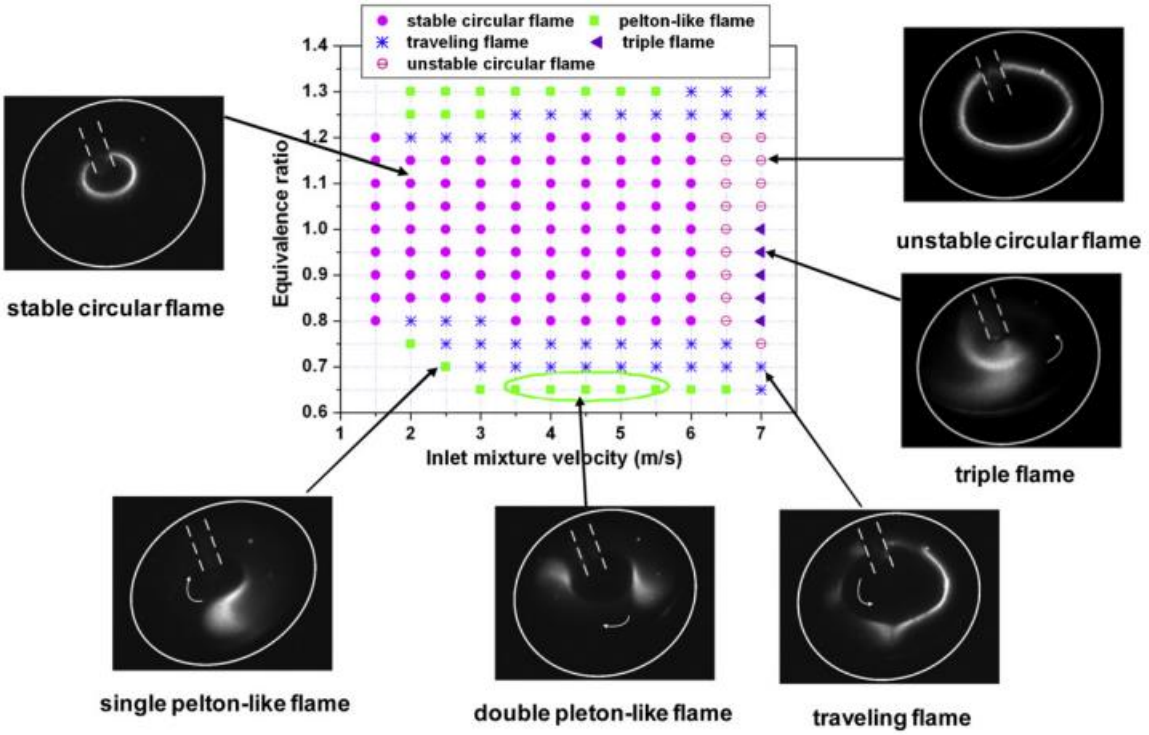

Figure 9: Flame patterns observed in radial micro-channel and their regime diagram for methane/air mixtures at the gap between two plates is 2 mm [75].

A consistent circular flame in a radial microchannel is similar to a steady normal flame in a straight tube. Single or double flames circling around the middle of the channel, known as Pelton (wheel)-like flames [187], can be observed under both fuel lean and rich circumstances. These revolving flames were semi-circular in form and had rotational speeds ranging from 15 to 50 Hz. The whirling flames resemble a classic Pelton wheel since they rotate continuously and have a semi-circular form. These flame formations were found to emerge at velocities ranging from 1.5 to 6 meters per second. At comparable operating circumstances, the domain exhibits one, two, and three rotating flame fronts. A traveling flame is a circular flame split into fractions that move tangentially [188]. Travelling flame can be observed between circular stable flames and Pelton-like flames region. Regime diagram for various flame propagation modes at Φ= 0.85 for methane-air mixtures is given in Fig. 10.

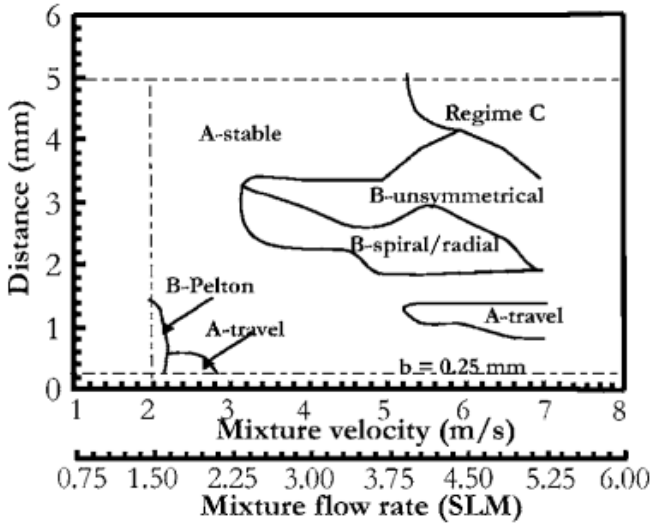

Figure 10: Regime diagram for various flame propagation modes at Φ= 0.85 for methane-air mixtures with mixture flow rate varying from 1.5– 5.25 SLM (U~2–7 m/s) and b~0.25–5.0 mm. The width of the radial channel is changed from 0.25– 5.0 mm in 0.25 mm steps. Flame quenching occurred for channel widths smaller than 0.25 mm and not addressed in the figure.[80]

Experiments have shown that the inner and outer borders of Pelton and moving flames correspond with the ignition and extinction of FREI events [81]. Two-dimensional transient simulations [81] are used to simulate single/double Pelton and spiral flames and analyse their structure. The computational and experimental analysis of reignition in FREI events is presented [82,83]. Splitting flames which have two reaction fronts, one moving upstream and the other downstream has been observed. This is because FREI's regeneration begins at a specific location that is close to the edge of the fresh mixture rather than at the edge of the recharging fresh mixture. Splitting flame behaviour is said to be crucial for the creation of patterns [81]. Using two-dimensional DNS, splitting flame behaviour for hydrogen-air mixtures is also independently determined [79].

2.4 Research Gap

Various studies which have been conducted in the field of flame dynamics for micro and meso scale combustor has been discussed in the literature review section. Many parameters such as combustor geometry, flow rate, fuels, duct lengths, equivalence ratio etc. have been varied and different flame behaviours have been observed by scientist. However, varying the ducts diameter and its effect on the flame dynamics has not been studied for mini scale combustor.

On the other hand, scientist have studied flame dynamics using numerous fuels such as methane, propane, butane, hydrogen etc. but there are not research work on the LPG flame behaviours.

LPG is widely used for domestic and industrial use as well as it is used for transportation. It is used by the whole world to produce power. So, it is a very useful fuel so it needs to be tested as if it can fuel mini combustor powered portable power sourced. Another characteristic of LPG which makes it suitable for use in a portable power source in mini scale is that it can be stored in liquid form easily and when it comes out in atmosphere it becomes in vapour form. This characteristic of LPG reduces the complexity of the system. Suppose any liquid fuel such as diesel or petrol is used that it needs to be turn into small liquid particle or vaporise it before it can mix well with air which increases complexity for a mini scale device. But as LPG is vaporised in atmosphere it can be mixed pretty well with the air without the complexity of making it into small particles. Also, as LPG is stored in liquid form therefore the energy density is also higher compared to gaseous fuels.

So here for the flame behaviour study of mini scale combustor flame LPG has been used as fuel.

2.5 Objective of The Study

As the space where flame is constructed that space is reduced then the heat loss in the combustor walls increases and due to higher heat loss than the heat produced by burning fresh mixture the flame is quenched for mini scale combustors. Also, many instabilities such as FREI flame, spinning flame, spiral flame patterns pattern etc. has been observed for mini scale combustion which has been explained in detailed in the literature review section.

The objective of the current study is to identify the different flame patterns and instabilities for a mini scale combustor using LPG as fuel source and different duct diameters. Due to the instabilities observed for the mini scale combustion it becomes very important to predict in which condition the instabilities can occur and predict which is the safe zone of operation for it. Therefore, in this study the safe zone for combustion is studied and flame regime map has been obtained for different flow rates and different equivalence ratio for the different diameter ducts used in the experiment.

CHAPTER 3: EXPERIMENTAL SETUP AND PROCEDURE

The mini scale combustor has been shown in the image as well as the schematic of experimental setup has been shown in the Fig. 11, Fig. 17-. The required instruments are listed below.

- ***Combustor:*** This part is the heart of the experimental setup. Here the air fuel mixture will be supplied then spark will be supplied through a gas lighter. Then the flame will take place in the combustor.

  The length of the combustor is 23.5 cm including the cap at the top of the combustor. The diameter of the combustor body is 59.61mm (outer diameter) while the inner diameter of the combustor body is 51.18mm. There is another cylindrical pipe made of steel present inside the combustor body through which the air fuel mixture is coming to the combustion zone. The inner diameter of the inner pipe is 13.7mm and the outer diameter is 16.18mm. Between the inner wall of the combustor body and the inner pipe a net made from metal is placed which will prevent flashback to provide accidental safety during the experimental operation.

- ***LPG cylinder:*** For supplying LPG as fuel. Domestic LPG cylinder of 14.2kg is used for the experiment.
- ***Flow rate controller(air):*** To control the supplied air amount for the experiment. For air rotameter (variable area flow meter) is used to control the air flow rate supplied for the experiment (Fig. 14). Rotameter measures the volumetric flow rate of the working fluid.

  The manufacturer of the rotameter used is CVG Technocrats India. The range of the rotameter used is 0-50 LPM. The rotameter is calibrated for nitrogen but for the experiment the rotameter is used to measure the flow rate of air therefore the rotameter

reading has been multiplied by gas correctional factor to convert the reading from nitrogen to air.

Gas correctional factor, GCF=($\frac{\rho_{N_2}}{\rho_{AIR}}$)^1/2

ρ_{N_2}=density of nitrogen, ρ_{AIR}=density of air

Density of air can be found out from the simple formula, $\rho = \frac{P \times M}{R \times T}$

Where,

P=pressure of the gas

M=molecular weight of the gas

R=universal gas constant

T=absolute temperature

For P=1atm and T=298.15K

Density of air = $1.184 kg/m^3$

Density of nitrogen=$1.13 kg/m^3$

Therefore, CGF= $\sqrt{\frac{1.13}{1.184}}$ = 0.98

- ***Flow rate controller (fuel/LPG):*** To control the fuel supplied for the experiment.

Fuel flow rate controller is manufactured by alicate. The range of the alicate is 0-10 slpm. Model number is MC-10SLPM-D-DB9M. This model can measure both mass flow rate and volume flow rate. In this particular experiment alicate is used to measure volume flow

(Fig. 15) rate of the fuel (LPG). LPG is taken as 60% propane and 40% butane, and the mixture is set as combination of propane and butane and used as working fluid.

- ***Fuel delivery pipe:*** To deliver fuel from LPG cylinder to fuel flow rate controller then supplying from the flow rate controller to the premixing chamber.

  Pu pipe has been used as delivery pipe along with pu connector where connection is required.

- ***Premixing chamber:*** The fuel and air will be mixed here (Fig. 13). Premixing chamber is basically a hollow cylindrical. Length of the premixing chamber is 32cm and the diameter is 75mm. The metered air and fuel will be supplied here so that air and fuel can be mixed together.

  The premixing chamber is made in such a measurement so that the air and fuel can be mixed properly and make a homogeneous mixture of required equivalence ratio.

- ***Air delivery pipe:*** It will deliver air from the compressor to the flow rate controller of air and then the metered amount of air will be supplied to the premixing chamber.

  For air delivery pipe pu pipe has been used just like the fuel delivery pipe.

- ***Compressor:*** It is used to supply the required air for the experiment to the setup. It is run by electricity (Fig. 12).
- ***Air fuel mixture delivery pipe:*** It is used to supply the the air fuel mixture from the premixing chamber to the combustor.
- ***Cap of the combustor:*** This is the part which is used so that quartz tubes can be fitted with the combustor body.

- ***Glass tube:*** Three glass tube of outer diameter 2.818cm,2.48cm and 2.142cm are there which will be attached in the cap of the combustor to observe the three cases. The inner diameter of the three tubes is 2.48cm, 2.142cm and 1.818cm. These ducts are referred as big duct, medium duct and small duct respectively (Fig. 16).
- ***Microphone:*** To record the produced due to instability in the combustor microphone of one plus nord ce 2 lite smartphone has been used.

Figure :11 Combustor used for the experiment

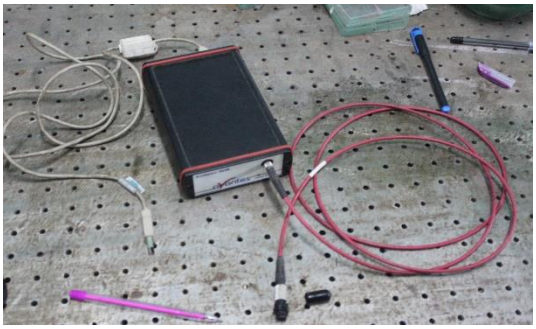

Figure :12 Compressor and Spectroscope

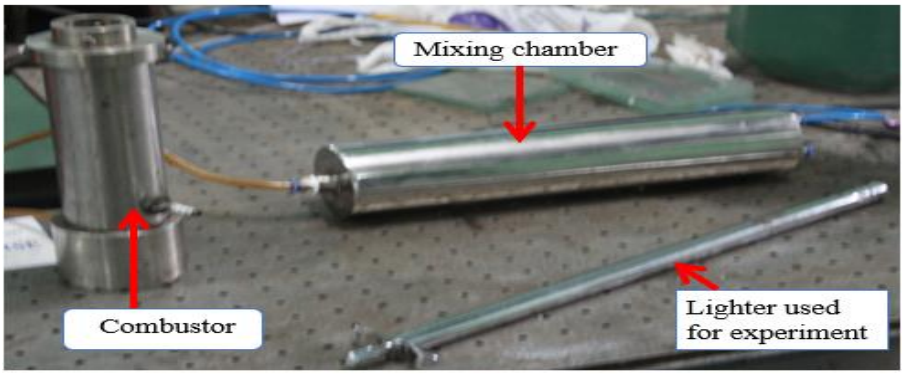

Figure :13 Combustor, mixing chamber connection with the used for experiment

\

Figure :14 Rotameter

Figure :15 Mass/volume flow controller (ALICATE)

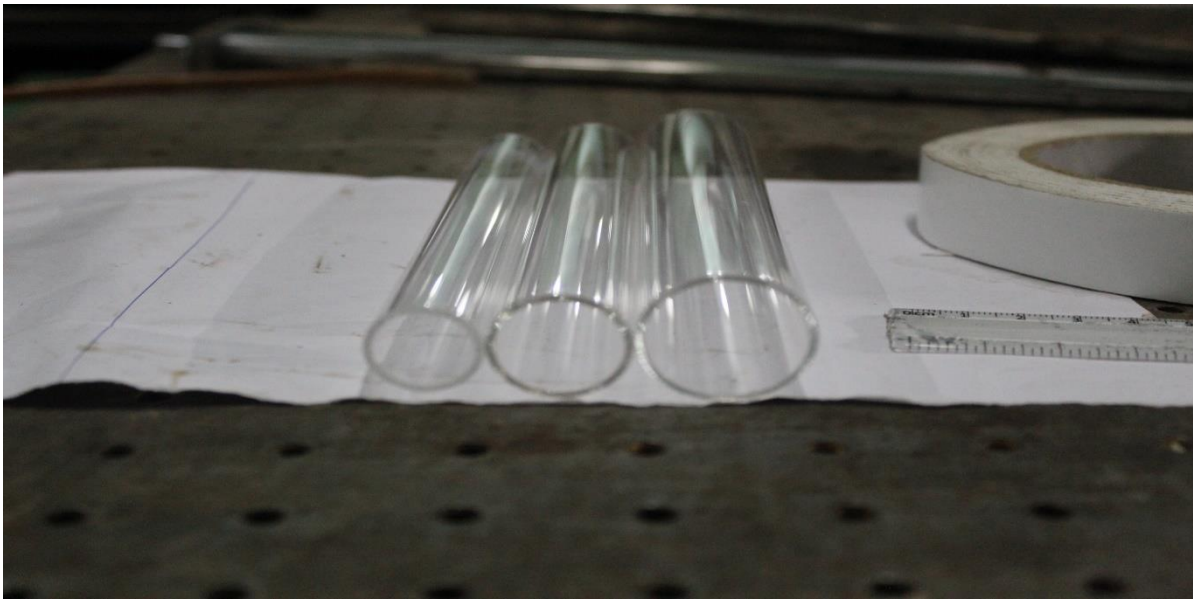

Figure :16 small, medium and big ducts used in the experiment

The way in which the experiment carried out is discussed in this section. The compressor supplies air required for the experiment. Then the air volume flow rate is controlled through the rotameter. Then from the rotameter outlet the air is supplied to the premixing chamber.

The fuel (LPG is used as fuel in this experiment) supplying cylinder supplies the fuel. The fuel volume flow rate is controlled through flow controlling device for fuel alicate which is volume flow rate controller. Then from the outlet of the volume flow rate controller the fuel goes to the premixing where the fuel meets with the air.

In the premixing chamber required amount of fuel and required amount of get mixed with each other and makes an air fuel mixture required for the particular equivalence ratio.

By keeping volume flow rate constant, the flame dynamics has been studied for various equivalence ratios. The equivalence ratios are changed by changing the volume flow rate of the fuel supplied. Both the volume flow rate controller and the rotameter measure the volume flow rate of fuel and air in litre per minute or lpm unit. As the volume flow rate of LPG is very small in comparison with the air flow rate therefore total volume flow rate can be taken as constant.

The flame dynamics has been studied through various parameters of the flame obtained in the combustor. The parameters are studied here are as follows

1. Flame height
2. Flame color
3. Flame flicker
4. Sound produced inside of the combustor

The flame height and flame diameter are needed to determine the geometry of the flame obtained in the combustor. Flame height and diameter are determined through image processing by using an open-source software image j. The scale for which one particular image is calibrated needs to be determined first and set accordingly in the image j software. As an image

is made of pixels so the height and width of one pixel can be determined, from there the height and diameter can be determined.

At first a straight line of known length to be selected. Then from set scale option the known value and unit needs to be put for determining the pixel height and width.

Then the value of distance between any two points in terms of pixels and be found out easily and multiplied that by height or width of one pixel to find out the flame height and diameter for one particular case.

Then this method is repeated for other cases to determine flame height and diameter for each case.

Flame colour is determined by using a spectroscope (Fig. 12) whose specifications has been given already in the experimental instrument section. The probe which scans the object and gives spectroscopy data is set at a height of 5mm from top of the combustor cap. Integration time for spectroscopy is set as 3500ms. Through this method the spectroscope generated intensity vs wavelength data for each case of the flame. From the spectroscopy graph the exact color present in one particular flame can be determined.

Some operations such as image smoothening, sharpening is used to find out the flame base and flame tip clearly as the flame tip and base has been selected manually.

Flame flicker is another very important parameter to determine or quantify the about the instability present in the flame. Generally, the lower flickering flame is more stable compared to a higher flickering flame.

Videos of flame has been taken for every instant through the digital camera whose specifications has been discussed in the experimental setup section. To determine the flicker

frequency of the flame first Fourier transformation has been applied on the fame video and flicker frequency has been obtained.

The FFT has been performed on the video data through programming in python language. To run the python code Kaggle notebook has been used which is a cloud-based environment to run code. The algorithm of code to perform the fft is

1. Video Processing:
    - Using OpenCV (cv2) to read a video file which contains the footage of flickering flames.
    - The video is cut frame by frame.
    - Each frame is preprocessed to isolate the flame region. The preprocessing is done by converting each frame to grayscale, then applying Gaussian blur, and then applying thresholding which creates a binary image highlighting the flame.
2. Flame Tip Tracking:
    - The flame region is located in the thresholder image by identifying contours.
    - The highest point inside the contour(s) is taken as the flame's tip.
    - It logs this tip's coordinates (X and Y) for every frame, along with the time and frame number that relate to it.
3. FFT Analysis:
    - The program uses the time data and recorded tip locations to construct a Data Frame (df) after processing each frame.
    - 'flame_tip_data.xlsx' is the Excel file where this Data Frame is saved.
    - After that, the algorithm extracts the information from this Excel file and uses the tip coordinates (X and Y individually) to do FFT analysis.
4. FFT Analysis (X and Y Coordinates):

- It takes the time and X coordinate information out of the Data Frame for the X coordinate analysis.
- Assuming uniform time intervals, it computes the time step.
- FFT is applied to the X coordinate data in order to extract the frequency and amplitude data.
- Plots the frequency vs. amplitude findings from the FFT and finds the frequency peak.

5. Similar Analysis for Y Coordinates:
    - The process is repeated and the same FFT analysis process for the Y coordinate data which finds frequency peaks for Y direction.

The code has few assumptions such as:

- The video is clear and it has consistent footage of a flickering flame.
- Through contour analysis the flame tip can be accurately determined.
- Uniform time interval between frames for FFT analysis.

Another important parameter to study the behaviors of flame is the analysis of sound produced for various reasons in the combustor. The sound is recorded through microphone and then the recorded sound has been analyzed by first Fourier transformation. To perform fft Kaggle notebook has been used to run the code. The code is written in python. The algorithm of the fft code is as follows

1. Load Audio File:
    - soundfile library is used to read the audio file specified as path.
    - Then it Checks if the audio is stereo and, if the audio file is stereo then keep only one channel (left channel).

2. Perform FFT:
    - uses the Fast Fourier Transform (fft from scipy.fft) to calculate the frequencies and amplitudes.
    - creates a Data Frame (df) with the associated amplitude values and frequency (Hz).
    - saves this Data Frame as "frequency_vs_amplitude.xls," an Excel file.
3. Plot FFT:
    - Positive frequencies are plotted against equivalent amplitudes in the FFT data.
    - sets the x-axis limit to 20 kHz, shows the grid, and configures the title and axes labels.

The different flames behaviours have been studied through different equivalence ratios all the way from equivalence ratio of 2 to lean blowout limit. The equivalence ratios have been studied over three air volume flow rate 8lpm,10lpm and 12lpm. Also, for a particular air flow rate there are three cases for three diameters of ducts (higher, medium and lower) as well as for the burner without any duct. The ducts have been represented as big/higher duct for 24.8mm diameter duct, for 21.4mm duct as medium duct and for 18mm duct lower/small duct.

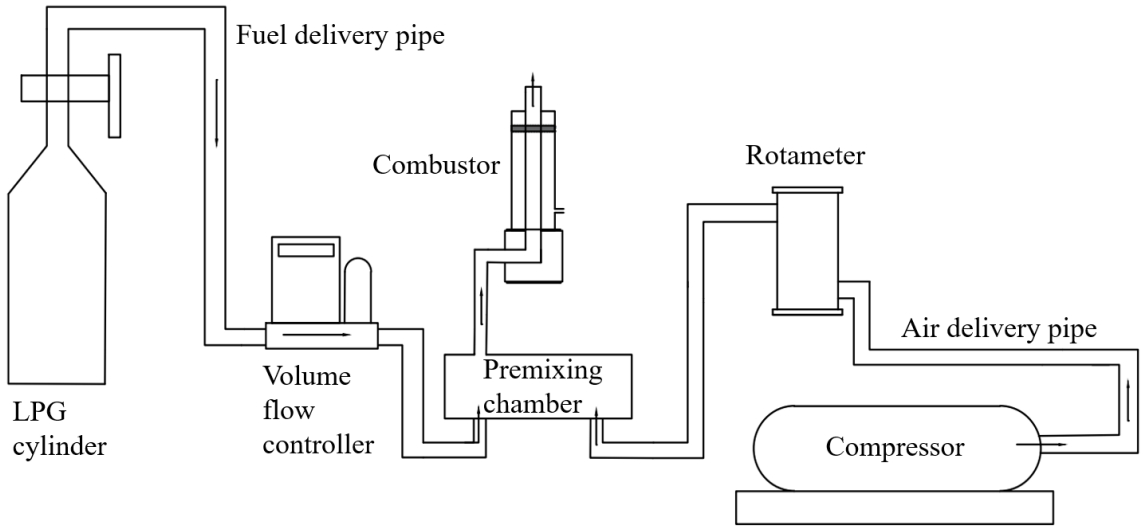

Figure 17:Schematic diagram of experimental setup

Table 2: Experimental procedure

8 LPM air flow rate	No Duct φ=2-LBO
	Big Duct φ=2-LBO
	Medium Duct φ=2-LBO
	Small Duct φ=2-LBO
10 LPM air flow rate	No Duct φ=2-LBO
	Big Duct φ=2-LBO
	Medium Duct φ=2-LBO
	Small Duct φ=2-LBO
10 LPM air flow rate	No Duct φ=2-LBO
	Big Duct φ=2-LBO
	Medium Duct φ=2-LBO
	Small Duct φ=2-LBO

CHAPTER 4: RESULTS AND DISCUSSION

4.1 Details Of events for 8 lpm air flow rate

As discussed in the experimental method the airflow rate has been kept at a constant value. However, the fuel flow rate is adjusted via volume flow rate controller to obtain the desired equivalence ratios.

For equivalence ratio of 2, all the ducts show the same flame region, this region is named as open flame region. Here the flame is located at the top of the glass duct. The flame is at the top due to high velocity of flow and lower value of flame speed. As the flame speed is lowered compared to the flow velocity therefore the flame cannot propagate inside the duct as the reaction speed between fuel and air is lower than the flow velocity of the premixed air fuel mixture therefore the whole combustion process occurs at the top of the duct.

At the same time, in this region the flame has a visible yellow light present as seen in the photographs and confirmed by the spectroscopic analysis of the flame. This yellow color appears due to incomplete combustion in this region.

At equivalence ratio of 2 and 1.9 open flame region is observed for big duct while for medium duct this region is observed for equivalence ratio of 2,1.9 and 1.8.

Finally, for small duct the upper flame region can be seen for equivalence ratios up to 1.6.

Images of flames in the open flame region for φ=2 for 3 ducts in Fig. 18 and for φ=1.8 when big duct shows FREI and other 2 ducts show open flame is given in Fig. 19.

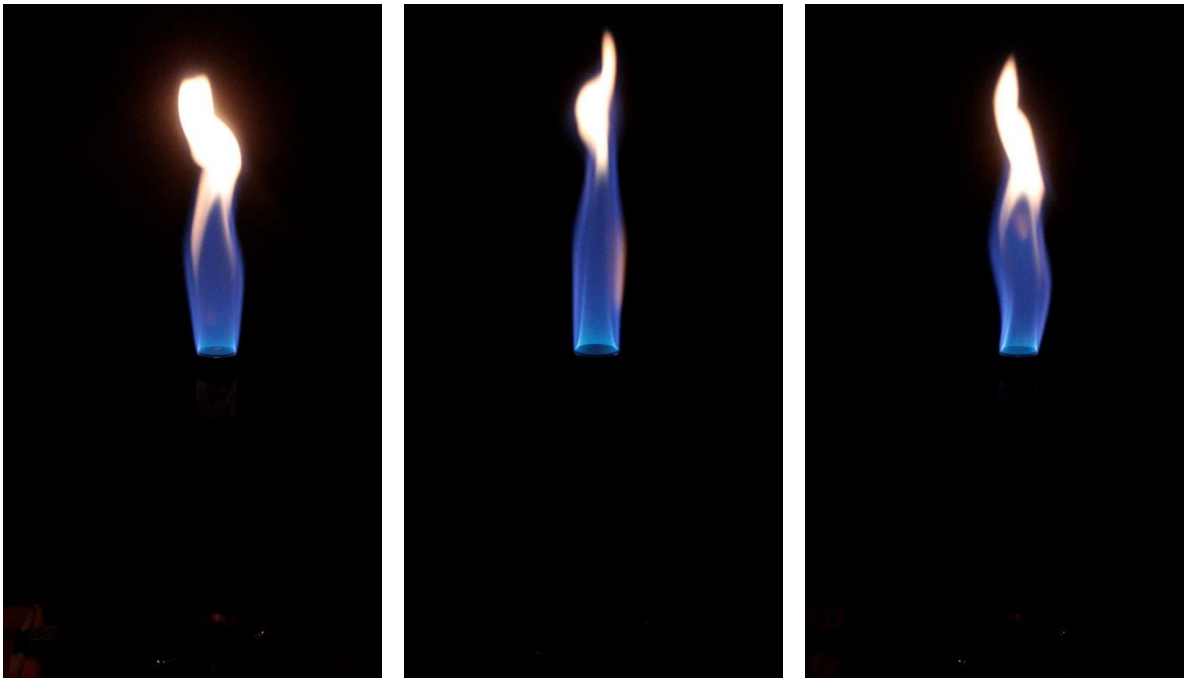

a. Big duct *b. Medium duct* *c. Small duct*

Figure 18: Flame images for equivalence ratio of 2.0 for duct of different diameters

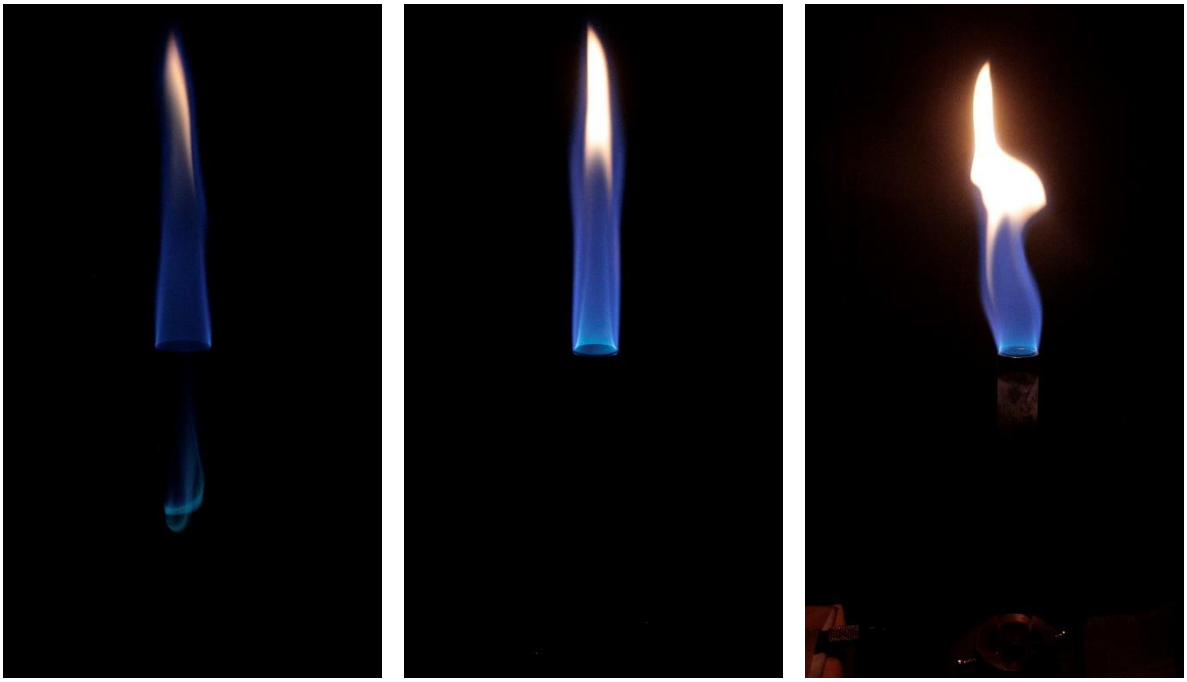

a. Big duct *b. Medium duct* *c. small duct*

Figure 19: Flame images for equivalence ratio of 1.8 for duct of different diameter

Now, the fuel flow rate is further reduced to obtain lower equivalence ratios. Therefore, the flame speed increases that means the reaction speed between air and fuel also increases which causes the flame to propagate inside the ducts. This phenomenon causes the shift in flame zone or flame dynamics and the flame reaches a new zone named flame repetitive extinction and ignition or FREI.

Here the flames show the extinction and ignition periodically. Therefore, the position of the flame changes with change in time at the same flow condition and same equivalence ratio. The frequency of FREI flame also changes with change in equivalence ratio as well as the change in diameter of the glass duct attached with the combustor.

The flame repetitive extinction and ignition is observed at equivalence ratios 1.8,1.7,1.6,1.5 for big duct. However, for medium duct the flame repetitive extinction and ignition zone is found out at equivalence ratios of 1.7,1.6,1.5. The small duct showed the FREI zone at equivalence ratio 1.5.

Here, the reason behind the FREI zone starting to appear at relatively lower equivalence ratios for medium duct and further lower equivalence ratio for small duct is the difference between the flow rate of the duct (Fig. 20). With decreasing value of inner diameter of the duct the cross-sectional area also decreases which results the flow velocity to increase as the total flow rate has been kept constant for the all three different ducts. Therefore, the though the flame speed increases with lowering equivalence ratios such as 1.7 or 1.6 but still it is not enough strong to counter the relatively higher flow velocity of the small duct. Due to this reason the FREI zone occurs at relatively lower equivalence ratios for ducts with relatively lesser diameter.

Flame images for 1.5 equivalence ratio is given in Fig. 21 for visualizing the flame behaviours in different ducts.

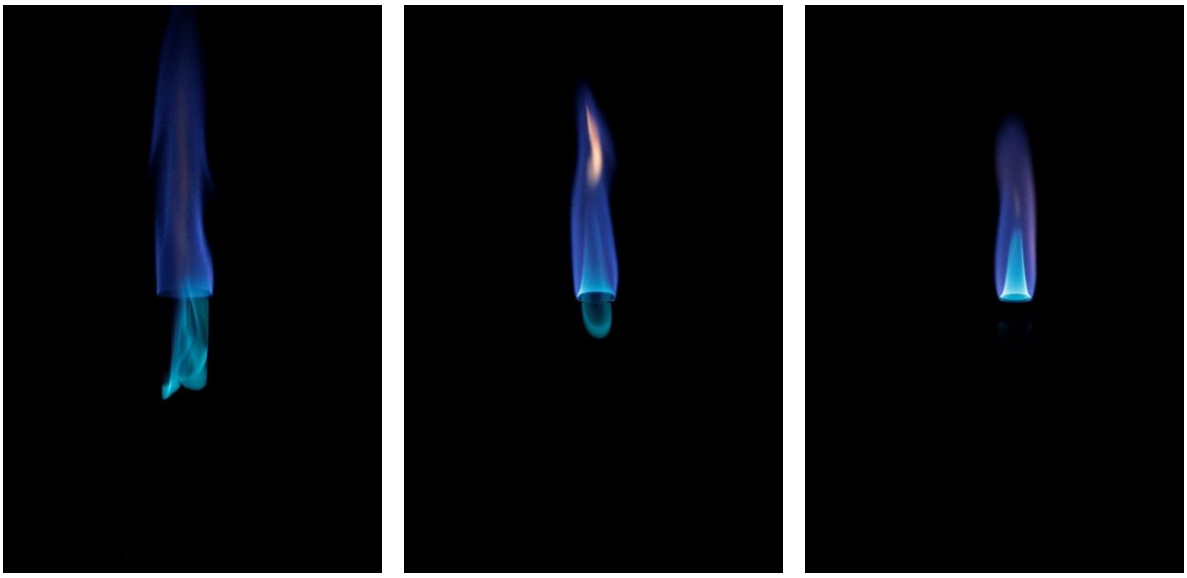

a. Big duct *b. Medium duct* *c. Small duct*

Figure 20: Flame images for equivalence ratio of 1.6 for duct of different diameters

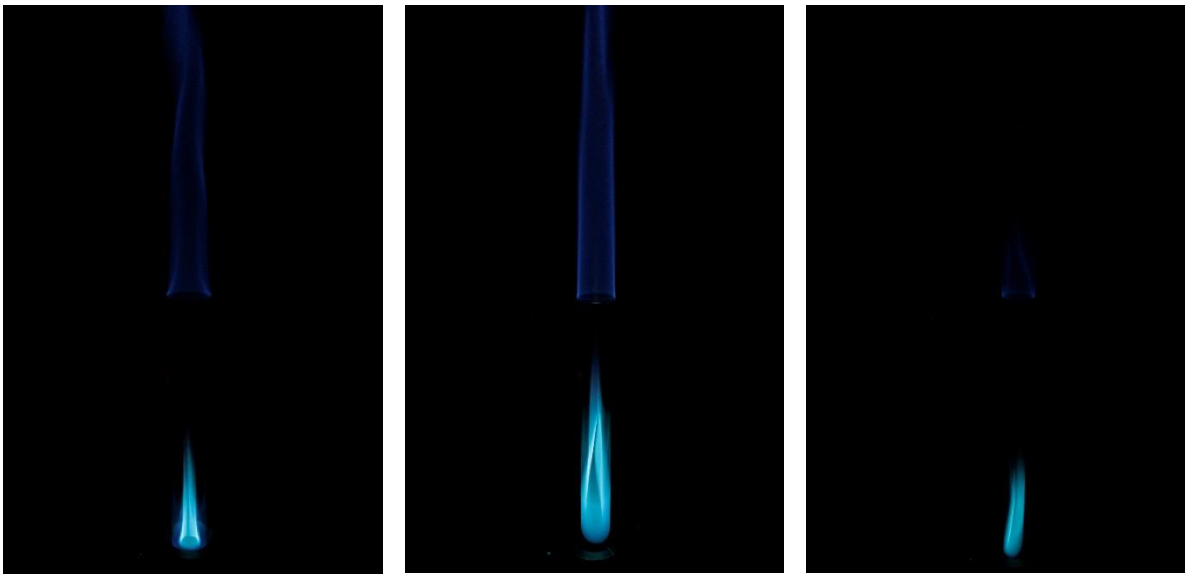

a. Big duct *b. Medium duct* *c. Small duct*

Figure 21: - Flame images for equivalence ratio of 1.5 for duct of different diameters

In this zone for the equivalence ratio 1.5 the upper flame intensity gets reduced compared to other higher frequency.

When the equivalence ratio is further lowered to 1.4 flame speed increases further. Therefore, the flame speed started to become the dominating factor in comparison with the flow velocity. Therefore, for equivalence ratio 1.4 a stable flame zone is observed. The stable flame obtained can be clearly seen from the Fig. 22.

Here the flame has propagated to the base of the duct. However, as the flame speed is not very high compared to the flow velocity and operation zone is still in the rich side of stoichiometric ratio therefore a volume of unburnt mixture escape combustion inside the duct. This unburnt mixture burnt at the top of the duct. Therefore, this flame zone is named as open + duct(stable) flame zone.

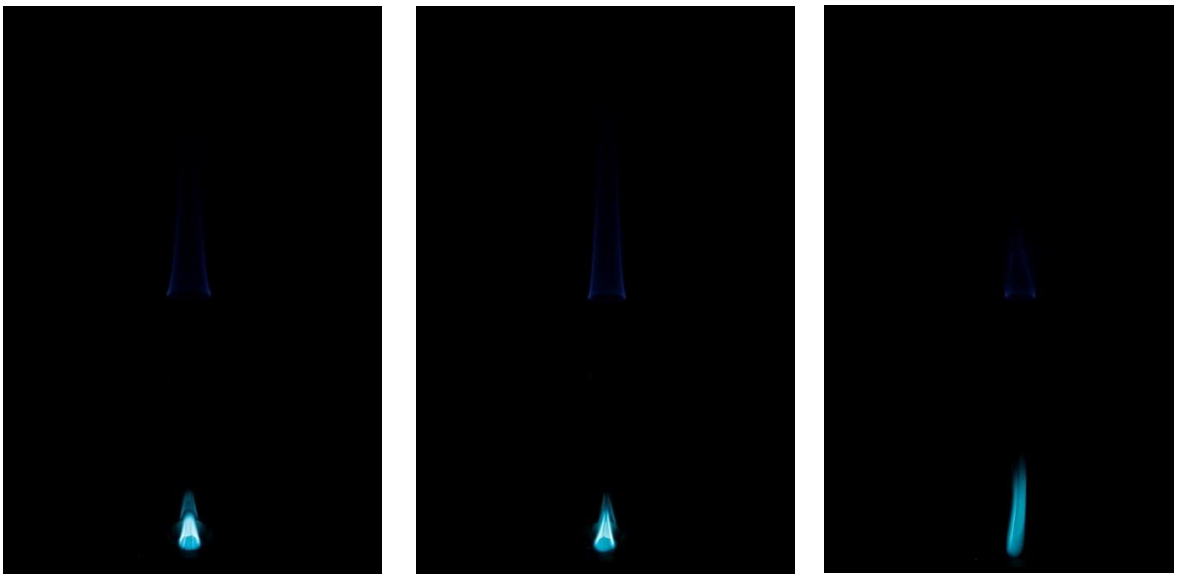

a. Big duct *b. Medium duct* *c. Small duct*

Figure 22: Flame images for equivalence ratio of 1.4 for duct of different diameters

In this zone while the flame stabilizes and the lower flame intensity becomes greater than it was there throughout FREI zone. This is due to the domination of flame speed over flow velocity.

When the equivalence ratio is further lowered then the flame speed value becomes bigger. For this zone the flame speed becomes much more dominating compared to the flow velocity. Therefore, the flame propagates further downstream. Due to which flashback phenomenon is observed here. This zone is named as flashback zone.

At the same time thermo acoustic instability can be observed in this flashback zone. The characteristics of the sound created in this flashback zone can be used to predict the instability zone and necessary steps needs to be taken to obtain a stable combustion for a real-life portable power device made of micro combustor. The flashback zone is observed at the equivalence ratios of 1.3, 1.2, 1.1, 1, 0.9, 0.85 and 0.83 for the big duct. While for medium duct the flashback zone is seen from equivalence ratio of 1.2, 1.1, 1, 0.9, 0.85, 0.83 and 0.8. Although, the flame speed is high for equivalence ratio of 1.3 but due to its lesser inner diameter the medium duct does not show the flashback phenomenon at equivalence ratio 1.3(Fig. 23).
For the small duct however, a different zone can be observed at equivalence ratio 1.3. Here the inner flame at the bottom of the duct spins with time and the upper flame can be observed as lifted off. And the flashback zone is from 1.2 to 0.83 equivalence ratio.

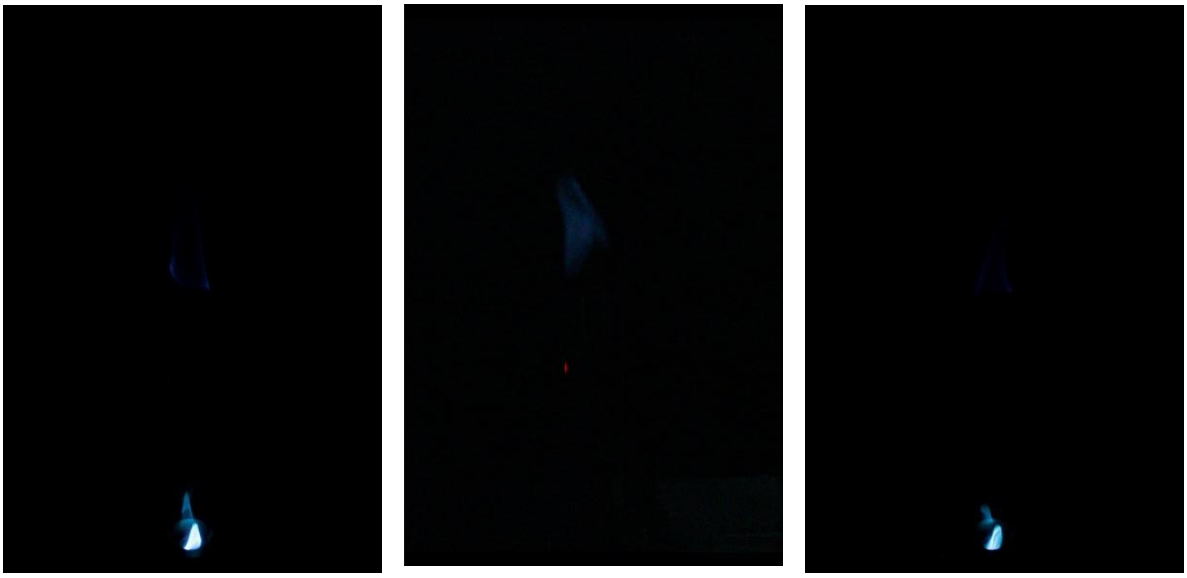

a. Big duct b. Medium duct c. Small duct

Figure 23: Flame images for equivalence ratio of 1.3 for duct of different diameters just before starting of flashback zone

In the transition phase from the stable open + duct stable flame zone to flashback zone is occurring through the through spinning flame. In the transition phase due to thermal wall coupling spinning phenomenon for flames is observed. In the transition phase the upper flame is lifted off position. The position change of flame font in spinning manner occurs. In the Fig. different frames of spinning flame has been given with time to show the behavior of flame font with time.

The spinning flame images are given in Fig. 24 to visualize the different position of the flame with time when the flame moves in spinning way. The spin direction can be clockwise and anticlockwise here the observed direction is clockwise spin.

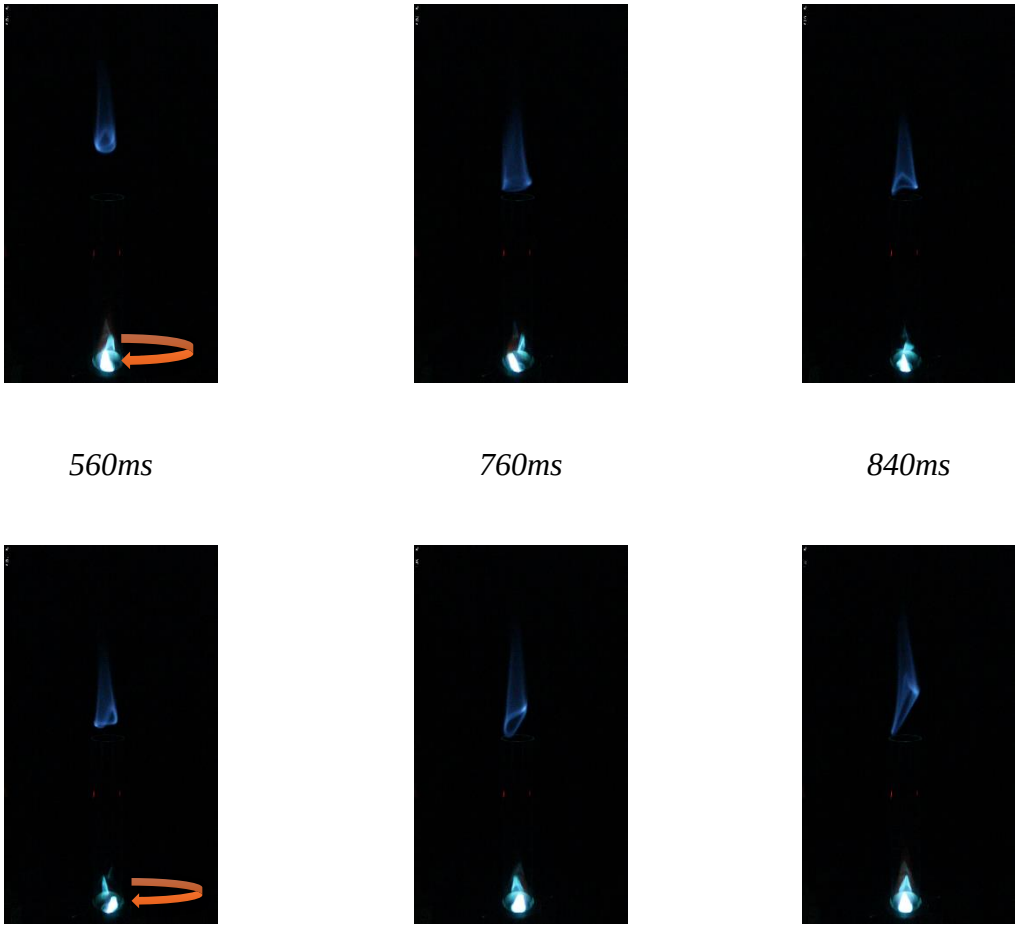

Figure 24: Spinning flame visualization with time for transition zone between the shift from open + duct stable flame zone to flashback zone

When the operating zone reaches equivalence ratio of 0.8 or lower here with the air fuel mixture being in the lean side of stoichiometric ratio the flame speed decreases with decreasing value of equivalence ratio. Here again the flame speed and flow velocity balances each other and a stable blue flame is observed at the bottom of duct. This zone is named as duct flame zone (Fig. 25). When the displacement of the flame tip is obtained from the video of flame, the position of the tip always remains almost constant. which means lower flicker and the lower flicker means more stable flame and combustion which can be used for a real-life power source device

made with micro or meso combustor. In a sense this zone can be used for safe zone of operation for stable combustion however further studies are required to investigate the efficiency in this zone as well as to determine emission characteristics of flames in this zone.

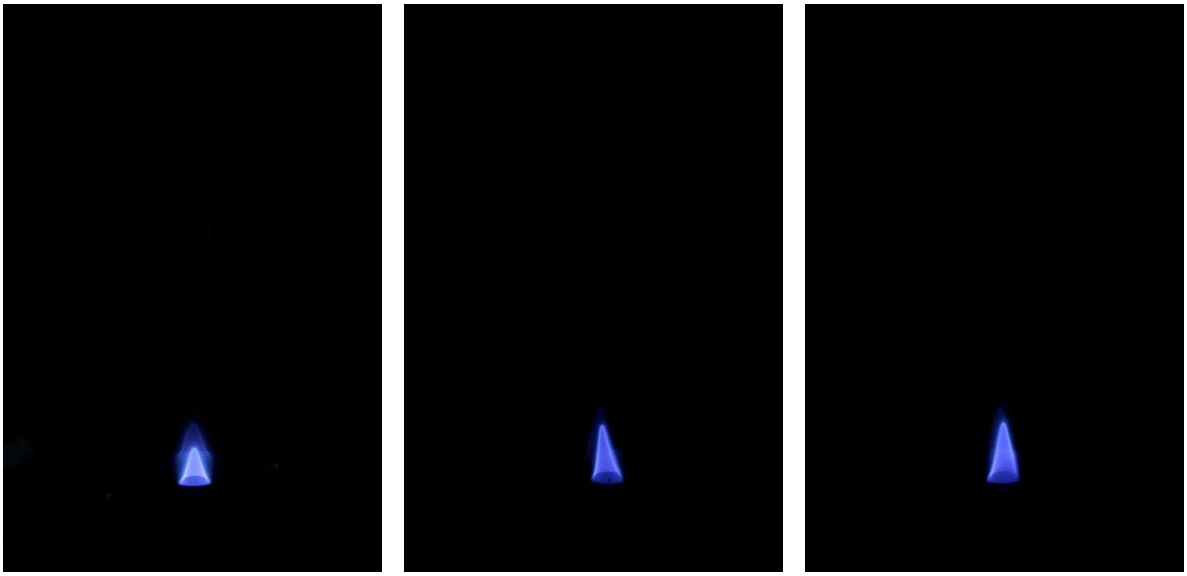

a. Big duct *b. Medium duct* *c. Small duct*

Figure 25: Flame images for equivalence ratio of 0.8 for duct of different diameters just before starting of flashback zone

Stable duct flame is observed from equivalence ratio of 0.8 to 0.68 for big duct, from 0.83 to 0.75 for medium duct and for small duct stable duct flame is seen only for equivalence ratio of 0.8.

Fig. 26 shows flame behaviors for three ducts for 0.75 equivalence ratio and the Fig. 27 shows flame behaviors for 0.80 equivalence ratio.

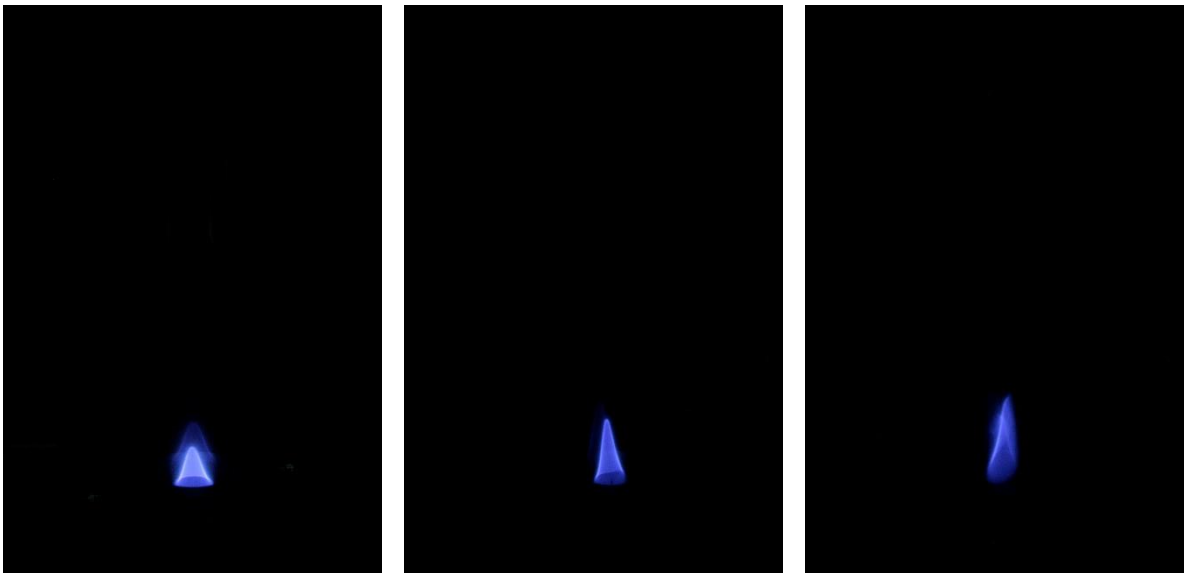

a. Big duct *b. Medium duct* *c. Small duct*

Figure 26: Flame images for equivalence ratio of 0.75 for duct of different diameters just before starting of flashback zone

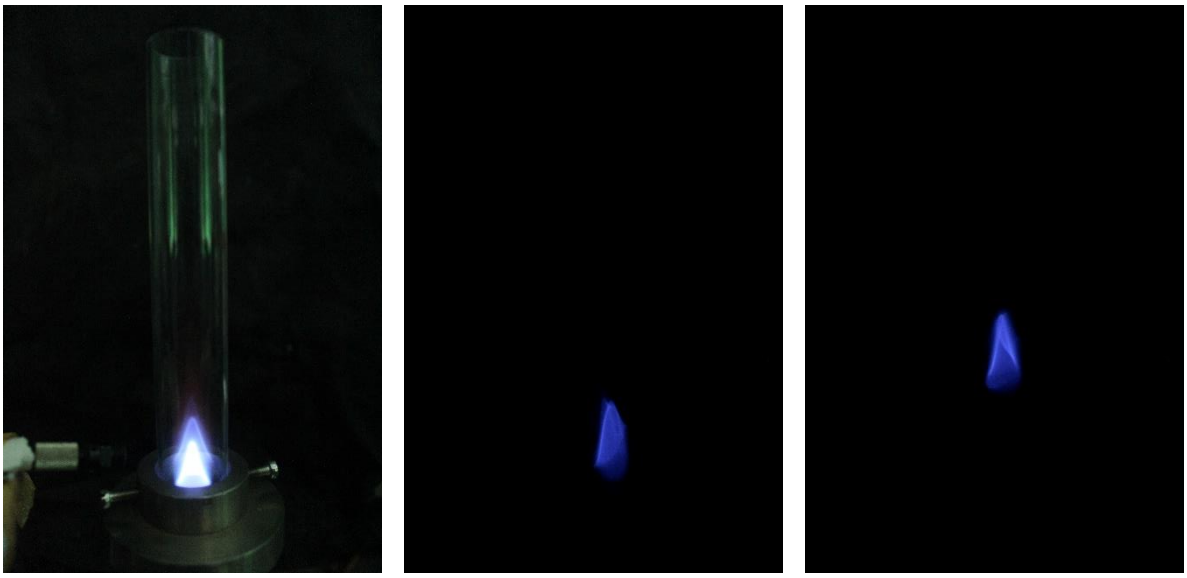

a. Big duct b. Medium duct c. Small duct

Figure 27: Flame images for equivalence ratio of 0.70 for duct of different diameters just before starting of flashback zone

From the above figure it is clear that here the flame for the duct with biggest diameter is duct flame while for the smallest diameter duct the oscillating flame has already started. At the same time the duct with medium value of diameter has just started to show oscillating flame region.

However, when the equivalence ratio is lowered further the flame speed is further reduced. But the flow velocity is not reduced that much compared to flame speed as the air supply is being kept constant. therefore, flow velocity of air fuel mixture become dominating factor compared to the flame speed. So, the flow velocity tries to push the flame which was located at the bottom of the duct upstream towards the top of the duct. This phenomenon give rise to another flame zone that is called the dancing flame zone. Here the flame dances with time inside the duct due to the reason explained above. Upon further lowering the equivalence ratio the dancing frequency increases as well as the chaos in the dancing pattern can also be observed to have increased. Eventually the flame will reach blowout point upon reducing the equivalence ratio further.

Oscillating flame for big duct is observed for equivalence ratio 0.68 to 0.60 and blowout occurs at 0.58 equivalence ratio. For medium duct dancing flame occurs from 0.70 to 0.64 and blowout equivalence ratio is 0.62. From the Fig. 28 it is observed that the big and medium ducts showing oscillating flame while for the small duct blowout already occurred. For small duct the oscillating flame zone is from equivalence ratio of 0.77 to 0.68 before eventually blowing out at 0.66. However, when no duct is used the blowout limit for the combustor is at equivalence ratio of 0.70.

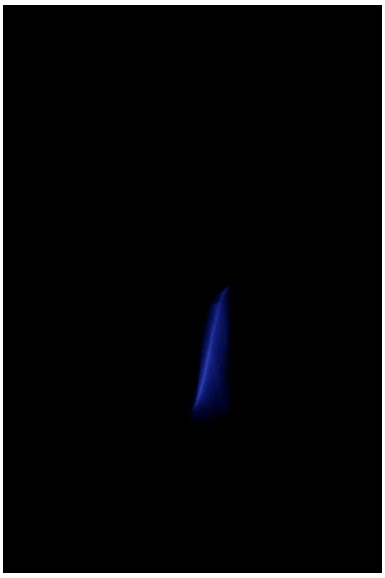

Already blowout occurred

a. Big duct b. Medium duct c. Small duct

Figure 28: Flame images for equivalence ratio of 0.64 for duct of different diameters just before starting of flashback zone

This above figure shows the flames for equivalence ratio 0.64 which is just above the blowout zone for medium duct. From the image one can get an idea about the increase in the chaos in the dancing pattern of flame just before blowout.

The blowout point is slightly higher with the decreasing inner diameter of the duct. This is due to the higher flow speed for same flow rate at ducts with lesser inner diameter. Also due to lower inner diameter the heat loss in the duct wall is higher which also causes the flame to blowout at higher equivalence ratio for small duct compared to the other two ducts. The comparison for blowout if in Fig. 29 for each case.

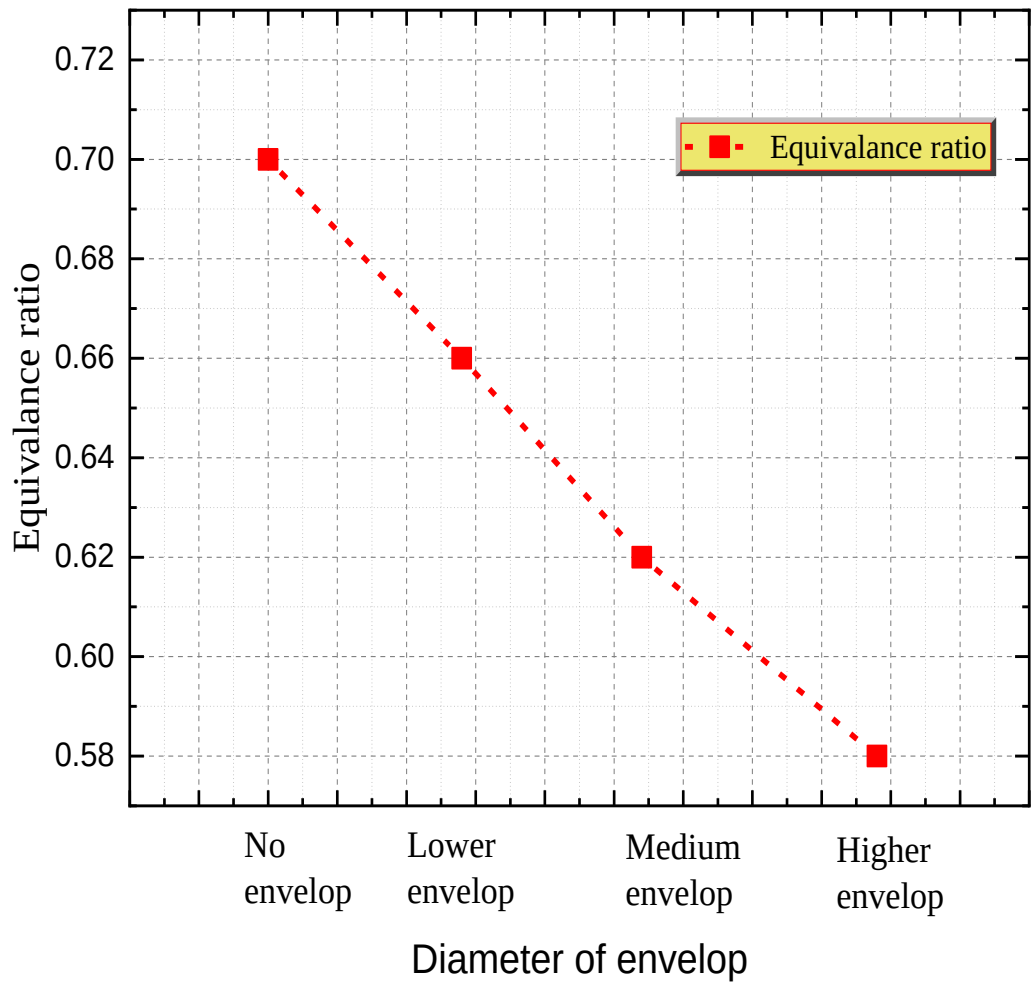

Figure 29: Equivalence ratio for blowout comparison for different inner diameters of duct attached to the combustor.

The comparison of flow velocity and flame speed which creates different flame regime for different equivalence ratio is given in the Fig. 30. From the graph it can be seen during the flashback zone the flame velocity is higher compared to flow velocity and when the flame speed decreases then the start of duct flame happed. Also when flame speed reduced further therefore the blowout occurred.

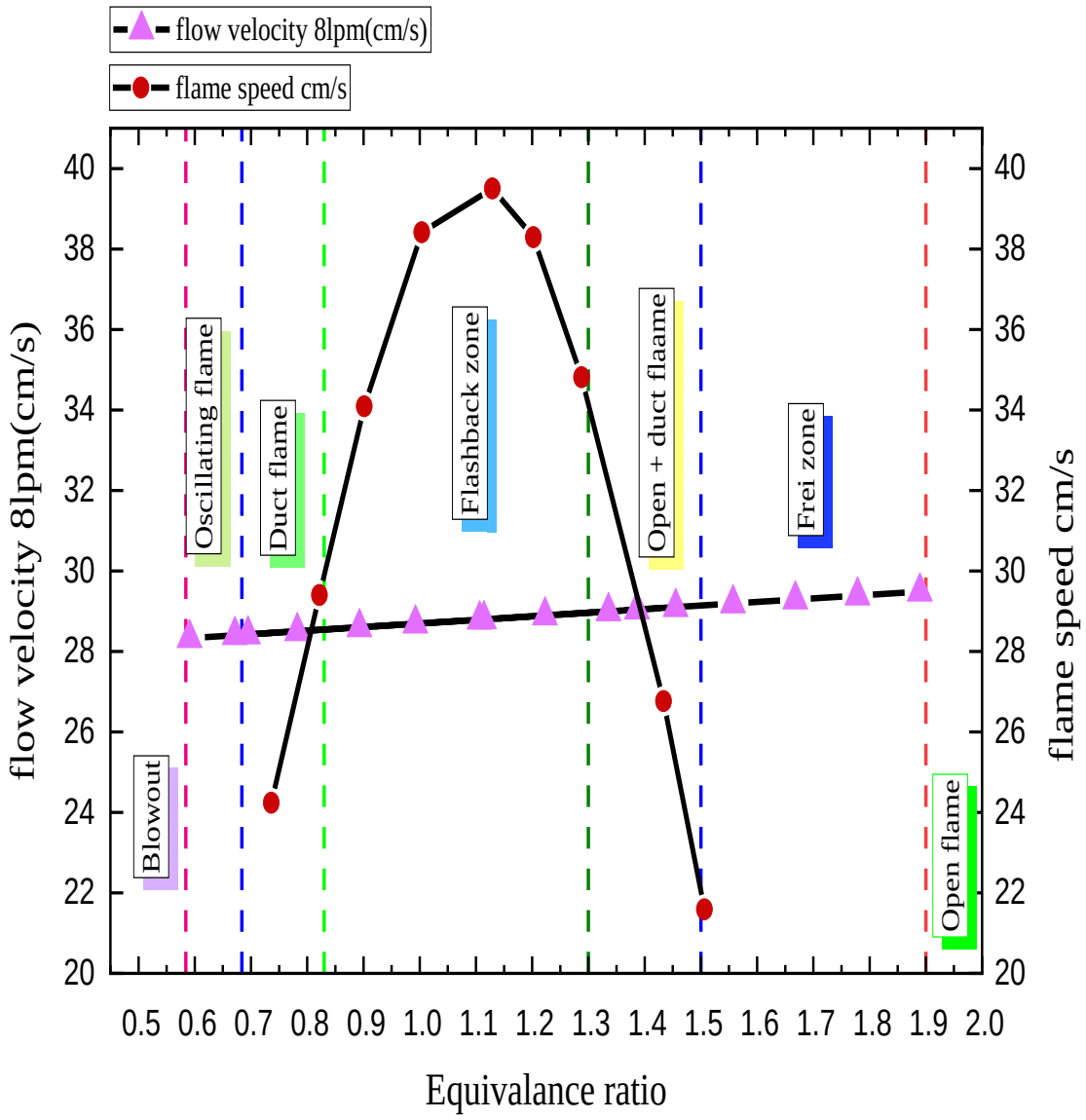

Figure : 30 Flame speed and flow velocity of LPG air mixture changing with equivalence ratio for 8 LPM

4.2 Details of happenings for 10LPM air flow rate

The experiment is conducted at a constant air flow. However, the fuel flow rate is being changed. Through this the equivalence ratio is being controlled. Although the exact total flow rate is not constant due to variation in fuel flow rate. But the change is very low compared to total flow rate.

3 different diameters of glass tubes have been attached with the combustor to study about the flame dynamics of mini combustor flame varying with different diameters of glass and also the comparison with flame of the combustor without any glass tube.

The experiment has been carried over for 3 different air flow rates i.e., 8LPM, 10LPM, 12LPM.

The Reynold's no for the different flow rates air given in the Fig. 31.

The experiment has been conducted over various equivalence ratio i.e., 2 – lean blowout limit which occurs from (Φ=0.8 to Φ=0.6 generally).

Here are the observations found out during the experimental process for fixed air flow rate 10LPM.

1.At Φ=2(Fig. 32) the flame present on the top of the glass duct. this is due to the interplay between the flame velocity and air fuel mixture flow speed. Due to the high velocity of air fuel mixture compared to the flame velocity the flame is constructed over the top of the duct. This flame region is called as open flame region. Due to high flow velocity of air fuel mixture and lower flame speed the flame can't be constructed inside the duct rather it constructs outside of it in open area. Therefore, this flame region named as open flame region.

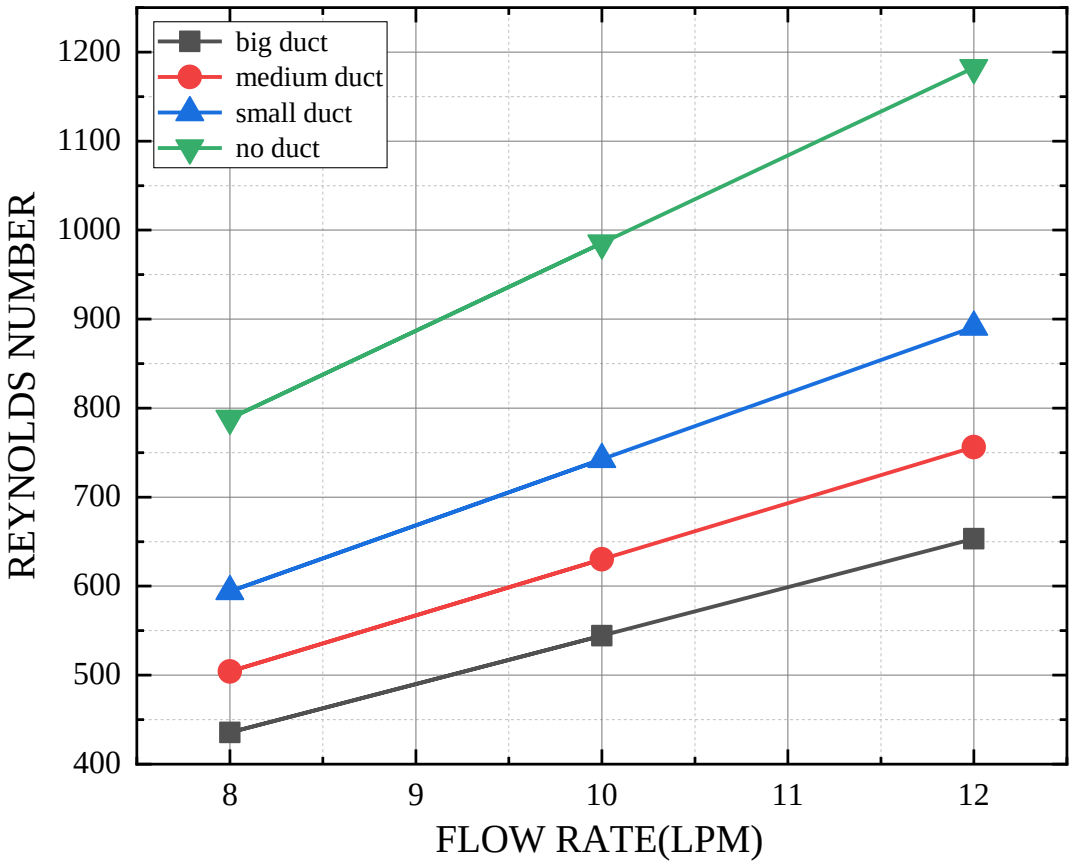

Figure 31: Reynold's number variation for different flow rates with change in duct diameter

a. Big duct b. Medium duct c. Small duct

Figure 32: Flame images for equivalence ratio of 2.0 for duct of different diameters

2.For Φ=1.9 the open flame region is present in the lower and medium ducts. But for the big duct the flame starts to propagate inside of the duct. Therefore, the flame in the big duct has started to showcase FREI flame domain(Fig. 33). As the air fuel mixture flow velocity is lower in the big duct due to the higher area inside the duct for flow therefore when the flame speed increases for the φ=1.9 therefore the big duct shows FREI region at higher equivalence ratio then the medium or small envelop.

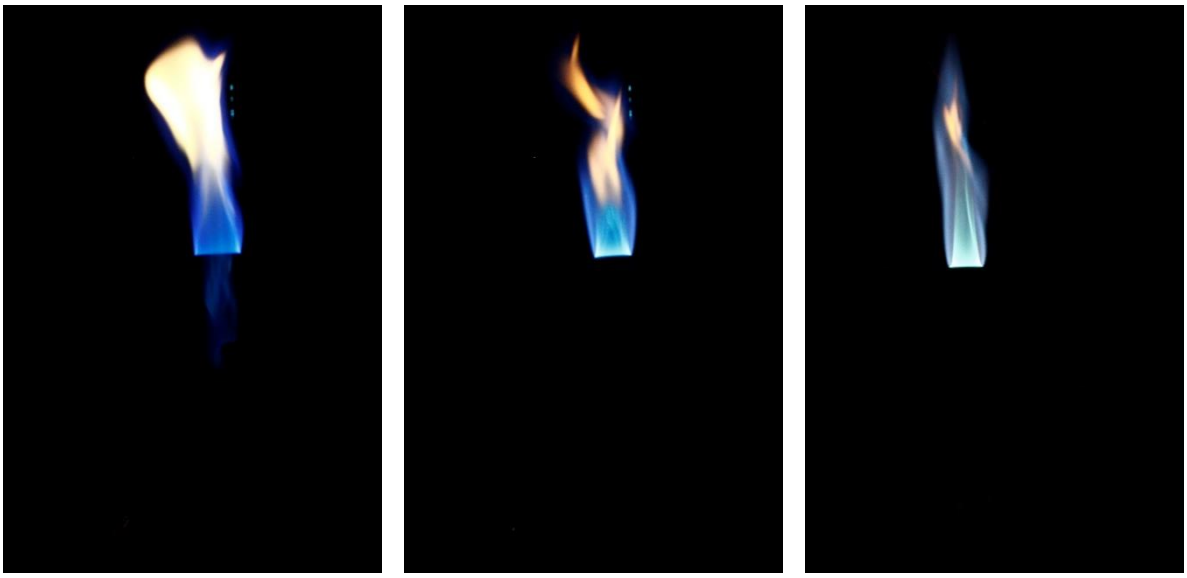

a. Big duct b. Medium duct c. Small duct

Figure 33: Flame images for equivalence ratio of 1.9 for duct of different diameters

3.When the equivalence ratio is further lower to 1.8 ,1.7 the medium as well as the big duct also starts to show the FREI flame region (Fig. 34). This phenomenon of FREI flame shift from open flame domain is due to the interaction between velocity of flow and flame velocity. For the big duct as the diameter of the duct is greater therefore the air fuel mixture velocity or flow velocity will be lesser than the duct with lesser diameter as discharge $Q = A \times v$

- Where A is inside area of the duct
- v is the air fuel mixture velocity.

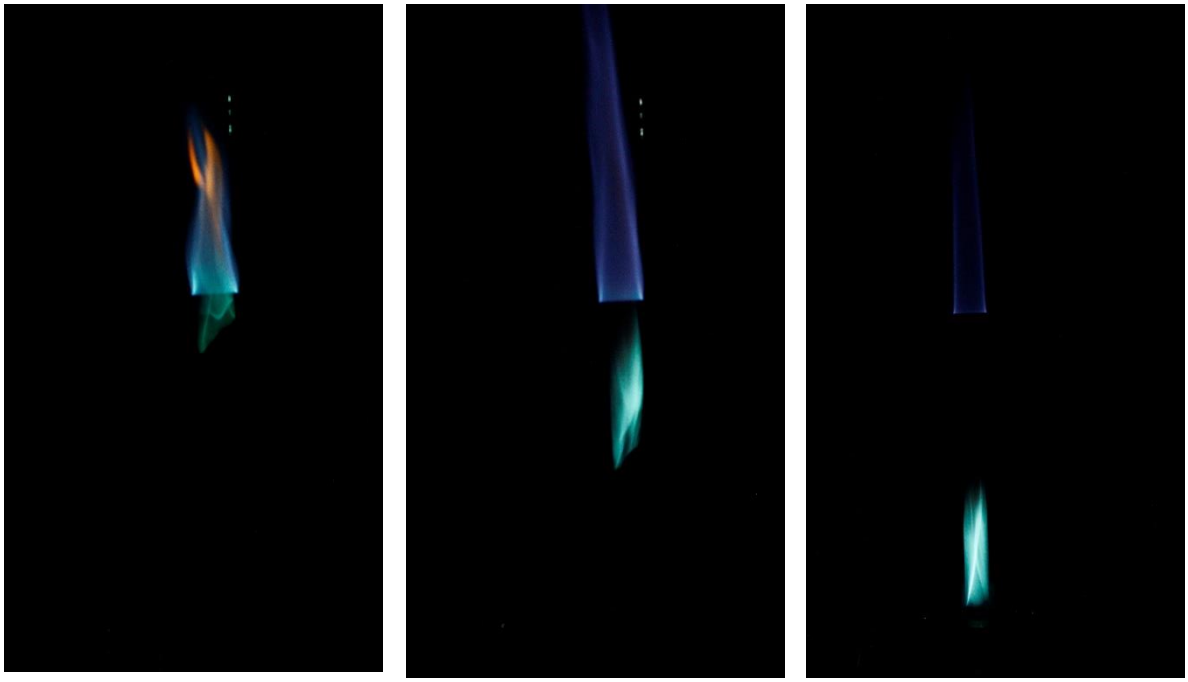

a. Big duct b. Medium duct c. Small duct

Figure 34: Flame images for equivalence ratio of 1.7 for duct of different diameters

4. For equivalence ratio of 1.6 (Fig. 35) the FREI flames in all the ducts tends to stabilize but the flame is not stable yet. For Φ=1.5 the flames of all the three ducts are stable and both upper and lower flames are present. Therefore, the flame goes from FREI flame region to the open + duct flame region which is shown in Fig. 36. While equivalence ratio shifts from 1.6 to 1.5 the flame speed increases therefore FREI to stabilized open + duct flame shift occurs in this equivalence ratio. Still the reaction speed between the air and fuel is not that fast to burn entire mixture inside the duct therefore the unburnt mixture burns as open flame.

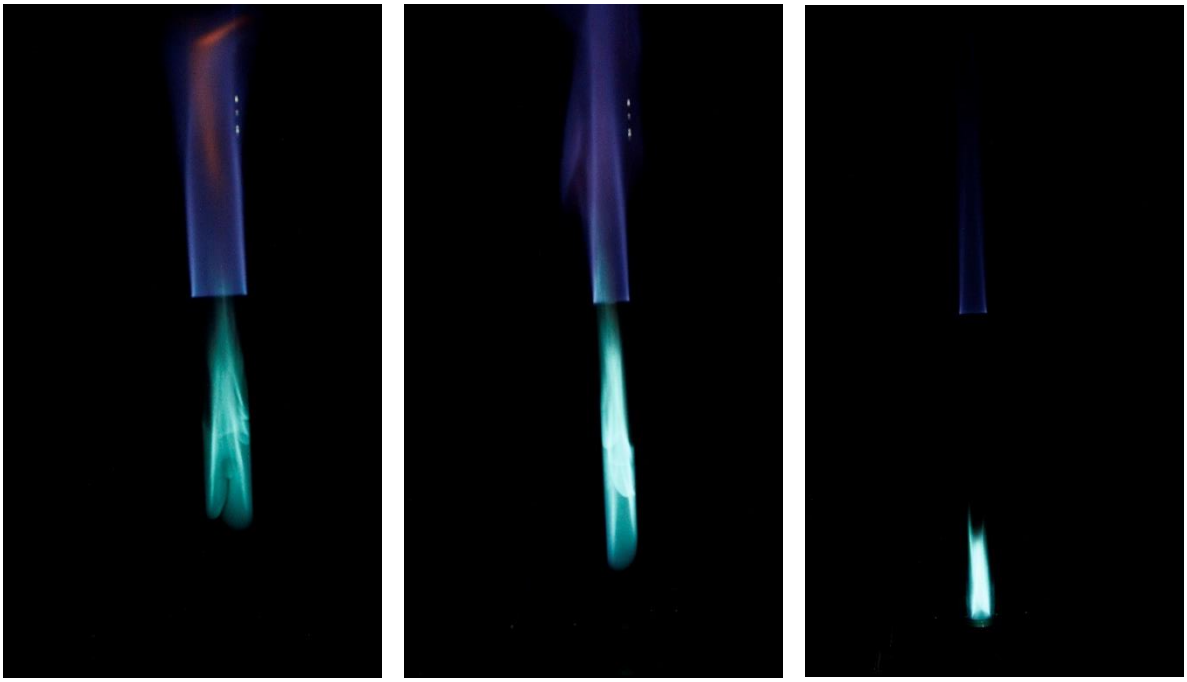

a. Big duct b. Medium duct c. Small duct

Figure35: Flame images for equivalence ratio of 1.6 for duct of different diameters

5. From Φ=1.5, Φ=1.4, Φ=1.3 the flame is in both inside the duct at bottom position (lower flame/inside flame) as well as outside of the duct in the top of the duct. there is also slightly reddish color present in the flames for equivalence ratio 1.4 and 1.3. However, the reddish color intensity is higher in the order of big>medium>small duct(Fig. 37).
6. Not only the redish colour intensity vary with different diameters of the duct but also it varies with the equivalance ratio. There is no redish colour apperaed for Φ=1.5 but then its intensity keeps growing for Φ=1.3 it becomes very prominat compared to Φ=1.4.

   The different flames obtained for equivalence ratio 1.3 are shown in Fig. 37.

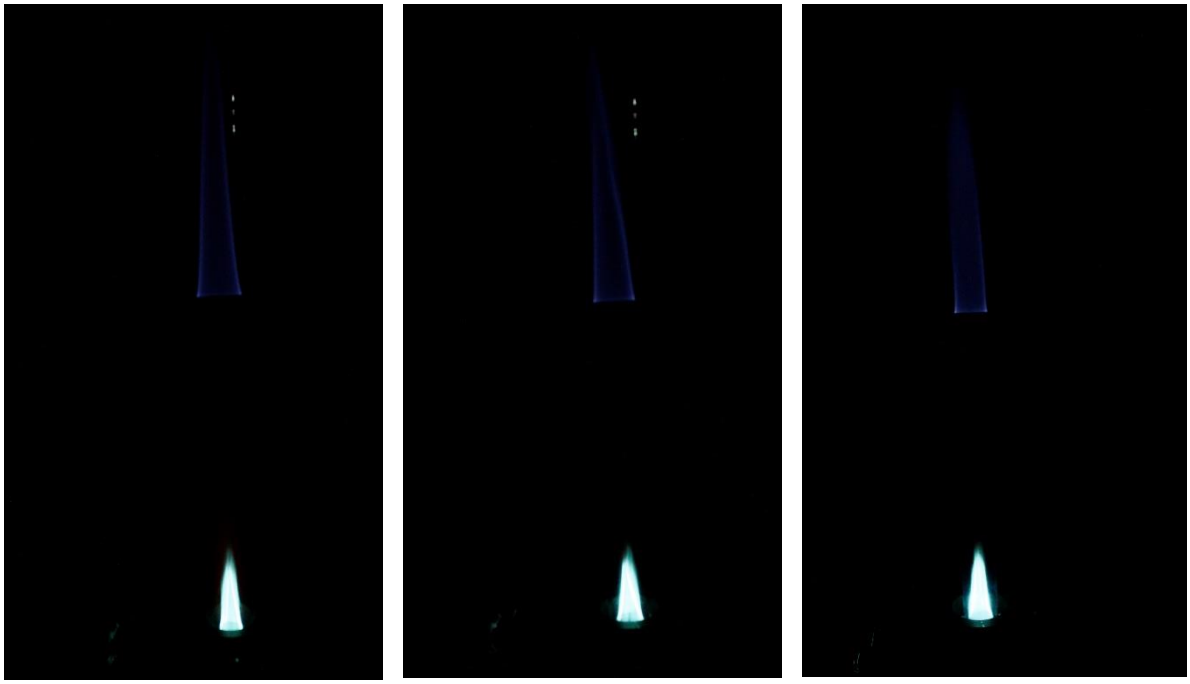

a. Big duct b. Medium duct c. Small duct

Figure 36: Flame images for equivalence ratio of 1.5 for duct of different diameters

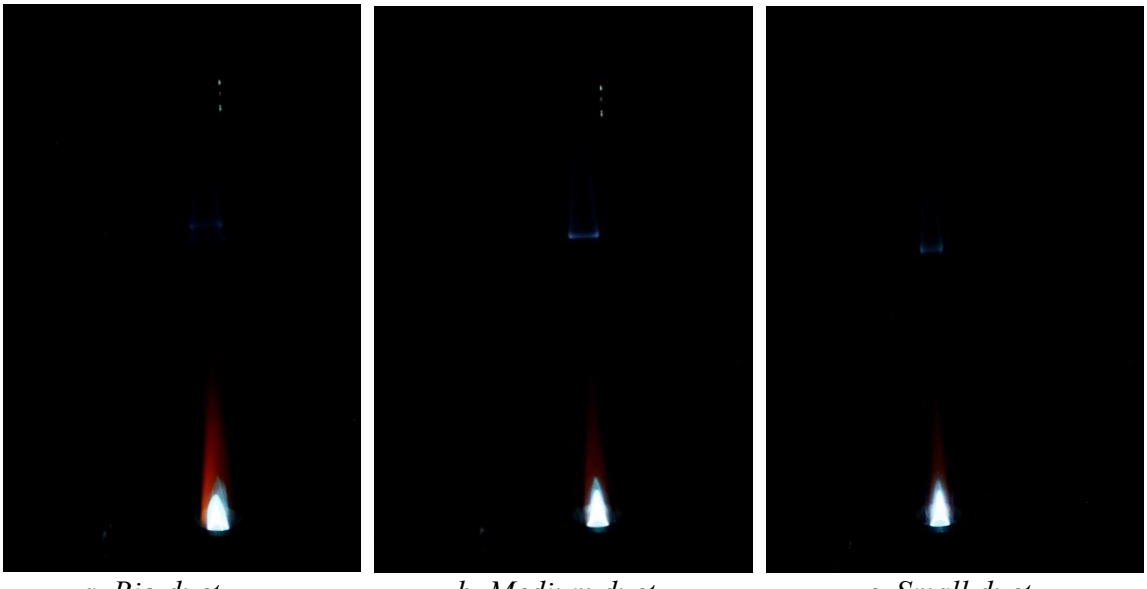

a. Big duct *b. Medium duct* *c. Small duct*

Figure 37: Flame images for equivalence ratio of 1.3 for duct of different diameters

7. From the above iamges it is also clear that with decresing value of equivalance ratio the uppar flame tends to loose its intensity which is visible from the photographs. The uppar flame appeared due to the difference between flame velocity and mixtuere velocity. Uppar flame was mainly the unburnt air fuel mixture that failed to burn inside the duct,therefore it keeps burning in the top of the duct.The uppar flame looses intensity as the mixture velocity decreases with the decreasing equivalance ratio. Therefore ,the unburnut mixture amount gets reduced .

8. Now for Φ=1.2 the flame speed is higher now compared to the mixture velocity therefore at this equivalance ration flashback starts (Fig. 38) inside the combustor the flame becomes weak however the flame top image inside of the combustor can be seen from the isometric view(figure) .

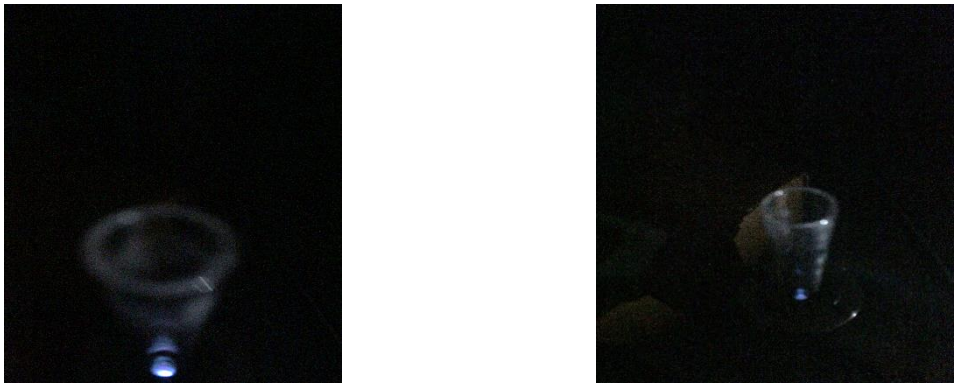

Figure 38: Flashback flame zone

9. This above phenomenon also repeats for Φ=1.1, there is also sound in the combustor due to this flashback phenomenon.

10. For Φ=1.0 ,now the mixtur velocity decreases furthur but also the flame speed decresed . For Φ=1.1 and Φ=1.2 the dominating force was the flame speed as it was higher than that of mixture

velocity but for Φ=1.0 the mixture velocity now the dominating force as the mixture velocity is higher than that of the flame speed. Therefore for Φ=1.0 there is a stable flame inside the duct. This is called duct flame regime(Fig39).

Big duct *Medium duct* *Small duct*

Figure 39: Flame images for equivalence ratio of 1for ducts of different diameters

11. Furthur,when the equivalance ratio is lowered then the stable flame is seen for some time but for Φ=0.8 (small duct) the flame starts to dance or the flame reaches to oscillating flame zone. This is basically blowout region . Dancing of the flame starts for the + first then it appeared for medium and then for higher. The blowout also happen in this order small>medium>big. When no duct is attached then blowout occurs at φ=0.80 which is higher equivalence ratio compared to the when ducts are attached. The duct flame obtained in 0.90 and 0.85 equivalence ratio has been showed in Fig. 40 and Fig. 41. and the flames obtained for different ducts for 0.8 equivalence ratio is shown in Fig. 42.

12. For the big duct the oscillating flame regime starts at φ=0.77 and continues to φ=0.72 and blowout occurs at φ=0.70 while for medium duct the oscillating flame is observed for φ=0.77 to 0.72 and blowout at 0.71 and for the small duct oscillating flame is observed for φ=0.80 to 0.77, at φ=0.75 the blowout occurs.

13. When the dancing stated for Φ=0.8 (small duct) the freequency of the dancing is less but when Φ decreases the the flame becomes more and more unstable therefore incresing in the freequency of the dancing . thereafter, eventually due to lower amount of fuel and more air present in the air fuel mixture the temparature obtained due to the burning of fuel cannot provide adequate heat to burn the incoming fresh mixture therefore blowout occurs.

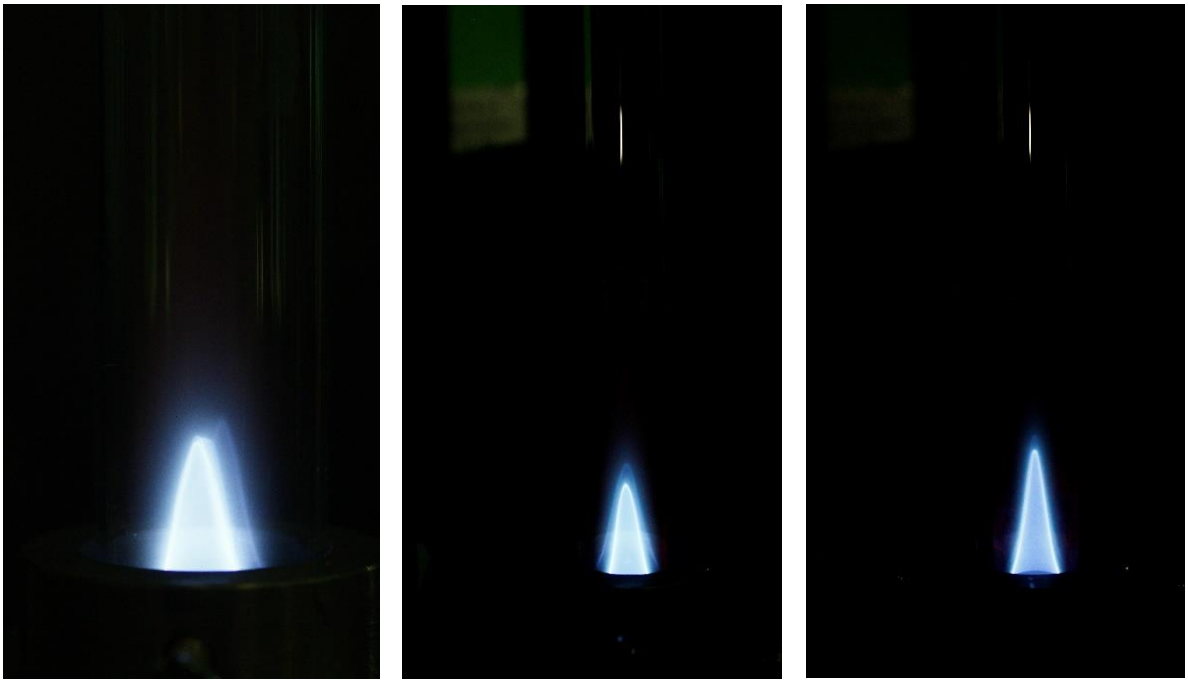

Big duct *Medium duct* *Small duct*

Figure 40: Flame images for equivalence ratio of 0.9 for ducts of different diameters

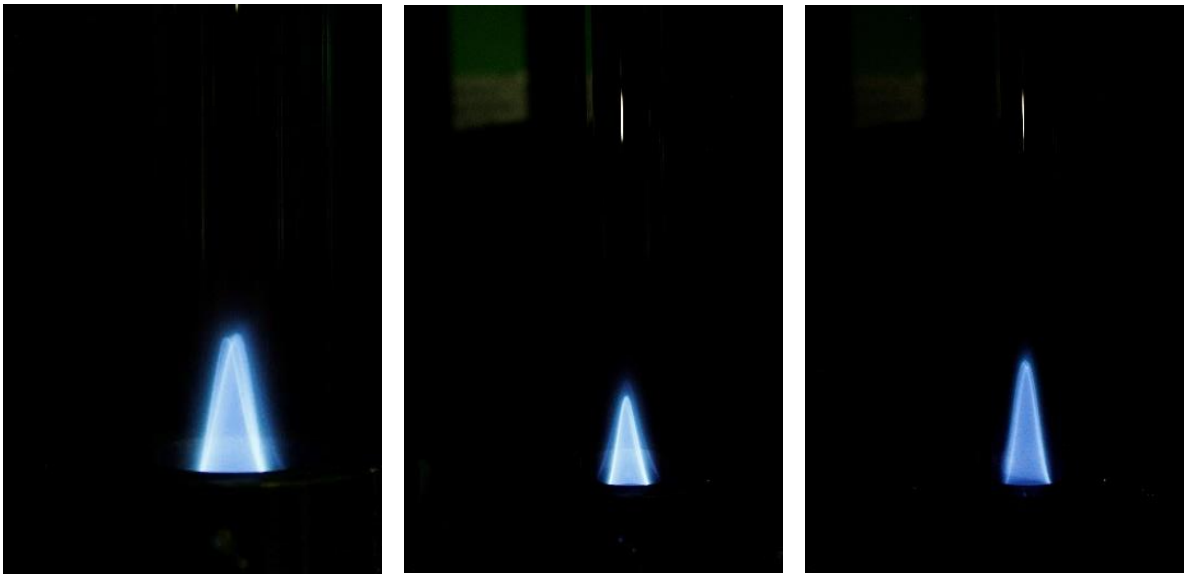

Big duct *Medium duct* *Small duct*

Figure 41: Flame images for equivalence ratio of 0.85 for ducts of different diameters

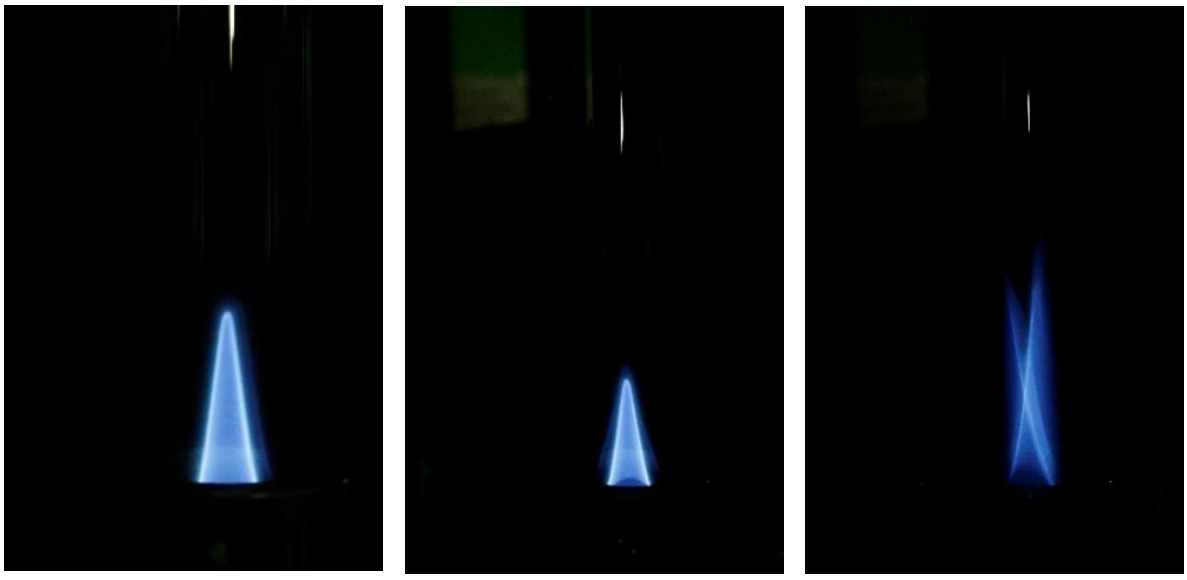

Big duct *Medium duct* *Small duct*

Figure 42: Flame images for equivalence ratio of 0.8 for ducts of different diameters

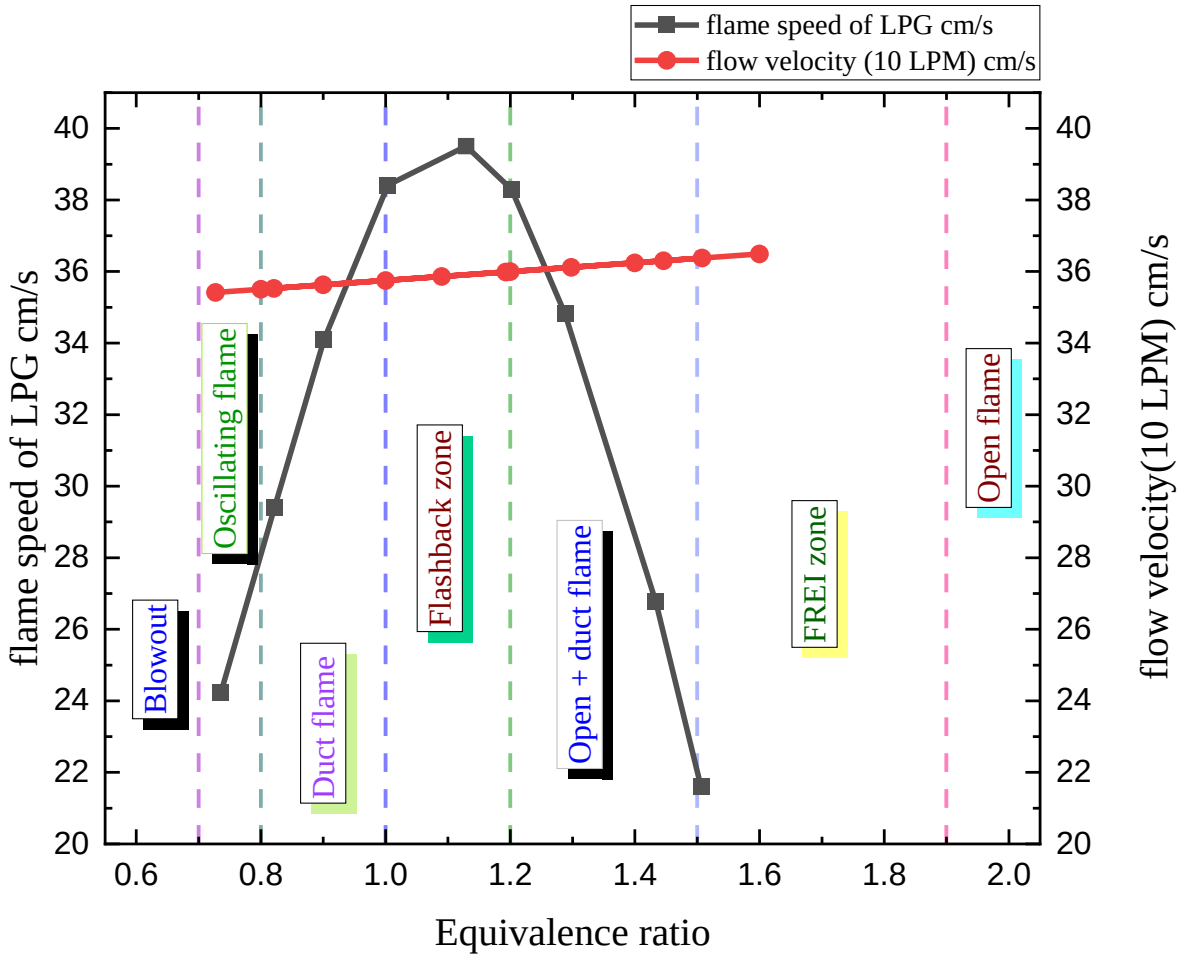

Figure 43: Flame speed and flow velocity comparison with different equivalent ratio graph for 10 LPM air flow rate with different flow zone.

From the above graph Fig. 43 the dominating factor between flame speed and flow velocity at different flame zones can be identified. This can use to predict different flame types possible for a particular equivalence ratio. Here , the flame zones observed at various equivalence ratio has been show in the graph and the difference between the flame speed and equivalence ratio gives an explanation behind the flame dynamics or flame behaviour at a particular equivalance ratio.

4.3 Details of events for 12 LPM air flow rate

When the air flow rate is kept at a constant at 12 LPM flow rate there are also similar types of flame regimes observed as observed for other two constant air flow rate 8 LPM and 12 LPM such as

a. Open flame

b. FREI zone

c. Open + duct flame

d. Duct flame

e. Oscillating flame

f. Blowout

However, in contrast to other two flow rates for 12 LPM constant air flow the flashback zone doesn't occur. This phenomenon is observed for this case due to higher flow velocity compared to other two cases. To put things into context the flow velocity for 12 LPM air flow at equivalence ratio of 1 is about 42.9 cm/s while for 10 LPM and 8 LPM this flow rate velocity is 34.75 cm/s and 28.6 cm/s respectively for the big duct (Fig. 44).

Fig. 44 shows the variation across flow velocity for different flow rates and different equivalence ratio.

For 12 LPM air flow rate the fuel flow rate has been varied to observed the flame dynamics for the mini combustor.

The experiment is started from equivalence ratio of 2. At the equivalence ratio of 2 the flow velocity is very high compared to the flame speed of LPG therefore the high flow velocity in the combustor system tries to push the air fuel mixture upstream but to the lesser flame

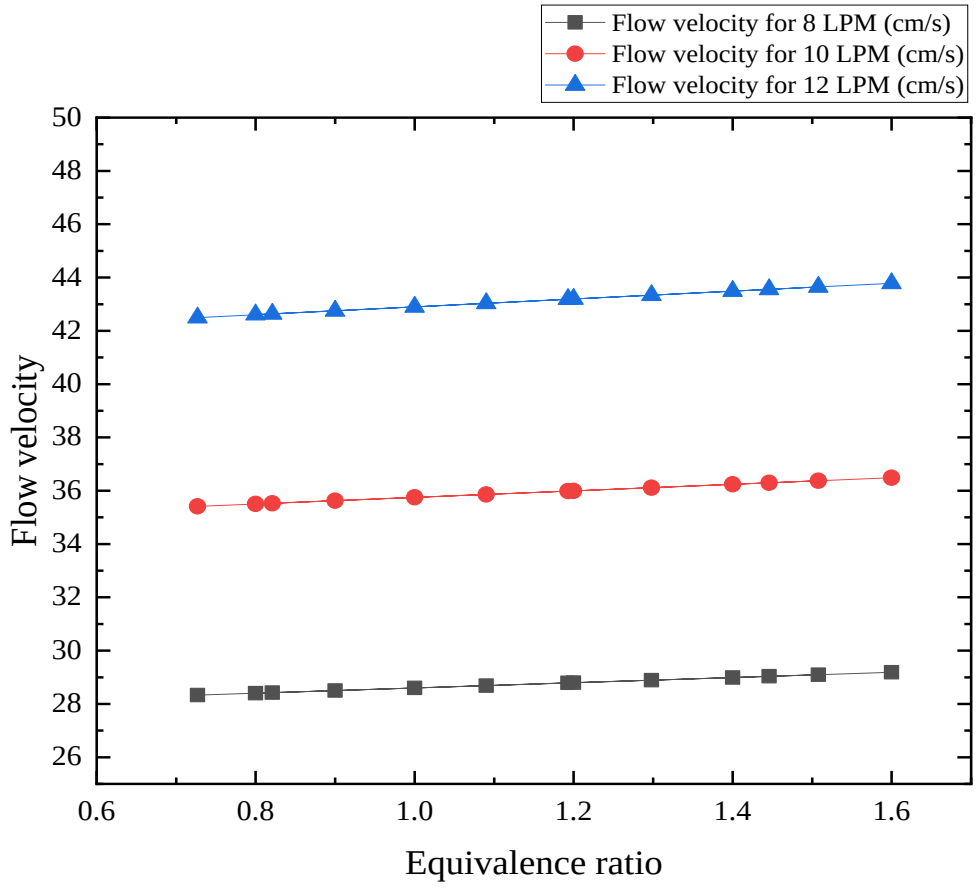

Figure 44: Variation across flow velocity for different flow rates and different equivalence ratio.

velocity the counter force against the flow velocity is not yet prevalent. Therefore, here the flame is constructed at the top of the duct.

Due to this dominating power of the flow velocity over the flame speed a flame regime is observed across several equivalence ratio and all three-glass duct. This zone is named as open flame zone.

Open flame zone is observed for equivalence ratio of 2 (Fig. 45), 1.9, 1.8 (Fig. 46) and 1.7 for big duct while for the 18 mm duct the upper flame zone is observed at equivalence ratio of 2, 1.9, 1.8,1.7 and 1.6. For the medium duct the equivalence ratio for the open flame zone is observed for the same equivalence ratio as for big duct.

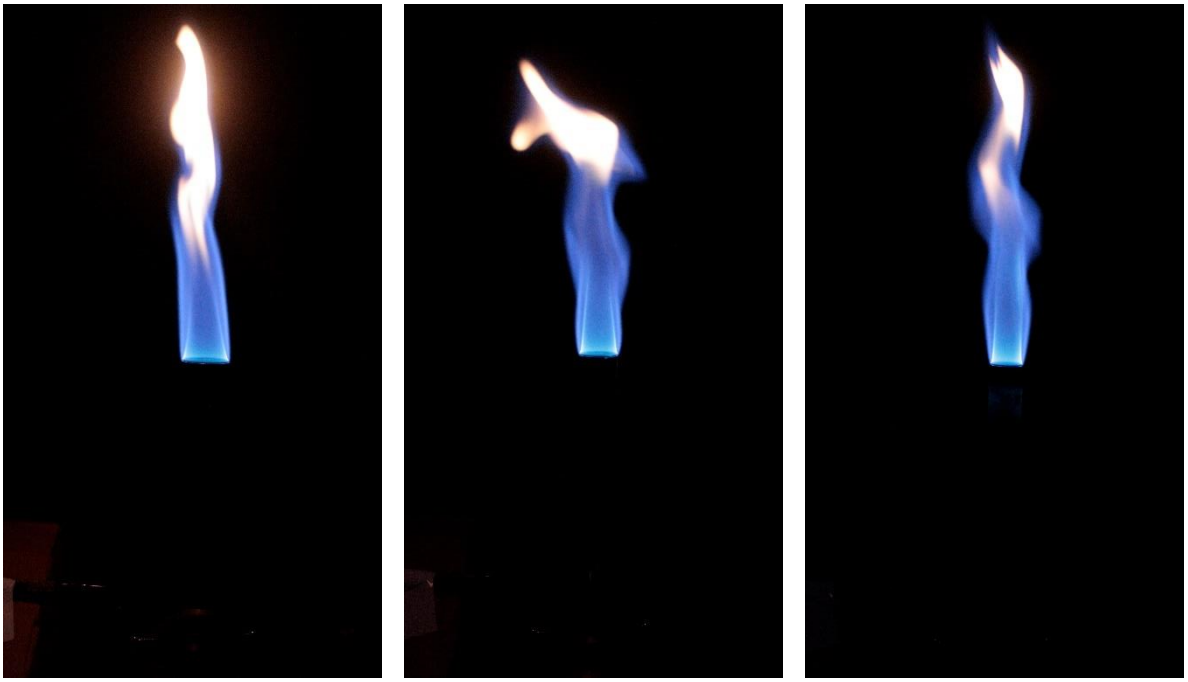

a. Big duct *b. Medium duct* *c. Small duct*

Figure 45: Flame images for equivalence ratio of 2 for duct of different diameters

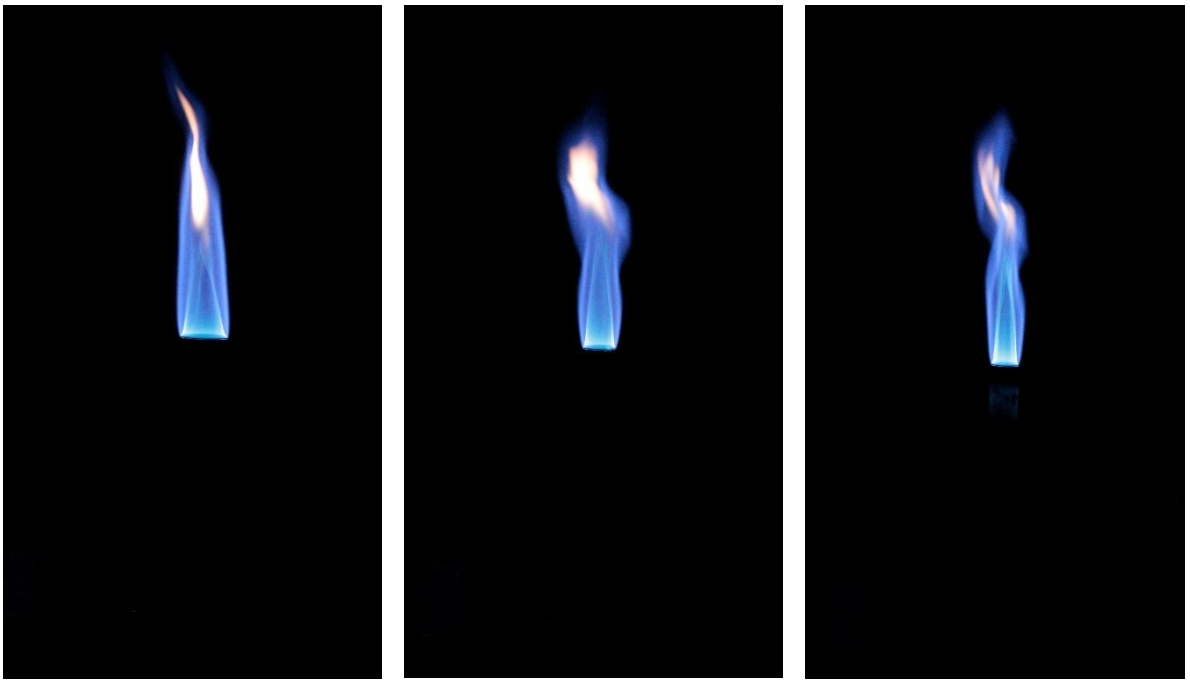

a. Big duct *b. Medium duct* *c. Small duct*

Figure 46: Flame images for equivalence ratio of 1.8 for duct of different diameters

The flame repetitive extinction and ignition zone (FREI zone) is also visible in the medium and big ducts when the equivalency ratio drops even further to1.6 (Fig. 47). The interplay between flow velocity and flame velocity is responsible for the free flame shift phenomena, which is limited to the upper flame domain. In the case of these ducts, the discharge $Q = A \times v$ (where A is the interior area of the duct and v is the air fuel mixture velocity) will result in a Lower air fuel mixture velocity or flow velocity than the duct with a smaller diameter. However, for the small duct due to smaller duct diameter the area will be lesser hence the flow velocity will be higher. Therefore, the small duct does not show FREI zone in 1.6 equivalence ratio.

When the equivalence ratio is further reduced for 1.5 the big duct shows FREI zone however for 21.4mm duct the lower flame starts to stabilize at the bottom of the duct and for this duct the flame shifts from the FREI zone to the open + duct flame zone. The same thing also happens for the small duct. For 1.5 equivalence ratio in small duct the flame is now at Open+ duct flame zone (Fig. 48).

This event of the shift from FREI zone to the open + duct stable flame zone can be explained through the flame speed and flow velocity interplay. As the equivalence ratio is reduced in the rich mixture the flame speed increases therefore it pushes the flame downstream and hence this increased flame speed causes the Lower flame to stabilize at the bottom of the duct.

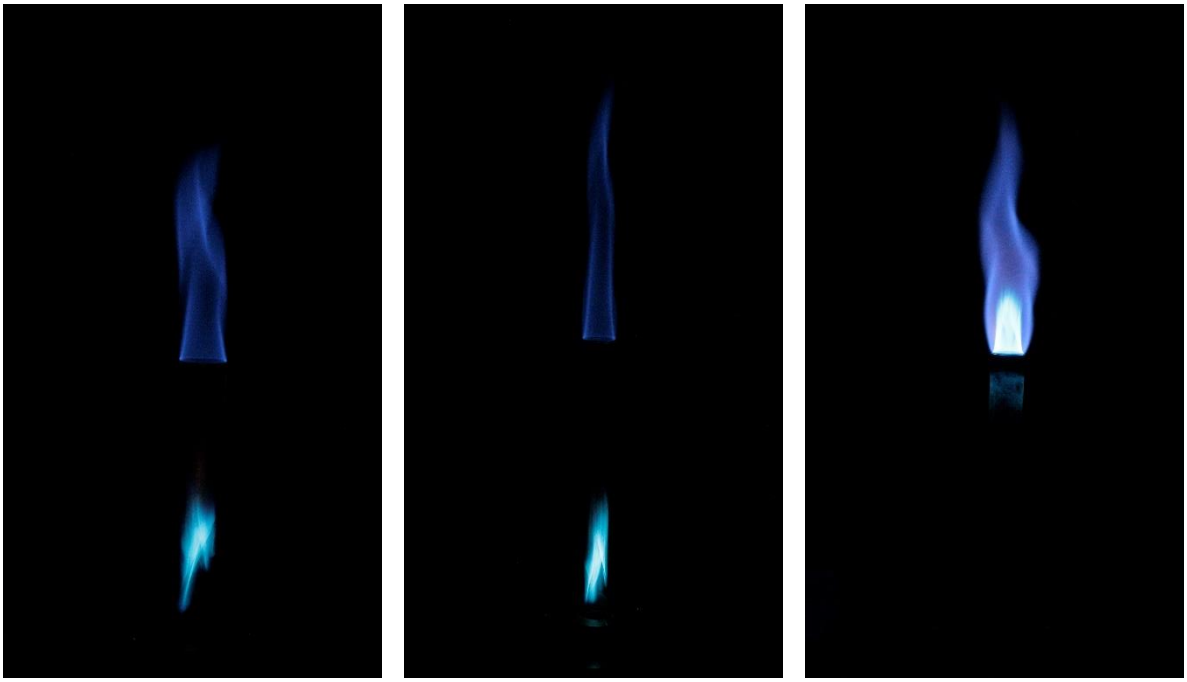

a. Big duct *b. Medium duct* *c. Small duct*

Figure 47: Flame images for equivalence ratio of 1.6 for duct of different diameters

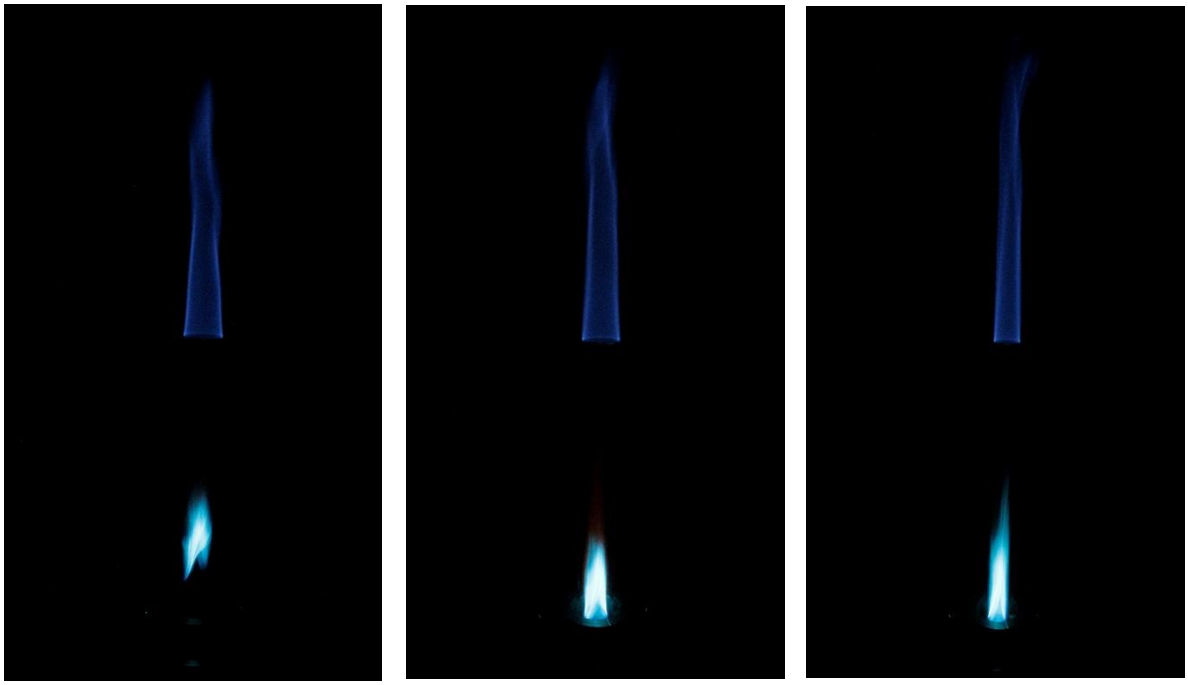

a. Big duct *b. Medium duct* *c. Small duct*

Figure 48: Flame images for equivalence ratio of 1.5 for duct of different diameters

When the fuel flow rate is further adjusted in volume flow rate controller to obtain equivalence ratio of 1.4 here all the duct shows the stable open + duct flame regime. In this zone the flame speed becomes dominating factor in comparison with the flow velocity therefore the flames get stabilized for all the ducts. This open + duct stable flame zone is observed at 1.4 (Fig. 49), 1.3, 1.2, 1.1 equivalence ratio for the big duct. While for the other two ducts this zone is observed for the equivalence ratio of 1.5, 1.4, 1.3, 1.2, 1.1.

From the images of flame for 1.4 and 1.3 equivalence ratio that for 1.4 equivalence ratio slight red color starts to appear for the flame. For 1.3 equivalence ratio the red color is visible for all 3 duct flames (Fig. 50).

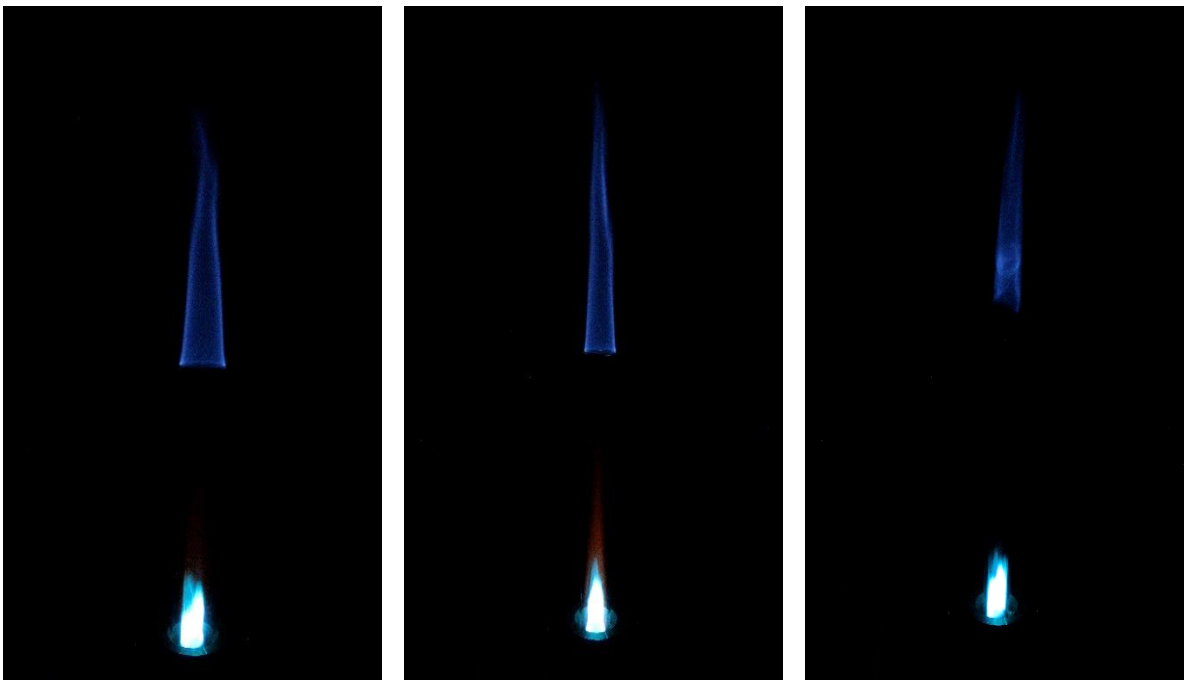

a. Big duct *b. Medium duct* *c. Small duct*

Figure 49: Flame images for equivalence ratio of 1.4 for duct of different diameters

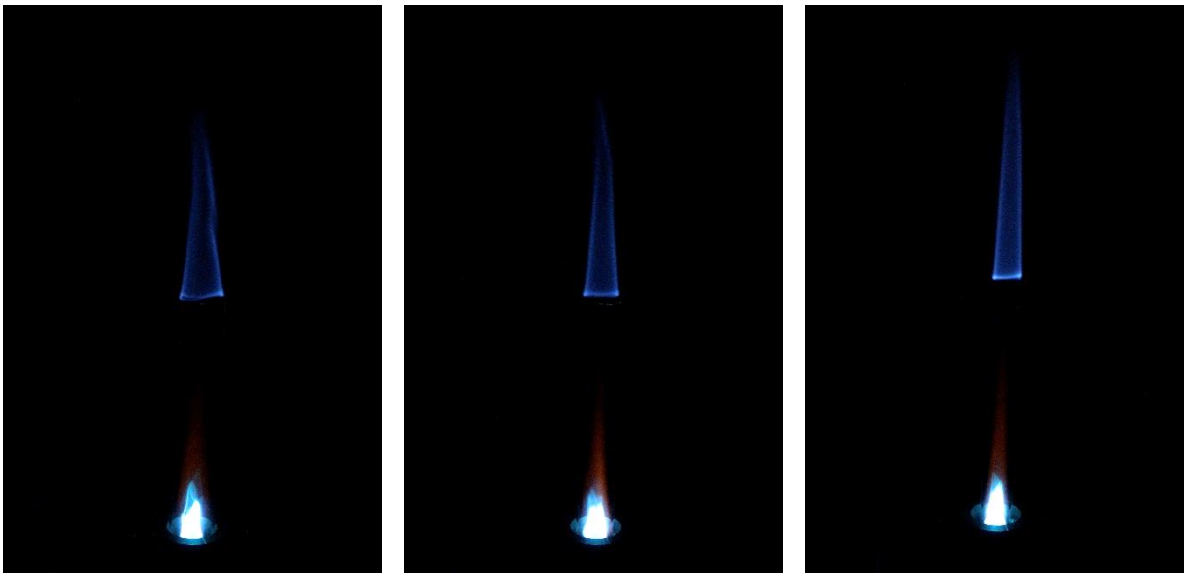

a. Big duct *b. Medium duct* *c. Small duct*

Figure 50: Flame images for equivalence ratio of 1.3 for duct of different diameters

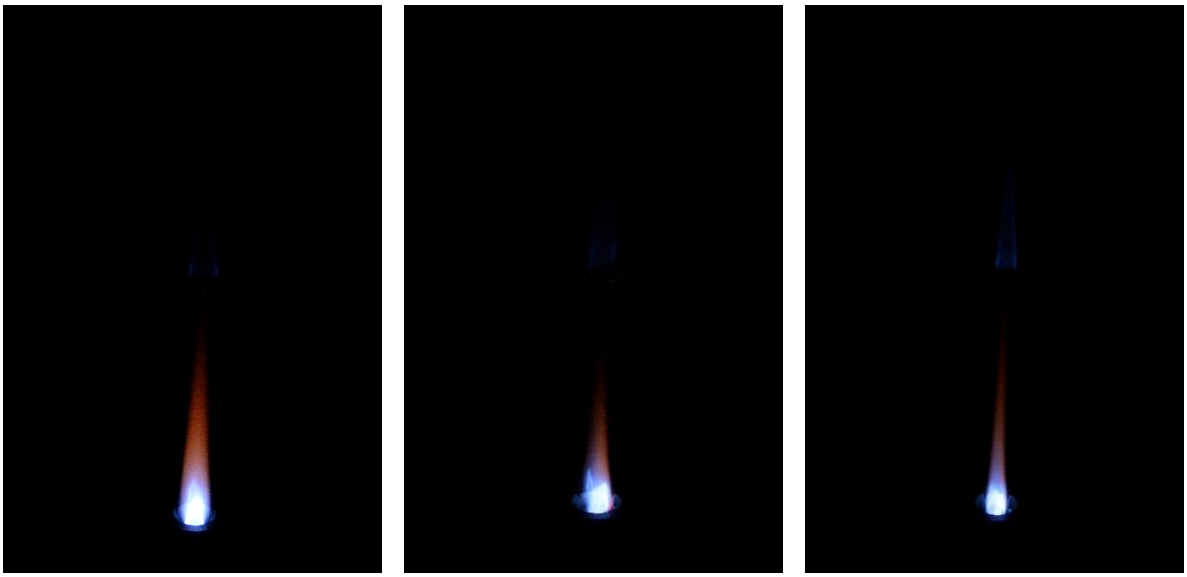

a. Big duct *b. Medium duct* *c. Small duct*

Figure 51: Flame images for equivalence ratio of 1.1 for duct of different diameters

For the equivalence ratio of 1.3 all the upper flame for 3 ducts starts to lifted off. After those upper flames started losing intensity and becomes very weak for equivalence ratio of 1.1 (Fig. 51). From the figures of flame at different equivalence ratio this phenomenon of upper flame losing intensity is very evident.

When the fuel flow rate is further Lowered to obtain the equivalence ratio of 1 for different ducts (Fig. 52) here the upper flame that was present fades away. It is the stoichiometric ratio therefore the air present in the mixture is sufficient to burn the total fuel present in the air fuel mixture. Therefore, no unburnt mixture gets released from the combustion which was burning at the top of the combustor for higher equivalence ratios such as 1.1,1.2 or 1.3.

Here again the flame regime shifts from the open + duct flame zone to the duct flame zone.

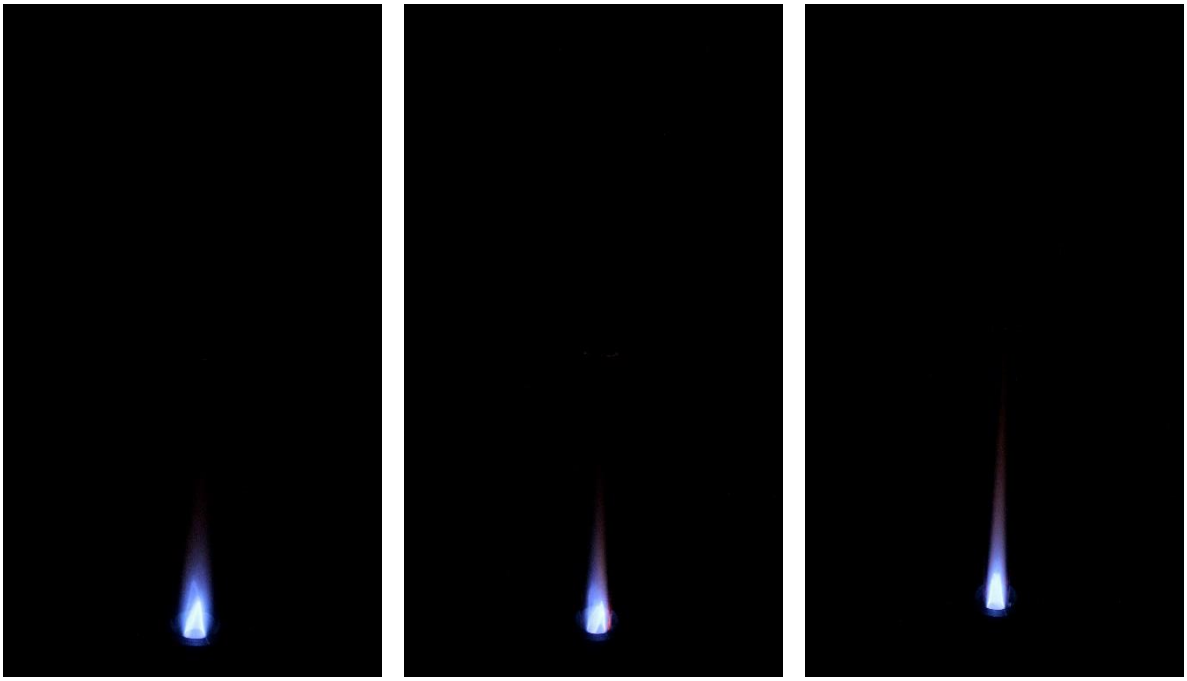

a. Big duct *b. Medium duct* *c. Small duct*

Figure 52 Flame images for equivalence ratio of 1 for duct of different diameters

Here we can observe from the image itself that the intensity of red color present in the flame gets reduced significantly though little amount of red color is still present. When spectroscopy is done for the flame a particular wavelength in this region is found that is 588 nm wavelength along with 765nm and 930nm wavwlength bands. 588nm is in yellow spectrum of visible light while 765nm is slightly after visible red colour ends at 750nm, while 930 is in the infrared spectrum range.

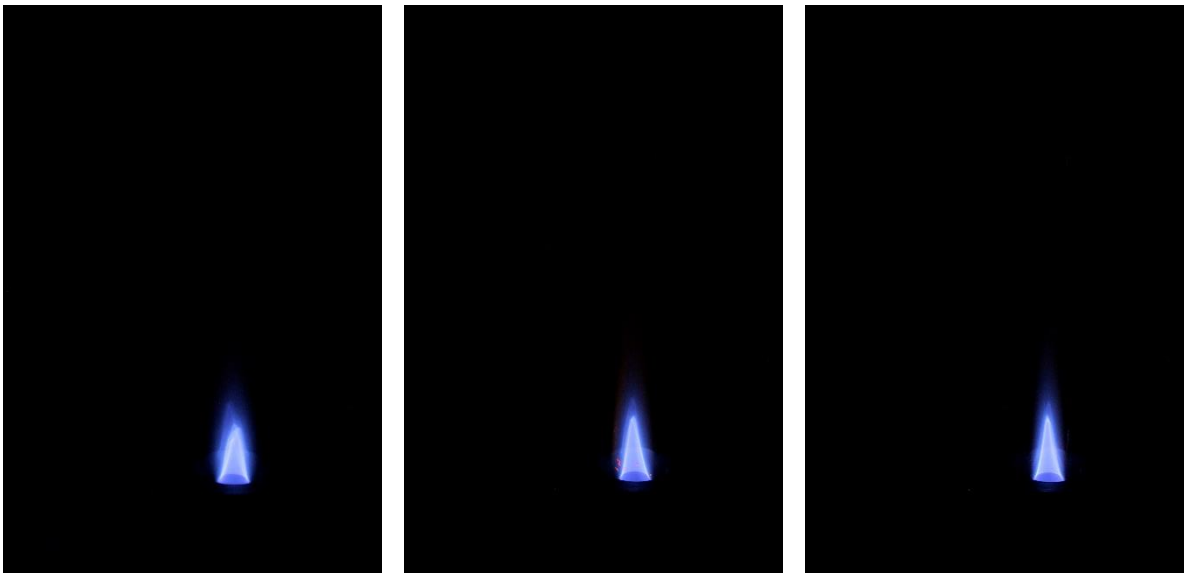

a. Big duct *b. Medium duct* *c. Small duct*

Figure 53: Flame images for equivalence ratio of 0.9 for duct of different diameters

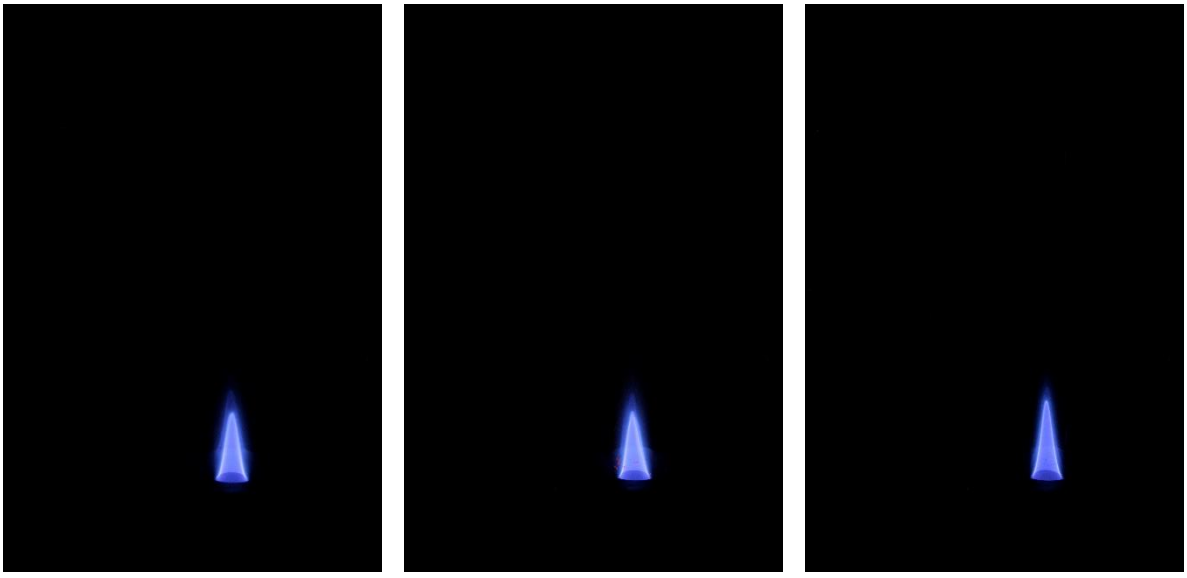

a. Big duct *b. Medium duct* *c. Small duct*

Figure 54: Flame images for equivalence ratio of 0.8 for duct of different diameters

For further lower equivalence ratios such as 0.9 (Fig. 53) the flames for all the 3 different diameter ducts shows duct flame. Here from image only this is clear that the orange color

presented in the images is completely gone due to shift of air fuel mixture from richer side of stoichiometric ratio to the leaner side of stoichiometric ratio. So, it can be concluded that here in the leaner side the combustion process is efficient and also the flame is stable.Fig. 54 shows the duct flame zone for 0.80 equivalence ratio and the flame is of blue color.

When the fuel flow rate is again lowered through volume flow rate controller and further lower equivalence ratios are obtained now the reaction speed also decreases and hence the flame speed also decreases therefore the flow velocity becomes dominating factor compared to the flame speed. Hence the flow velocity of air fuel mixture tries to push away the flame that was present in the bottom of the duct. Therefore, here the flame regime again shifts from duct flame zone to the oscillating flame zone. Here the flame tends to dance periodically with time. The oscillating flame zone starts at 0.77 (Fig. 55) equivalence ratio for the big duct and ends at 0.68 equivalence ratio.

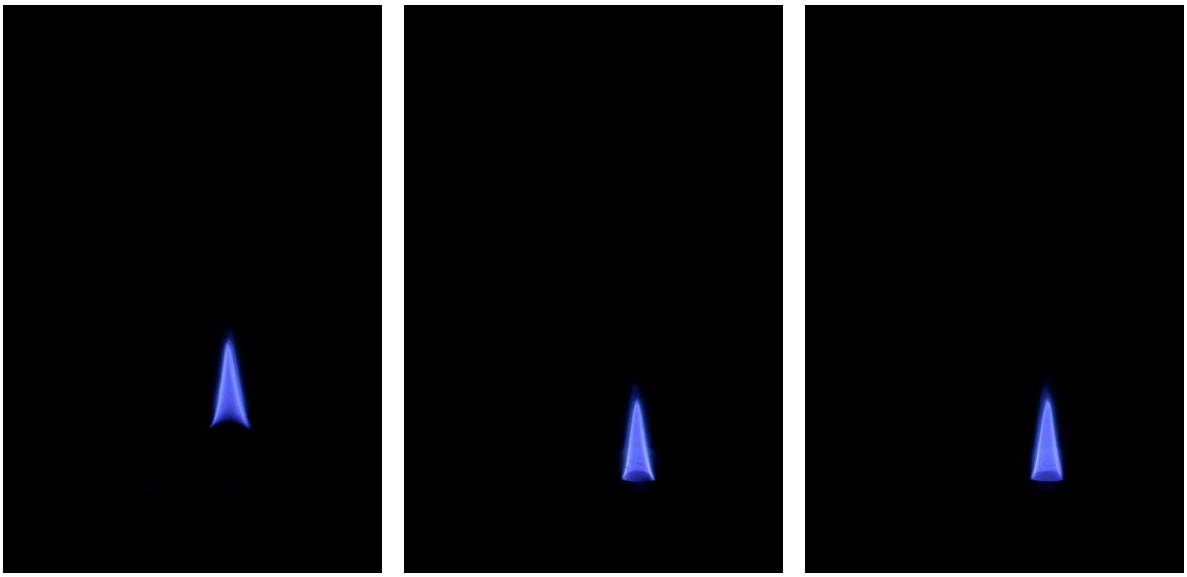

a. Big duct *b. Medium duct* *c. Small duct*

Figure 55: Flame images for equivalence ratio of 0.77 for duct of different diameters

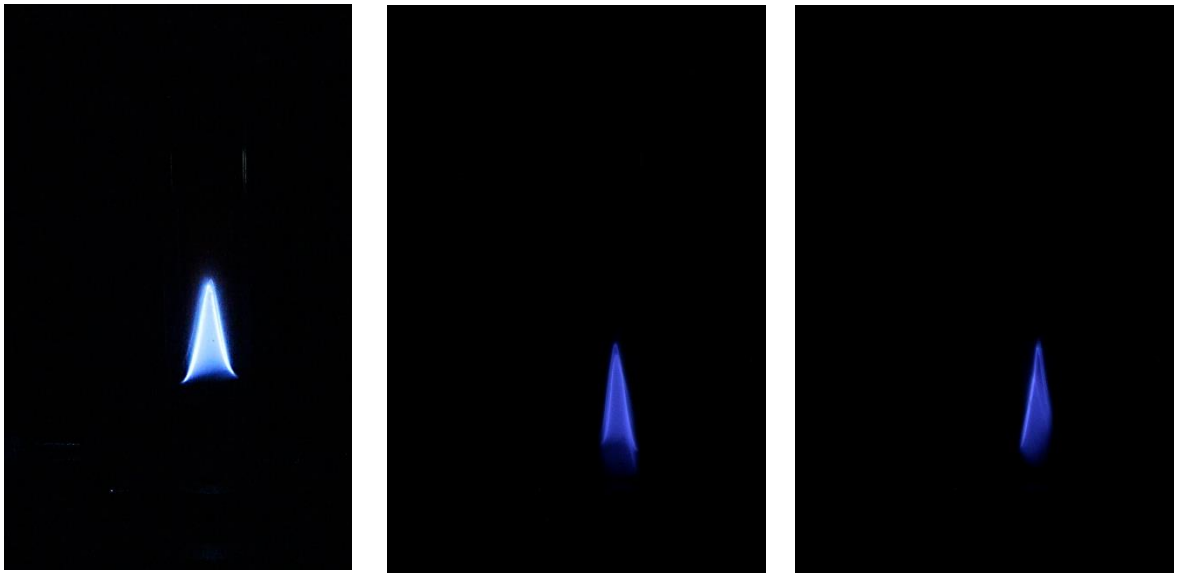

a. Big duct *b. Medium duct* *c. Small duct*

Figure 56: Flame images for equivalence ratio of 0.75 for duct of different diameters

For the medium duct the oscillating flame starts at an equivalence ratio of 0.75 (Fig. 56). The same thing happens for the small duct. The oscillating flame zone observed for from 0.75 to 0.66 equivalence ratio for the medium duct and for small duct oscillating flame is observed for 0.75 and 0.72 equivalence ratio.

When the equivalence ratio is reduced further the air fuel mixture becomes leaner. Therefore, in this case there are more air present compared to the fuel. Therefore, due to this excess air the heat propagation from the burning zone is not going to be adequate to burn the fresh charge. This phenomenon ensures the flame speed in this region reduced further lower values. Therefore, the flow velocity becomes more dominating factor here and pushes away the flame further upstream hence blowout occur. The blowout occurring point for the 24.8mm is at equivalence ratio of 0.66. For the 21.4mm duct blowout point is 0.65 and for the small duct the blowout occurs at 0.7 equivalence ratio.

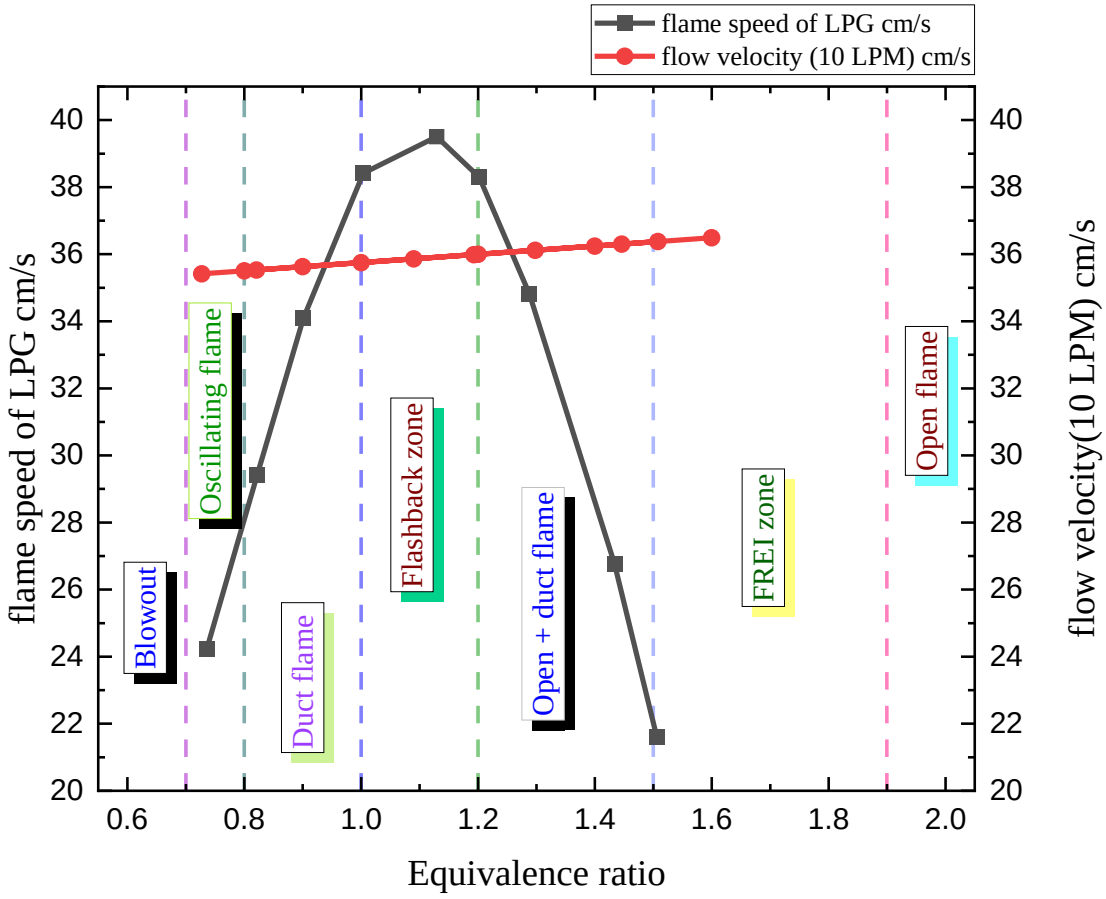

Figure 57: Flame speed and flow velocity comparison with different equivalent ratio graph for 10 LPM air flow rate with different flow zone.

Here the figure shows the values of both flame speed and flow velocity with equivalence ratio. The different flame regimes occurring for different equivalence ratios are also shown in the graph.

4.4 Lean Blowout:

When the air fuel mixture is supplied to the combustor is in leaner side of the stoichiometric ratio initially duct flame has been observed. But then when the air fuel mixture supplied made leaner than lean blowout occurs. This lean blowout point varies with different flow rates of air also it varies with the different duct diameters. lean happens when the air-fuel mixture gets overly lean, which lowers the flame temperature and causes instability in combustion.

As a result of lean air furl mixture supplied, there is more air present in this instance than fuel. As a result, the extra air will prevent the heat from the burning zone from spreading sufficiently to burn the new charge. This phenomenon guarantees even lower values of flame speed in this area. So, the flow velocity is higher in comparison of flame speed therefore the flow velocity push away the flame from the duct hence blowout occurs.

The lean blowout observed in the experiment occurs through the mechanism explained below. In the lean combustion zone firstly when flame speed decreases then the flame detached from the combustor base. Still the flame inside the duct near the bottom of the duct. However, upon further lowering the equivalence ratio causes the flame to be more unstable and it starts to show dancing phenomenon periodically. At the same time a sound emitted by the combustor can be heard. This sound is created due to the acoustic instability causes by the lean mixture combustion process. Initially the oscillating flame dance is very non chaotic and it occurs with low frequency and low amplitude. But reducing the equivalence ratio further causes the flame to dance with more frequency and amplitude. Further when the equivalence ratio lowered the frequency and amplitude of the oscillation becomes more intense and eventually blowout occurs. This change from little chaotic initially to much more chaotic at the time just before blowout can also be found for the FFT analysis of the sound heard from the combustion in the oscillating flame regime.

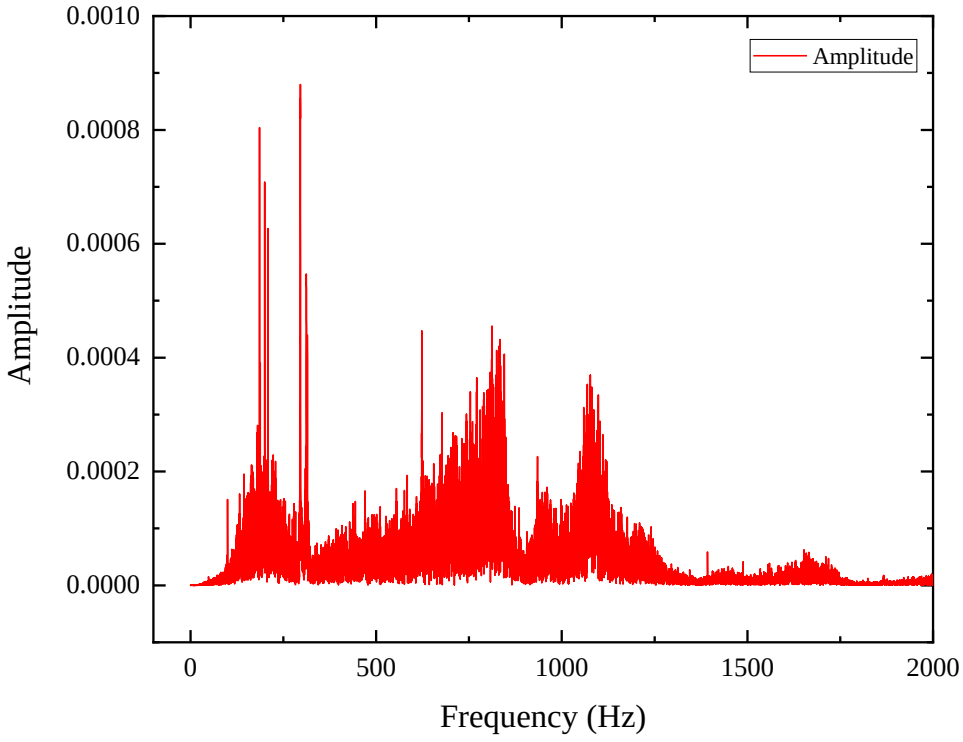

Figure 58.a: audio FFT for equivalence ratio of 0.75

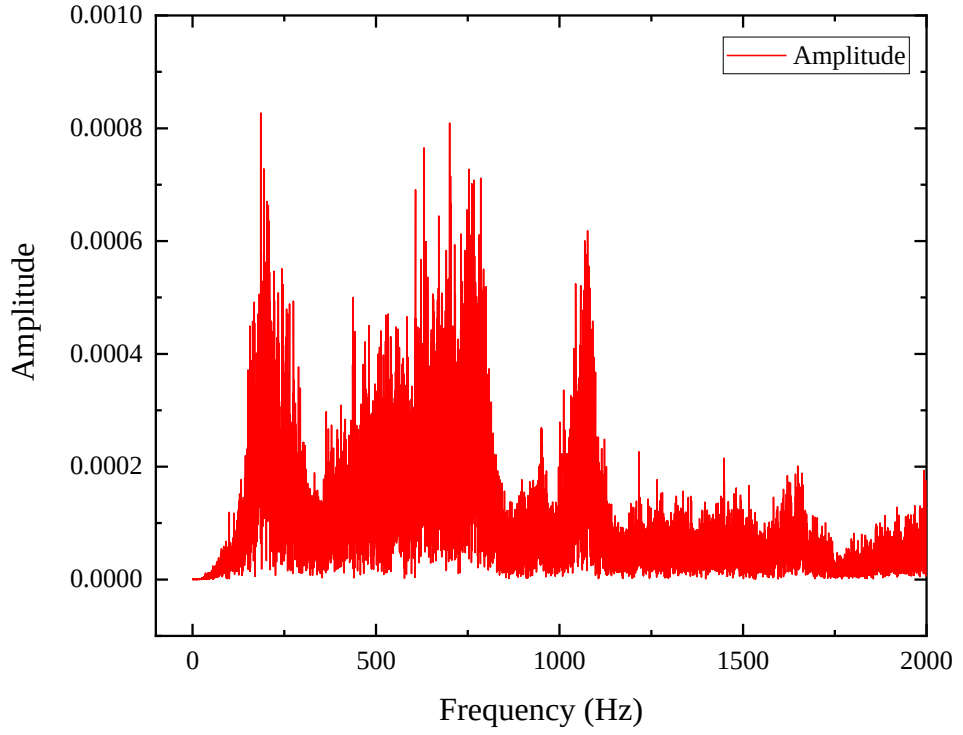

Figure 58.b: Audio FFT for equivalence ratio of 0.68

Figure 58: Audio FFT for equivalence ratio of 0.75 and 0.68

From the figures (Fig. 57, Fig 58) it is clear that initially the different frequencies present in the sound was with amplitude values on the lower side but for the equivalence ratio of 0.68 the amplitude various frequencies increase to a significant amount. Not only amplitude but also for Φ=0.75 the freequency peaks was around 150-300 Hz zone but as the flame approaches blowout the freequency peaks shifts to 600-750 Hz zone.

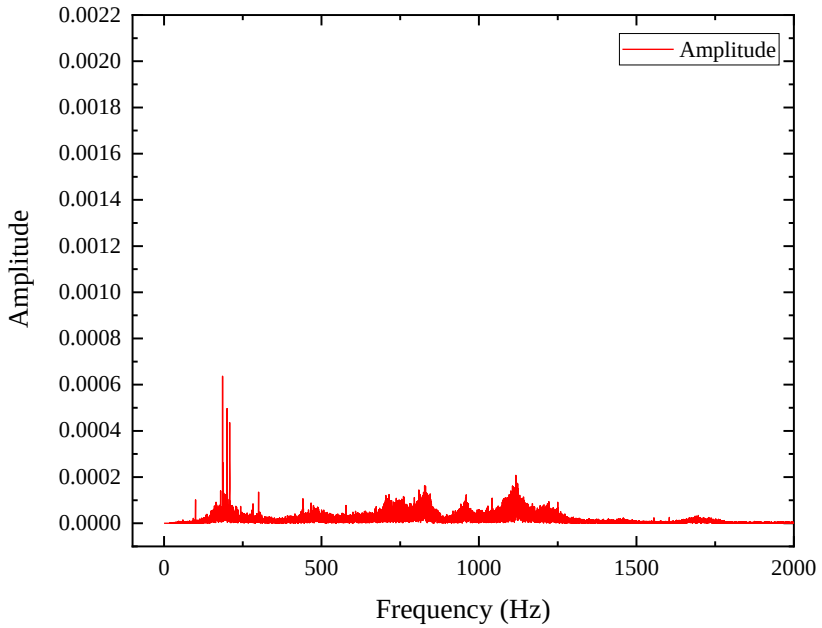

Figure 59: Audio FFT for equivalence ratio of 0.75(12 LPM medium duct)

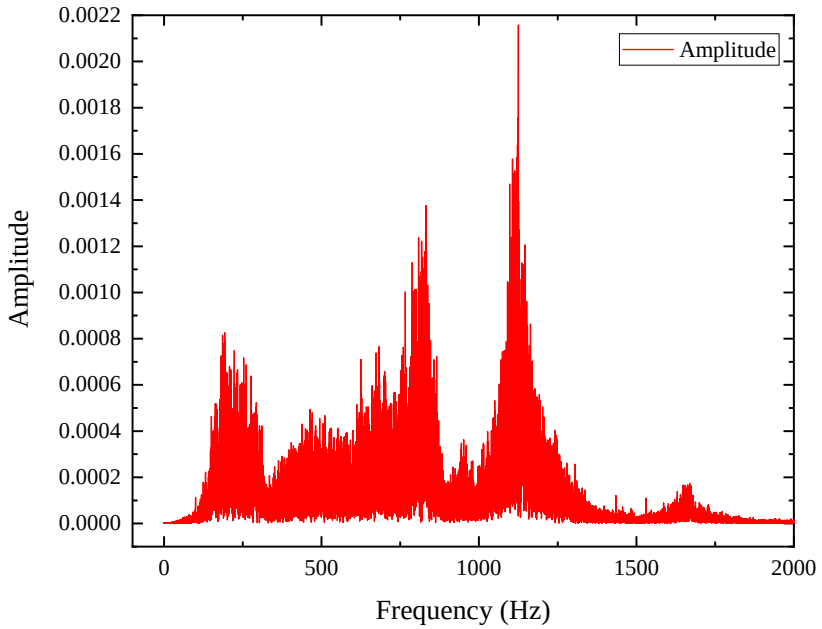

Figure 60: Audio FFT for equivalence ratio of 0.68(12 LPM medium duct)

For the medium duct the peak frequencies and amplitude attached to it is lesser for equivalenc e ratio of 0.75 (Fig. 59) compared to the equivalence ratio of 0.68 (Fig. 60) which is just befor e the blowout point. For more context in this case the oscilatinging flame zone starts at an equ ivalence ratio of 0.75.

The peak frequency for 0.75 equivalence ratio is 185.88 Hz with amplitude of 0.00063 while t he peak frequency for the 0.68 equivalence ratio is 1125 Hz with amplitude of 0.00215 which is significantly higher compared to 0.75 equivalence ratio.

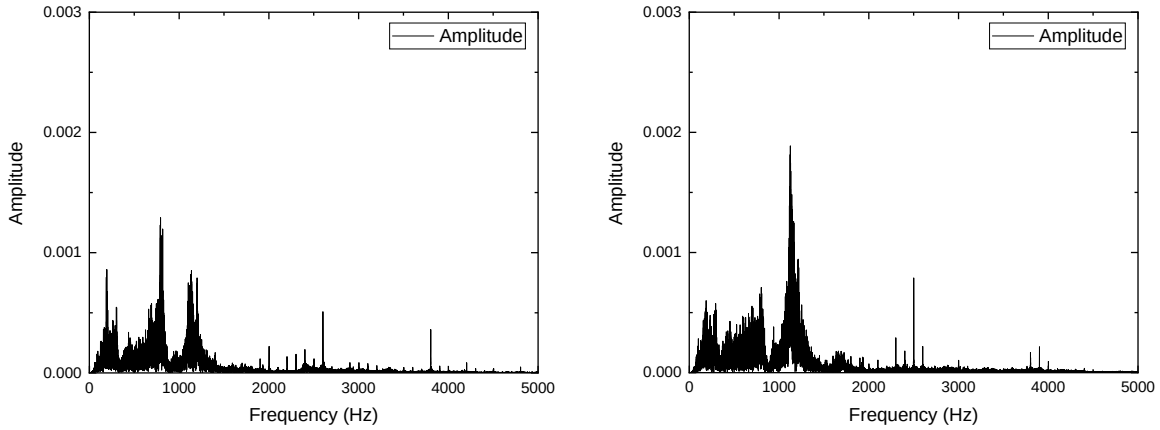

Figure 61: Audio fft for equivalence ratio of 0.80 and 0.77(10 LPM small duct)

For 10 LPM (Fig. 61) also for the audio captured during the blowout zone matches as previously discussed. The peak frequency and amplitude for Φ=0.80 is 789, 0.0012 respectively and at Φ=0.77 which is just above the blowout point the peak frequency and amplitude value increases and becomes 1134 and 0.0019 respectively.

When First Fourier Transformation is applied for the oscillating flame videos to find out the fft data the data revels some things for this zone.

FFT for 12 LPM big duct

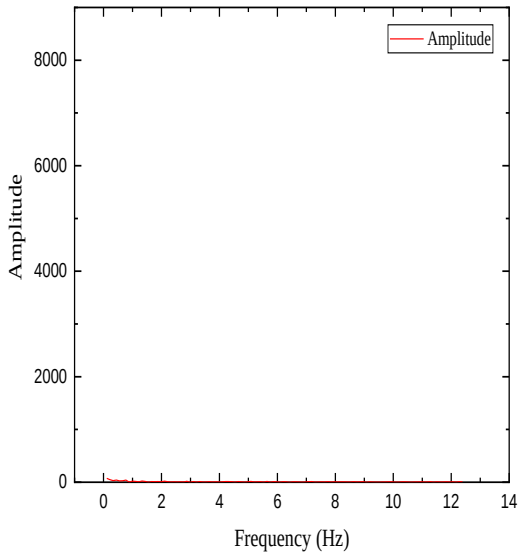

Φ=0.77

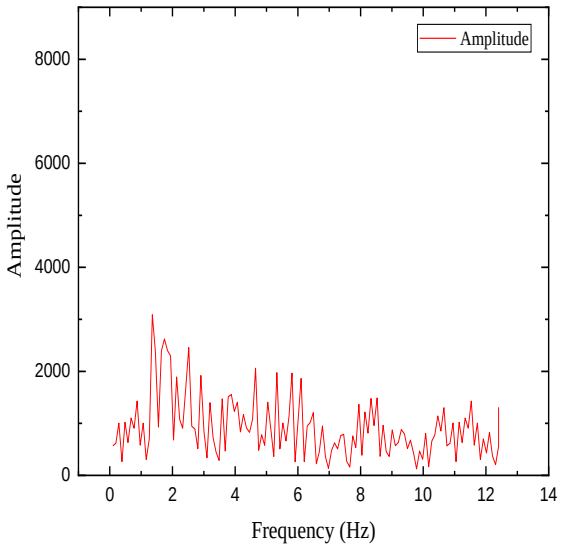

Φ=0.72

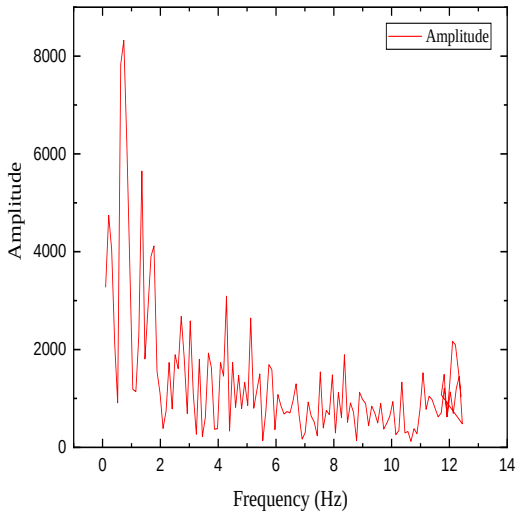

Φ=0.70

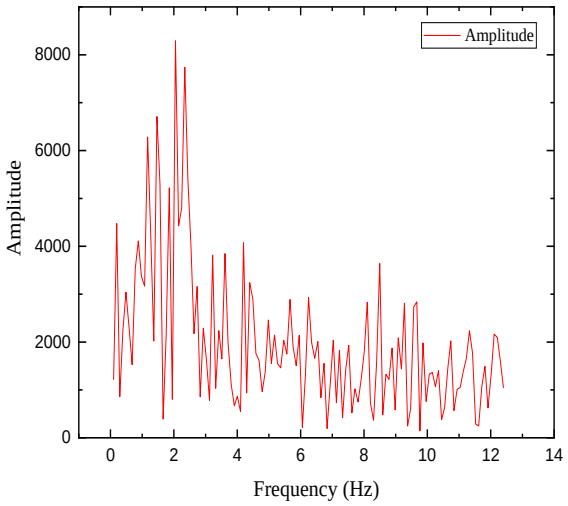

Φ=0.68

Figure 62: Oscillating flame FFT signal for different equivalence ratio for 12 LPM air flow rate (big duct)

For the oscillating flame regime obtained for 12 LPM (Fig. 62) flow rate initially when the oscillating started it started with a fft signal which almost doesn't exist. But as the equivalence ratio lower to 0.72 the fft signal become like a noise. Again, reducing to 0.70 equivalence ratio now there are many more no of peaks in the fft data as well as more amplitude. Finally at 0.68 equivalence ratio the peaks got even more in number with also increased in their amplitude. These large no of peaks with higher amplitude shows that there is more chaos shown by the flame as it gets closer to the lean blowout point. The peak frequencies for the equivalence ratios of 0.77 ,0.75, 0.72, 0.7and 0.68 are 0.11,0.67,0.68,0.95 and 2.05 respectively.

FFT for 12 LPM medium duct

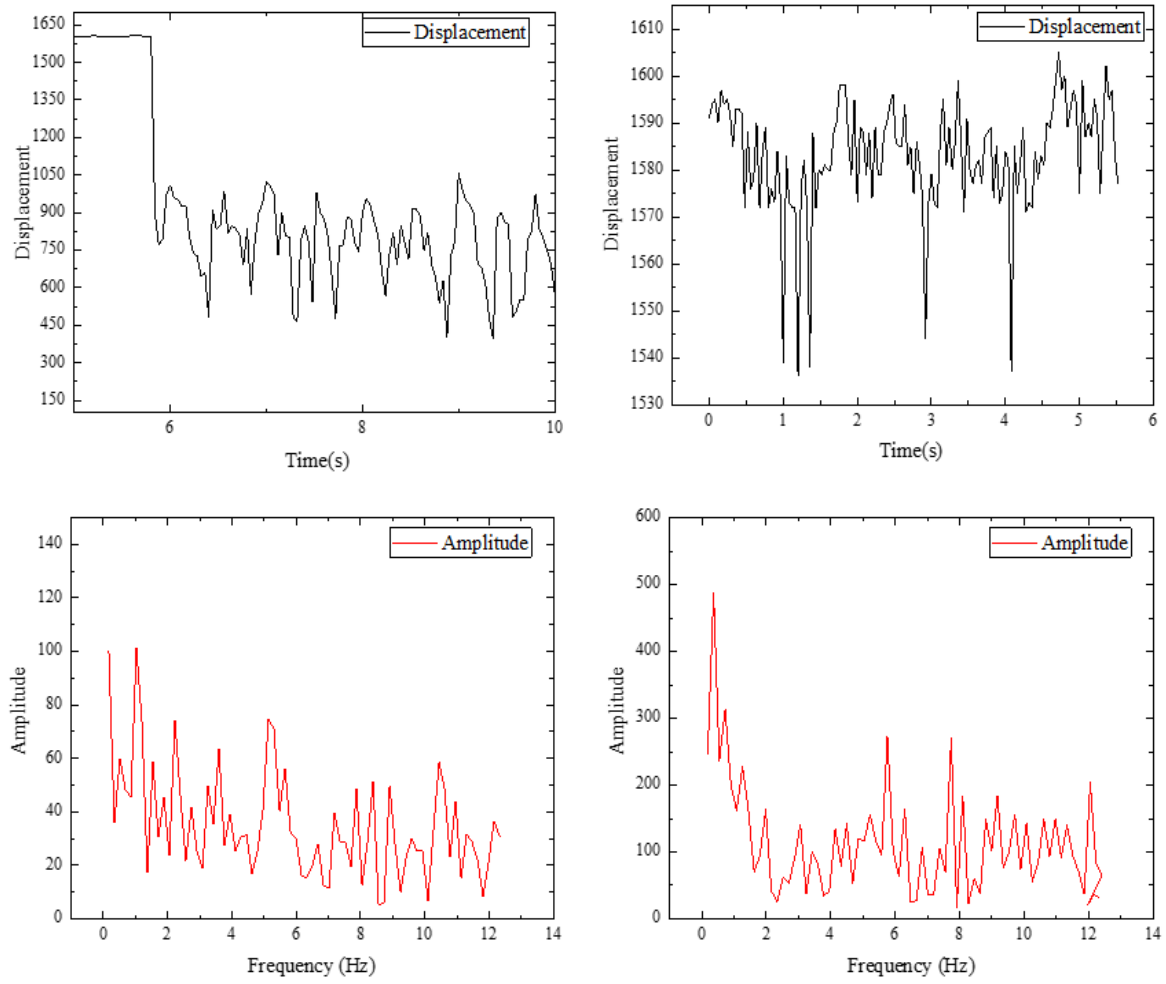

a. φ=0.75 b. φ=0.72

Figure 63: Displacement vs time and amplitude vs frequency graph for 12 LPM medium duct for different equivalence ratios

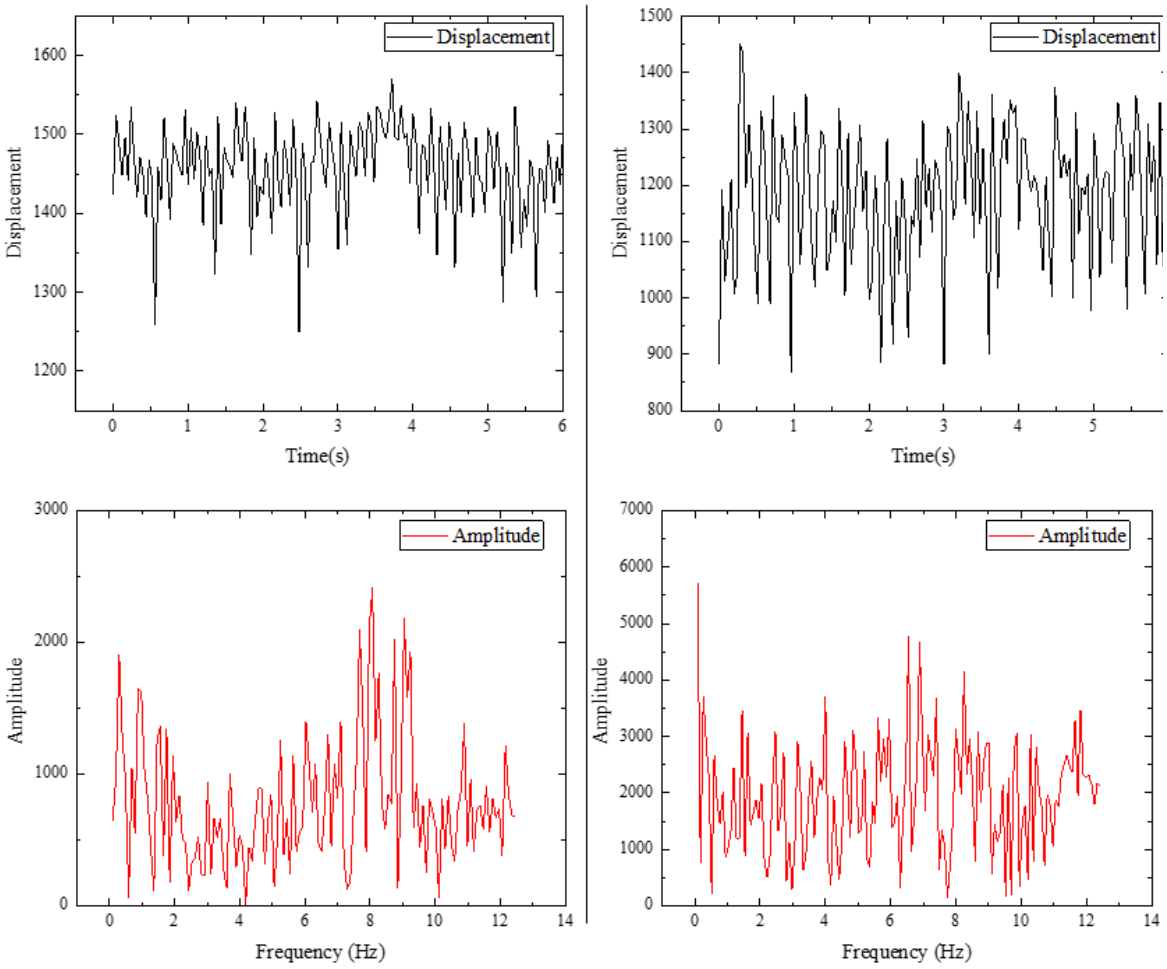

a. φ=0.70 b. φ=0.68

Figure 64: Displacement vs time and amplitude vs frequency graph for 12 LPM medium duct for different equivalence ratios

Here also (Fig. 63, Fig. 64) with decreasing values of equivalence ratios the amplitude for the peak frequencies increases. Also, from the graph it is clear that when the flame about to reach lean blowout limit the no of peaks with higher amplitude starts to show up much more when compared to higher equivalence ratios when the dancing flame regime started,

FFT FOR 8 LPM big duct

Here when the dancing flame zone started the fft signal is like a noise (Fig. 65). Then when the equivalence ratio lower towards the lean blowout point the flame FFT data shows the frequency at which the flame is oscillating and its amplitude. The peak frequency and the amplitude corresponding to the peak frequency increases as the flame gets nearer to the lean blowout zone. The peak frequency and amplitude value is shown in the figure (Fig. 66).

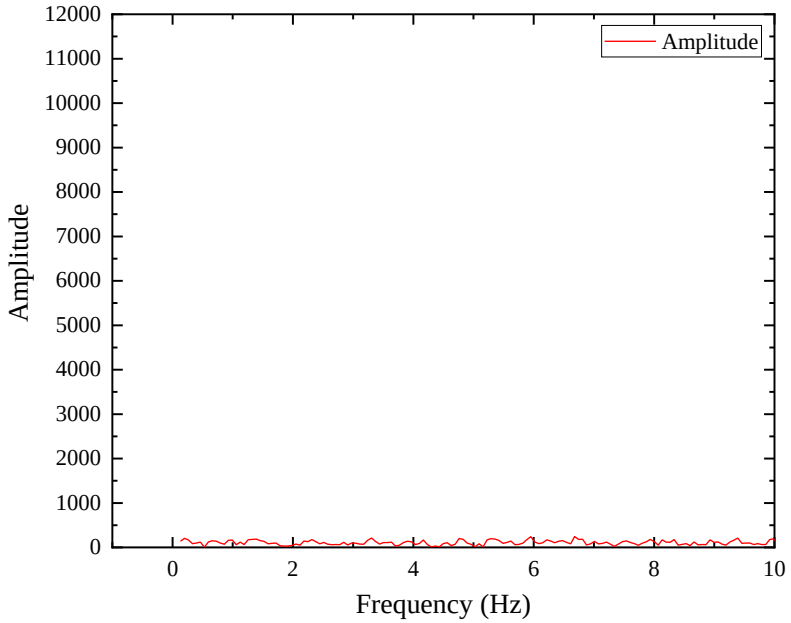

φ=0.66

Figure 65: Amplitude vs frequency graph for 8 LPM 24.8mm duct for different equivalence ratios of 0.66

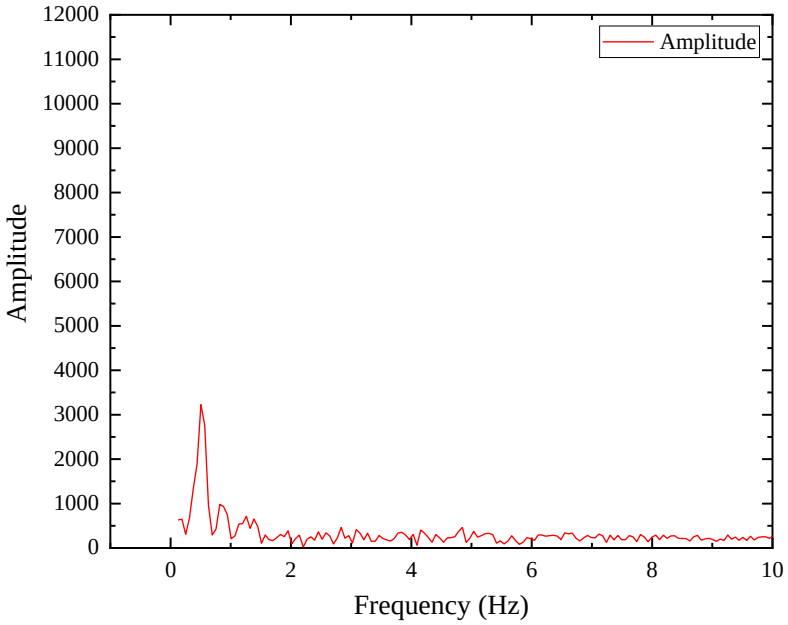

φ=0.62

Peak frequency=0.5, Amplitude=3174

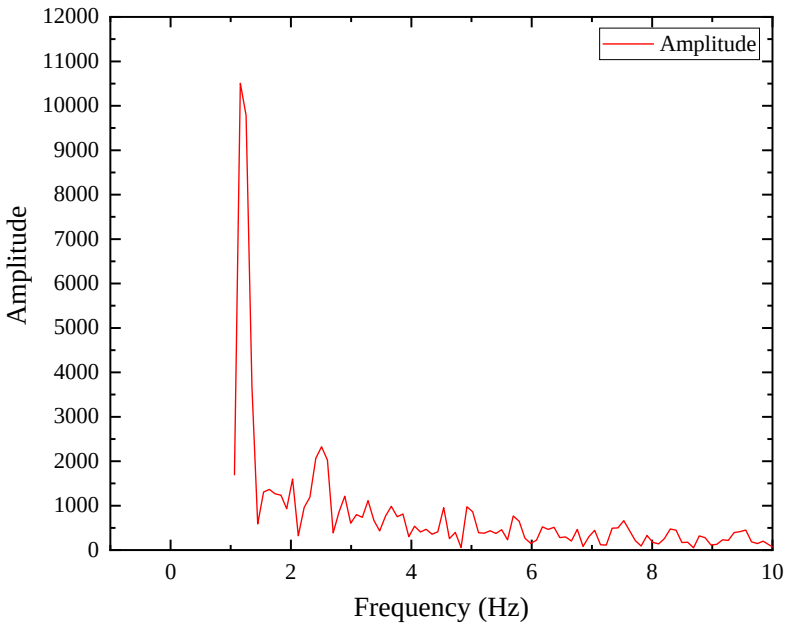

φ=0.60

Peak frequency=1.19, Amplitude=10366

Figure 66: Amplitude vs frequency graph for 8 LPM 24.8mm duct for different equivalence ratios of 0.62 and 0.60

FFT for 8 LPM medium duct

For this case also we can observe that the amplitude and peak frequency keeps increasing with the dancing flame being more unstable and chaotic (Fig. 67). The peak frequency and amplitudes are 0.56 and 958 for φ=0.70, 4.96 and 1167 for φ=0.68, 2.96 and 2250 for φ=0.66 and for φ=0.64 it is 8.62 and 3000. Not only the peak frequency and amplitude increased here but also the no of peaks with high amplitude to be shown just before the blowout zone.

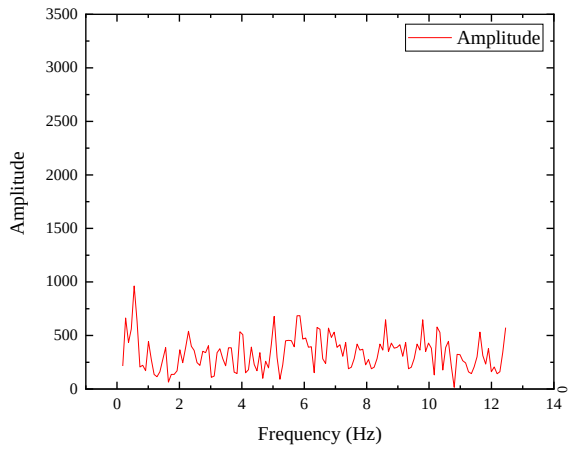

a. φ=0.70

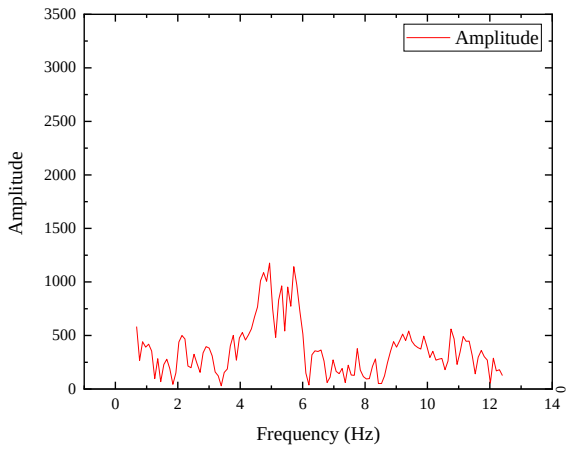

b. φ=0.68

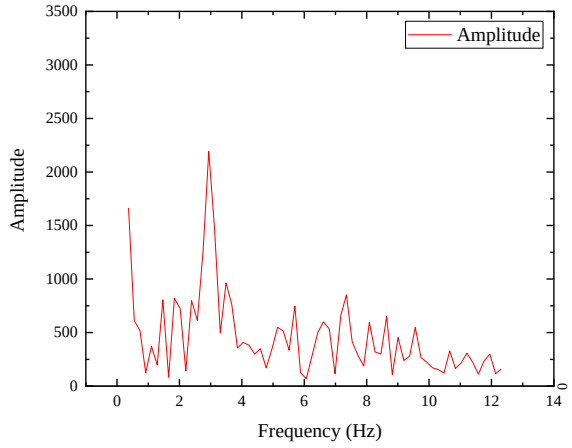

c. φ=0.66

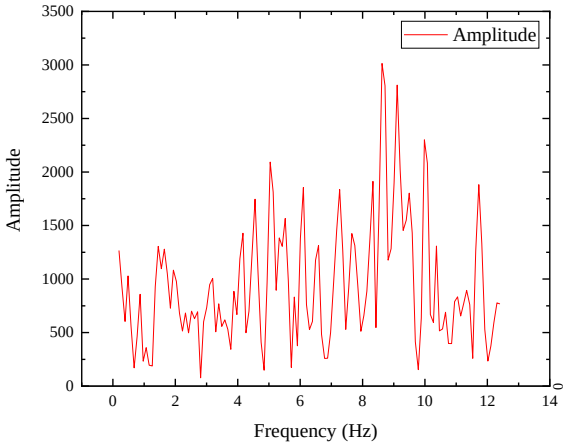

d. φ=0.64

Figure 67: Amplitude vs frequency graph for 8 LPM medium duct for different equivalence ratios

FFT for 10 LPM small duct

For the 18 mm duct or small duct the dancing flame zone is shown for the two equivalence ratios those are 0.80 and 0.77 (Fig. 68), for this case also initially at φ=0.80 when dancing flame started the amplitudes for different frequencies are much lower (250-350) but at φ=0.77 the peaks in the are more with more amplitude (1000-2000). Here for φ=0.77 the peak frequency is 3.78 with 4801 amplitude. The figure for the fft signal is given in the next figure.

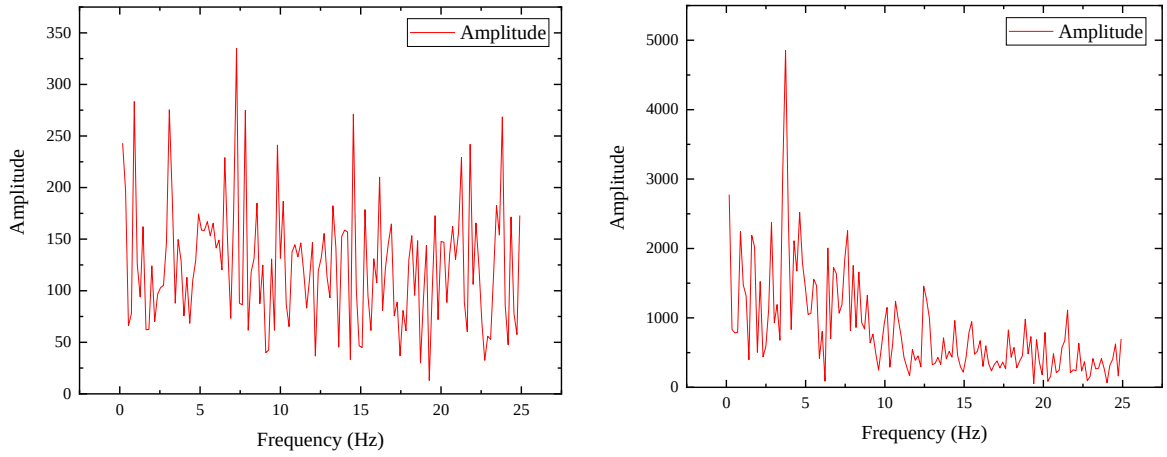

φ=0.80 φ=0.77

Figure 68: Amplitude vs frequency graph for 10 LPM 18 mm duct for different equivalence ratios (0.80 and 0.77)

FFT for 10 LPM medium duct

For 21.4mm duct or medium when the air flow is kept constant the lean blowout occurs at the equivalence ratio of 0.70, in the figure the fft signal for 0.75 and 0.72 equivalence ratio has been shown in Fig. 69. Just above the lean blowout occur at Φ=0.72 the fft shows many more peaks at higher amplitude compared to the dancing flame at Φ=0.75. For Φ=0.72 the peak frequency is 7.5 with amplitude 3597 while at Φ=0.75 the peak frequency is 9.17 with

amplitude 5794. Therefore, when the equivalence ratio reduced and the flame gets nearer to the lean blowout zone the flames peak frequency and amplitude both increases with many more local frequency peaks of high amplitude for just above the equivalence ratio is equals to the lean blowout.

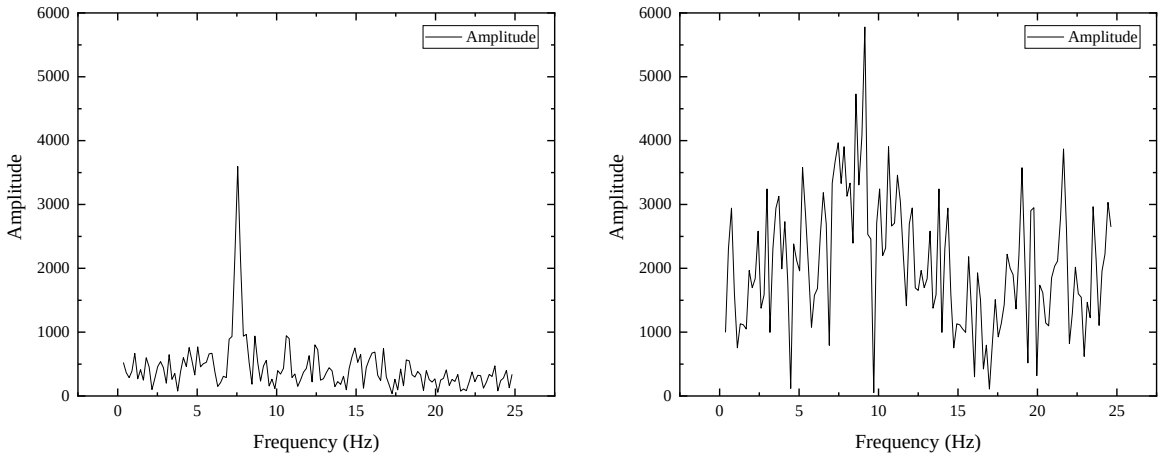

Φ=0.75 Φ=0.72

Figure 69: Amplitude vs frequency graph for 10 LPM 21.4 mm duct for different equivalence ratios

Lean blowout points have been shown in the Fig. 70 for different ducts. Understanding lean blowout is one of most important factors to design a portable power producing device that utilises the meso combustor as power source. Understanding lean blowout is important for a few reasons such as

Stability of combustion**:** LBO is the point of fuel-air combination that causes a premixed flame to become unstable and eventually the flame extinguishes. Properly understanding LBO thus facilitates the construction of combustors that sustain steady flames for better performance. Efficiency: The operation in combustor cannot proceed if the air fuel ratio is below LBO. This can cause safety issues as well as effects the efficiency. Therefore, for maximizing the efficiency the LBO must be avoided and flame operating zone should not be closer to LBO.

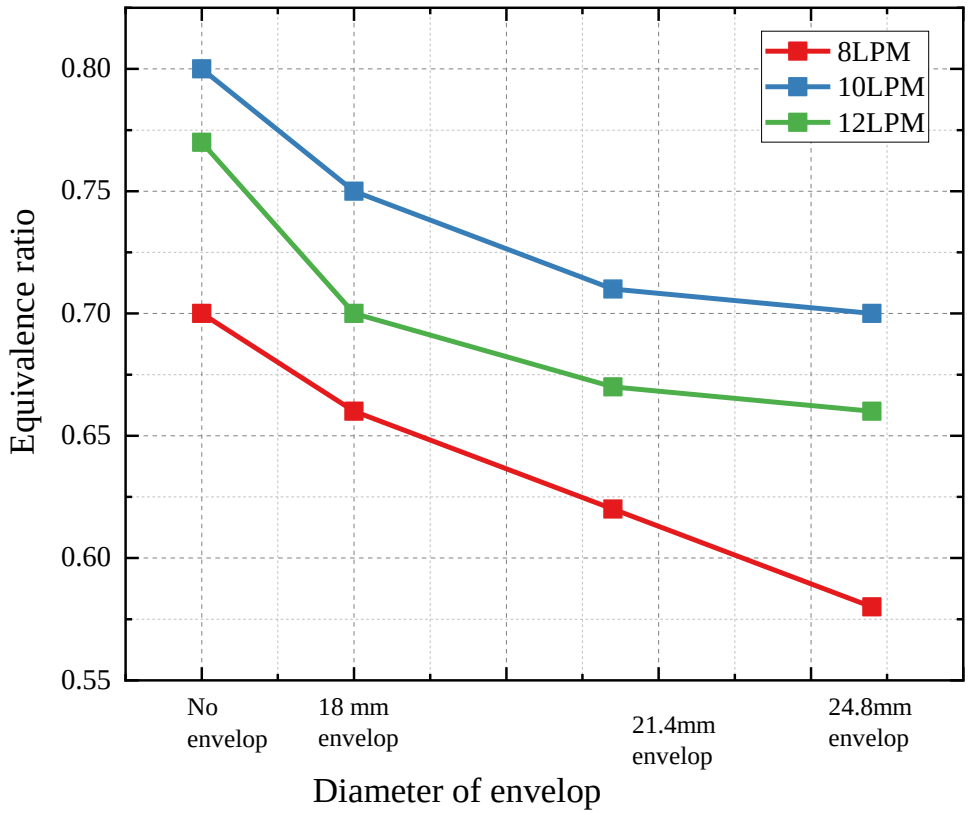

Figure 70: Lean blowout points for different diameters of duct

LBO prediction enhances overall performance and lowers maintenance costs thus it helps to design combustors that can resist blowout.

Numerous prediction techniques, such as semi-empirical models, data-driven models, hybrid approaches, numerical simulations, and experimental investigations, have been developed by researchers for predicting LBO.

In this section the different patterns shown in the before the LBO for the oscillating flame regime has been discussed. Due to instability growing during the dancing flame the sound emitted by the dancing flames become more chaotic this could be used for predicting the LBO.

At the same time the FFT of the oscillating flames has shown how the dancing flames increases its frequency and amplitude as equivalence ratio is lowered and the equivalence ratio approaches LBO. These fft result can also be useful to predict whether the flame is approaching the LBO so that the necessary steps can be taken to stop the flame to going into LBO and sustaining the stable flame for longer duration.

Also, the effect of varying diameter of the attached ducts has a significance role for difference in LBO. When the diameter is smaller i.e., 18mm then the flow velocity is higher compared to a duct with bigger diameter. The higher flow rate effects the LBO as higher flow velocity is more capable of pushing the flame from the bottom of the duct compared to a lower flow velocity for the at a constant equivalence ratio. Due to this reason for all 3 different air flow rates, there is a trend of LBO which goes to lower equivalence ratio for the big duct diameter. Also, when no duct is attached to the combustor the LBO occurs relatively higher equivalence ratios compared to when duct is attached. When duct is attached firstly the area of the duct is more than the steel tube present in the combustor therefore the flow velocity reduced and secondly due to the increase diameter a backward facing step type zone is created at the bottom of the duct hence it also helps in sustain the flames for lower equivalence ratios before going to LBO where eventually flame is extinguished.

4.5 Flashback

Flashback is basically propagation of flame into combustor or upstream rather than staying at combustor exit. Due to flame speed the flame front tries to move towards the unburnt air fuel mixture. Flow velocity of the unburnt mixture balances the flame speed and keeps the flame at a desired location. But when the flame speed is higher than the flow velocity the flame propagates successfully towards the unburnt mixture inside the burner or towards fuel system. This phenomenon is flashback. This is very much unwanted in combustion system. Due to the propagation of flame front towards the fuel system can cause explosion. Therefore, it is dangerous and should be avoided. At the same time flashback hampers the efficiency of the combustion process and might release several air pollutants gasses in higher concentration as well as flashback can damage the several components of combustion system.

The experiment carried out with the meso scale combustor to study the flame dynamics in meso scale combustion process in several occasion the flashback phenomenon has been observed. During the combustion process when the flame speed becomes higher compared to the flow velocity of the air fuel mixture then flashback has been observed. LPG flame speed becomes maximum when LPG is burn at an equivalence ratio of 0.9 to 1.2. So, the flashback is observed when the operating zone is within these equivalence ratios. For the 8LPM flow rate of air the flow velocity is lowest so it showcases the flashback zone for widest range of equivalence ratio from 0.83 to 1.3. For 12 LPM air flow rate the flow velocity is maximum so there is no equivalence ratio where the LPG flame speed is higher compared to the flow velocity therefore the flashback is not observed for 12LPM air flow rate. For 10LPM air flow rate the flashback zone is observed for equivalence ratio of 1.1 and 1.2.

During the flashback zone a sound is released by the combustor. Abrupt variations in pressure are caused by the quick igniting and expansion of gases. Sound waves are the result of these

pressure variations. These pressure fluctuations' strength might cause the combustor to make sound. The sound emitted by combustion system has been recorded by a microphone and First Fourier Transformation has been applied using python programming language to identify the characteristics of the sound.

FFT analysis for 8LPM

Big Duct

When big duct is attached with the combustor the flashback zone emitted sound has few differences between them if it is analysed. Form the figure of FFT given in the figure for various equivalence ratio the difference can be observed (Fig. 71). For the equivalence ratio of 1.3 where the flashback zone started the peak frequency and amplitude is 408,0.0447 respectively. For Φ=1.2 the peak frequency and amplitude is 386,0.0385 respectively. For Φ=1.1 the peak frequency and amplitude is 408,0.024 respectively. For Φ=0.85 the peak frequency and amplitude is 386,0.0072 respectively.

The peak frequency is observed to be at a range from 380 Hz to 410 Hz for this particular case over different equivalence ratios. However, the value of the amplitude corresponding to the peak frequency can be observed to be reducing. Initially the FFT signal gave a sharp peak with highest amplitude but when the flashback zone is about to be ended meaning the flame speed has been decreased due to change in the equivalence ratio so the flame speed and flow velocity balances and the flame that was propagated inside the burner now starts to stabilizes at the bottom of the duct the FFT signal has become like a noise with a very low amplitude compared to the higher equivalence ratios.

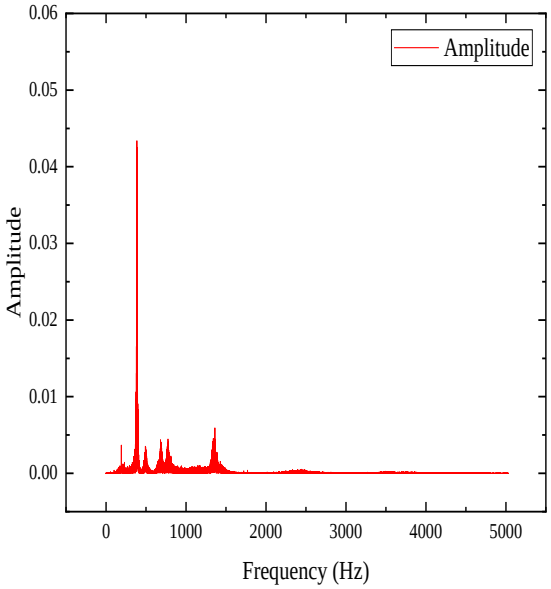

Φ=1.3

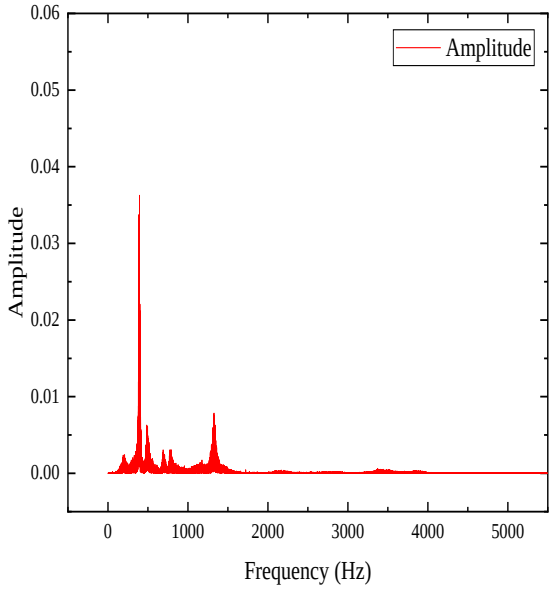

Φ=1.2

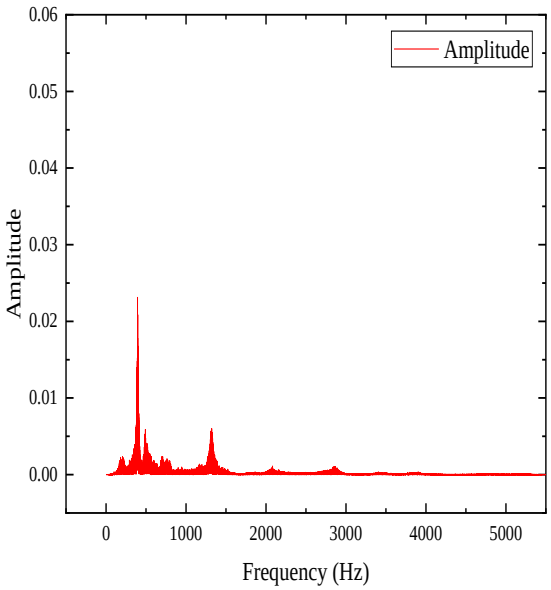

Φ=1.0

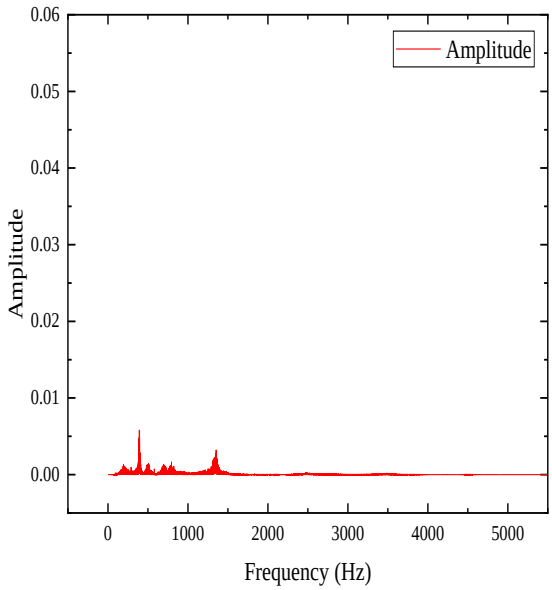

Φ=0.85

Figure 71: FFT analysis for 8LPM big ducts for different equivalence ratio

Medium Duct

Form the figure of FFT given in the figure for various equivalence ratio the difference can be observed (Fig. 72). For Φ=1.2 where the flashback zone started the peak frequency and amplitude is 361.8,0.030 respectively. For Φ=1.1 the peak frequency and amplitude is 386,0.1 respectively. For Φ=1.0 the peak frequency and amplitude is 364,0.057 respectively. For the equivalence ratio of 0.9 the peak frequency and amplitude is 408,0.0447 respectively. For Φ=0.85 the peak frequency and amplitude is 386,0.043 respectively. For Φ=0.83 the peak frequency and amplitude is 364,0.0086 respectively.

For duct 2 the frequency ranges from 360 to 390 Hz which is lesser frequency compared to the duct 1. However, in duct 2 initially at Φ=1.2 the amplitude is 0.030 where the flashback started. Then for Φ=1.1 the amplitude increases significantly to become 0.1. Thereafter, with decreasing equivalence ratio the amplitude associated with the peak frequency is decreased. For the equivalence ratio of 0.8 the amplitude becomes very less and the FFT signal looks like a noise.

Small Duct

Form the figure of FFT given in the figure for various equivalence ratio the difference can be observed (Fig. 73). For Φ=1.2 where the flashback zone started the peak frequency and amplitude is 342,0.041 respectively. For Φ=1.1 the peak frequency and amplitude is 364,0.06 respectively. For Φ=1.0 the peak frequency and amplitude is 342,0.0344 respectively. For Φ=0.83 the peak frequency and amplitude is 350,0.0013 respectively. For duct 3 the peak frequency range is from 340 to 370 Hz.

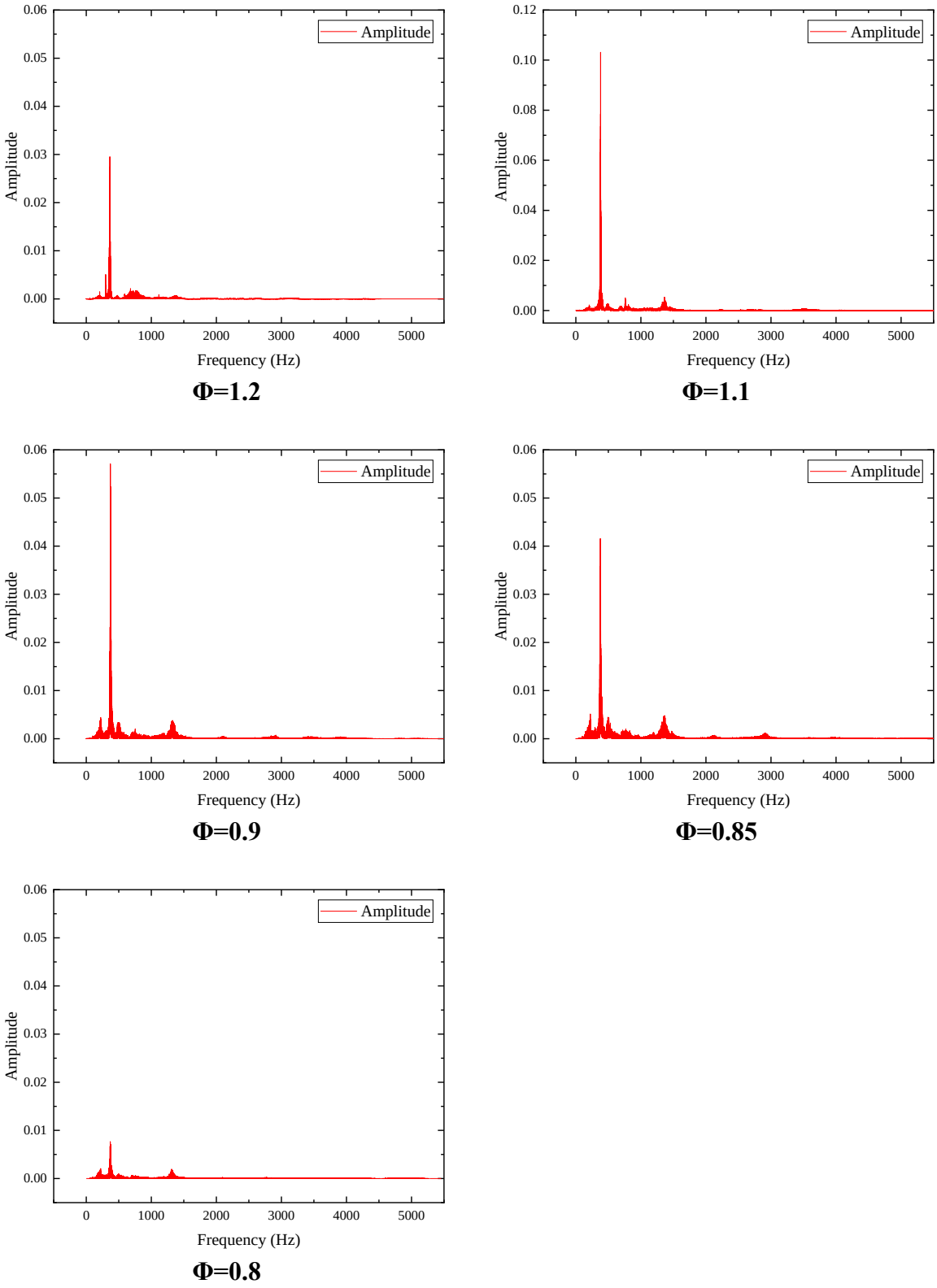

Figure 72: FFT analysis for 8LPM medium duct for various equivalence ratios

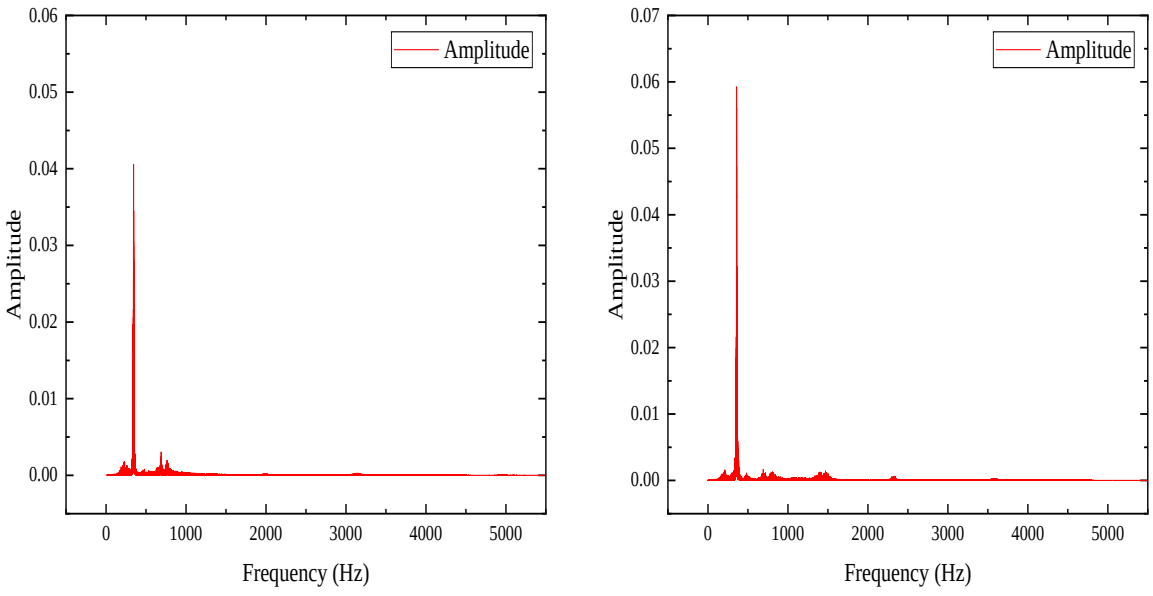

Φ=1.2 **Φ=1.1**

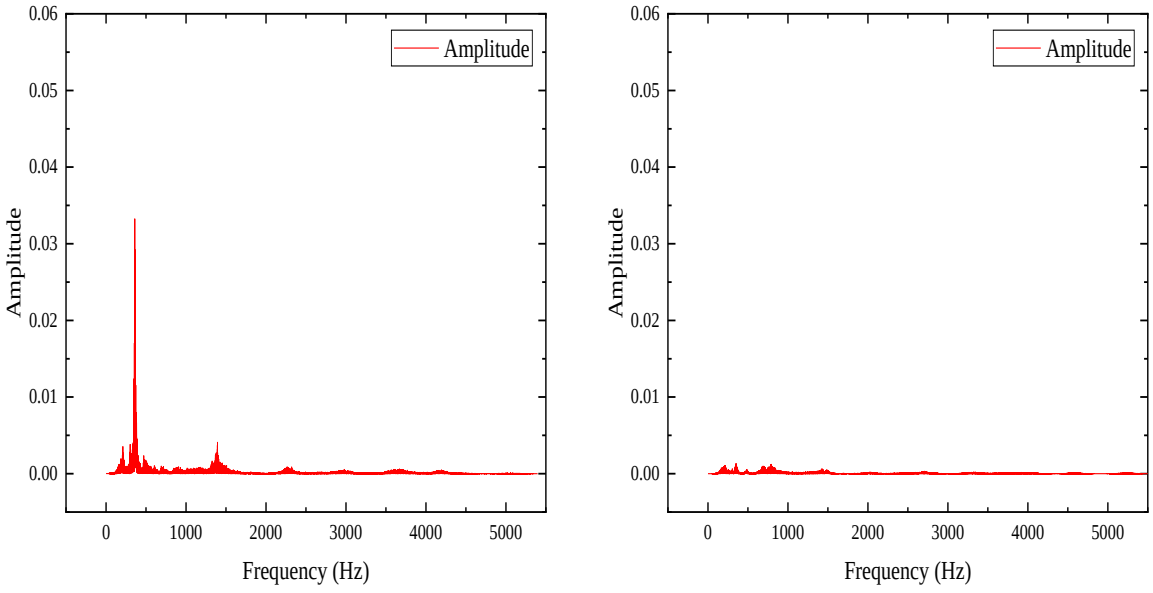

Φ=1.0 **Φ=0.83**

Figure.73: FFT analysis for 8LPM small duct for various equivalence ratios

For small duct also similar to the medium duct initially when flashback starts at Φ=1.2 the amplitude of the peak frequency is 0.041 and at Φ=1.1 it increases and becomes 0.06. After this with decreasing equivalence ratio the amplitude associated with peak frequency decreases. At Φ=0.83 the FFT signal becomes a noise like signal and the amplitude reduced to 0.0013. Here 0.83 is the equivalence ratio just below which stable duct flame appears.

No Duct

The FFT signal of the flashback zone has been shown in Fig. 74. Here for Φ=1.2 the peak frequency and amplitude is 408, 0.0197 respectively. For 1.1 equivalence ratio the amplitude increases and become 0.35 and the peak frequency remains the same. When the equivalence ratio id further lowered a range just before the stable duct flame is observed the FFT signal becomes like a noise with a amplitude of 0.0092 and 0.006 for equivalence ratio of 0.85 and 0.83.

So, form the above discussion it is clear that with equivalence ratio changing the amplitude and peak frequency changes. Initially when the flashback starts a sharp peak frequency is observed but then with equivalence ratio of 1.1 the amplitude increases. However, when the equivalence ratio is lowered further the amplitude decreases and eventually fall into a range that it appears to look like a noise. The amplitude lowered to such low values for those equivalence ratios which are just above the equivalence ratio where stable duct flame is constructed.

Also for the different diameters of the ducts the peak frequency range varies. For duct 1 the peak frequency range is 380 Hz to 410 Hz for duct 2 it is from 360 to 390 Hz for duct 3 the peak frequency range is from 340 to 370 Hz and when no duct is placed in combustor the peak frequency is 408 Hz before the FFT signal appeared like noise. So from this observation it is concluded that the peak frequency also depends on the duct diameters. For duct 1 to duct 3 with increasing order of the duct diameter the peak frequency range decreases.

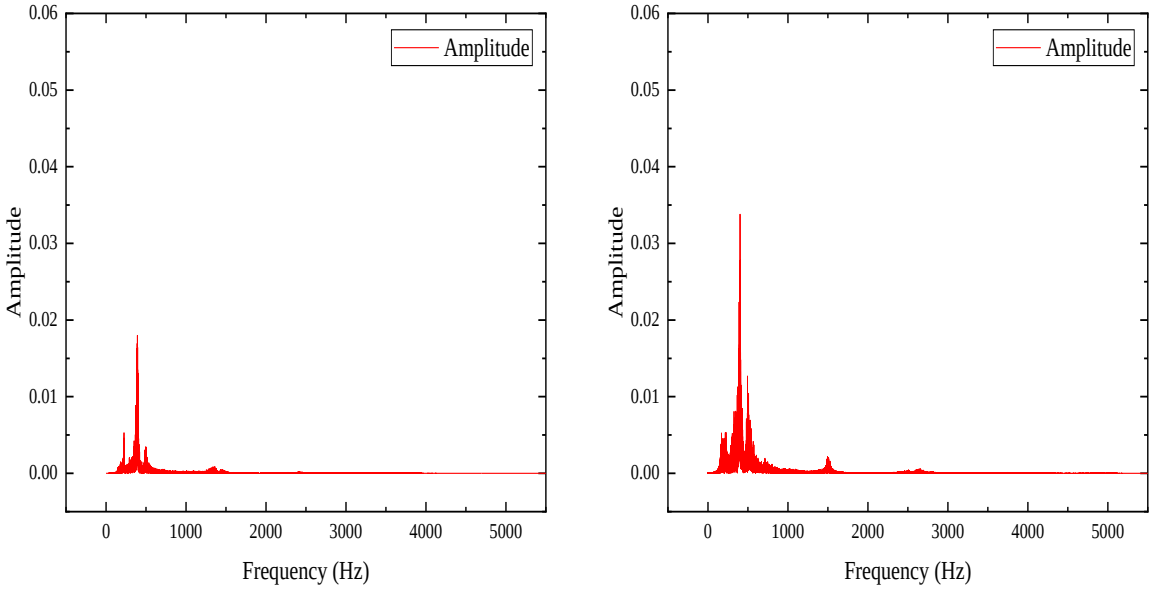

Φ=1.2

Φ=1.1

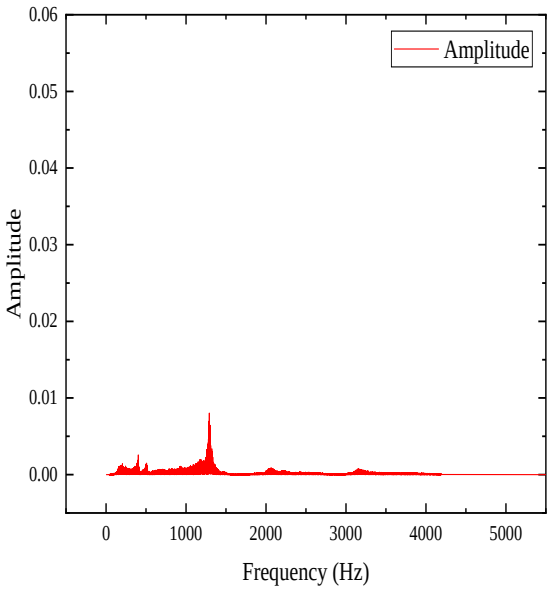

Φ=0.85

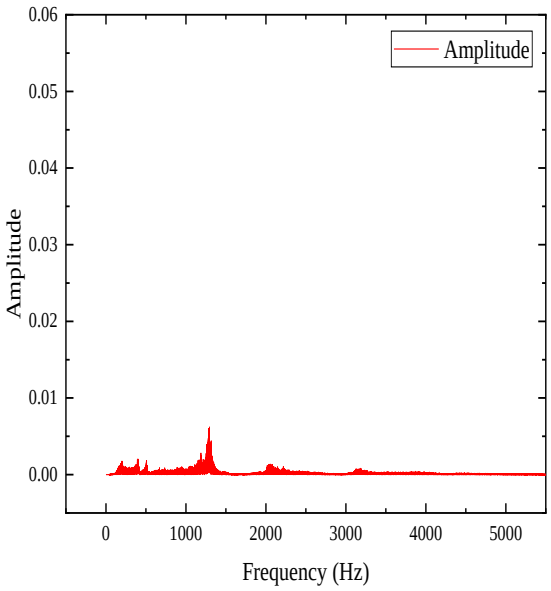

Φ=0.83

Figure 74: FFT analysis for 8LPM no duct for various equivalence ratios

4.6 Spectroscopy of flames

In the experiment the spectroscopy has been carried out to determine the colours emitted by the flame at different equivalence ratio. Through spectroscopy few characteristics has been observed which can lead to identifying the flame dynamics.

Blowout

If the spectroscopic data is observed for the flames just above the equivalence ratio before the blowout it gives away certain information. Here in Fig. 75 the spectroscopic data has been given for 8LPM flow rate of air at certain equivalence ratio that is just above the oscillating flame zone. As the oscillation observed in the flame is one of the instabilities for meso combustor therefore the operating zone cannot be in the oscillating flame zone. Therefore, predicting the oscillating flame, one becomes very important in that regard. The spectroscopy graph shown in the figure can help to identify the whether the operating zone falls inside the oscillating flame zone or it about to reach the oscillating flame zone.

The time vs intensity graph of the light obtained through spectroscopy shows peak wavelength at 308nm,431nm and 927nm. The peak with highest amplitude is generally for the wavelength of 308nm. The 308nm wavelength falls in the **ultraviolet (UV)** range of the spectrum. However, the 308nm wavelength is not in visible range of light spectrum.

The 431nm wavelength falls between the visible range of the spectrum. 431nm wavelength is basically blue-green colour zone. As this wavelength is in the visible spectrum therefore the flame colour observed with human eyes catches this blue green light emitted by the flame at equivalence ratio just higher than the oscillating flame equivalence ratios. It matches with combustion theory as for premixed mixtures the flame which is about to be extinguished is seen as blue-green colour.

Due to chemical reaction between LPG and air many intermediate radicals. These excited radicals emit several different wavelengths of light when move from higher energy levels to lower energy ones. The 431nm wavelength radiation is emitted due to the CH radicals. This 431nm is the strongest band emitted by the CH radicals.

Another peak is observed for the 930nm wavelength which does not falls into visible spectrum. It falls in near infrared spectrum.

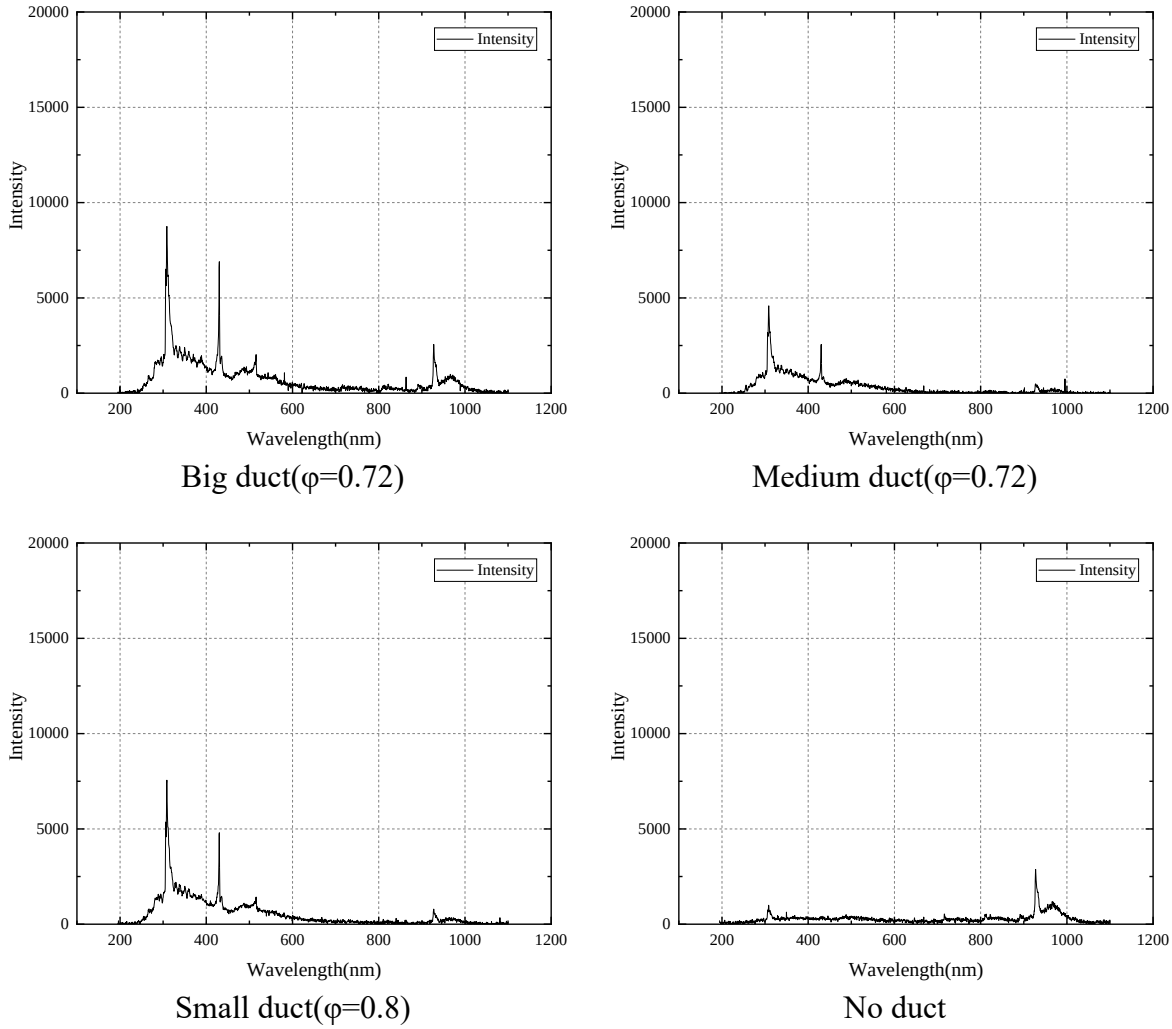

Figure 75:Spectroscopic graph of different duct for 8LPM air at an equivalence ratio just higher than equivalence ratio of oscillating flame

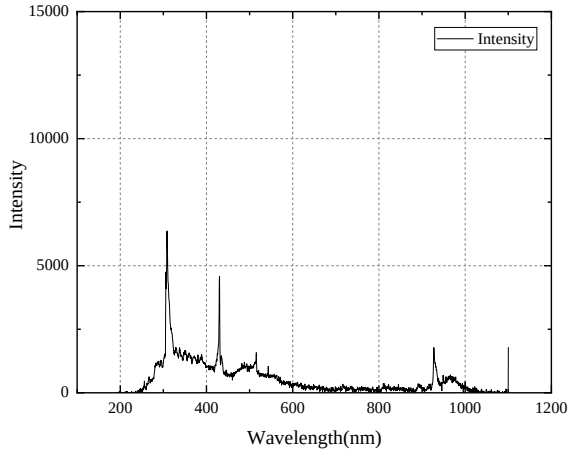

Big duct(φ=0.8)

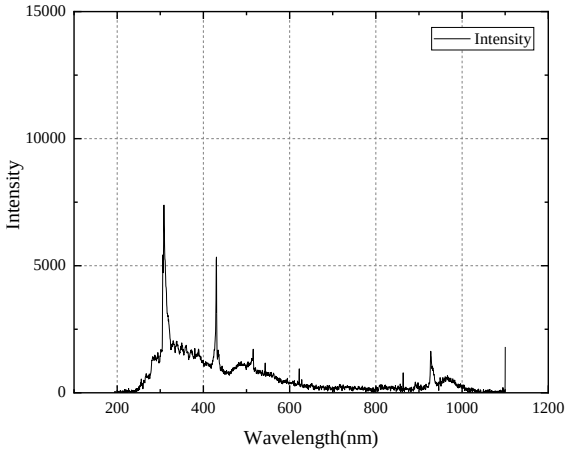

Medium duct(φ=0.8)

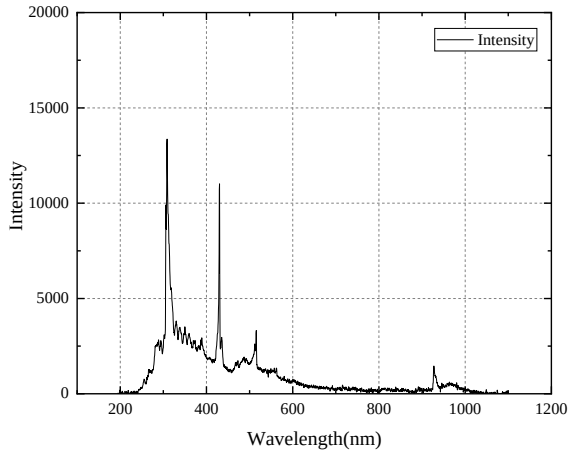

Small duct(φ=0.8)

Figure 76: Spectroscopic graph of different duct for 12LPM air at an equivalence ratio just higher than equivalence ratio of oscillating flame

Like the case with 8LPM air also for 12LPM (Fig. 76) air the peak wavelengths observed for the equivalence ratio just a little higher than the oscillating flame zone are 308nm, 431nm and 930nm.

The 308 nm wavelength is associated with OH radical formed during the fuel air reaction. LPG decomposes to smaller hydrocarbon and this hydrocarbon reacts with air to form OH radicals

as intermediate species. Fig. 77 shows the spectroscopy of 10 LPM just higher before oscillating flame zone starts.

However, the intensity of these wavelength bands doesn't matches with each other as the intensity also depends on many other factors.

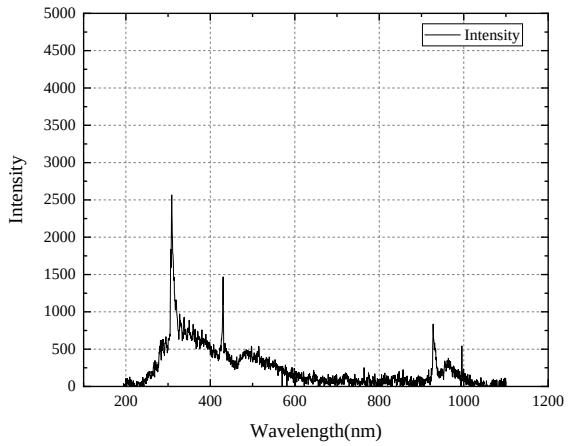

Big duct(φ=0.77)

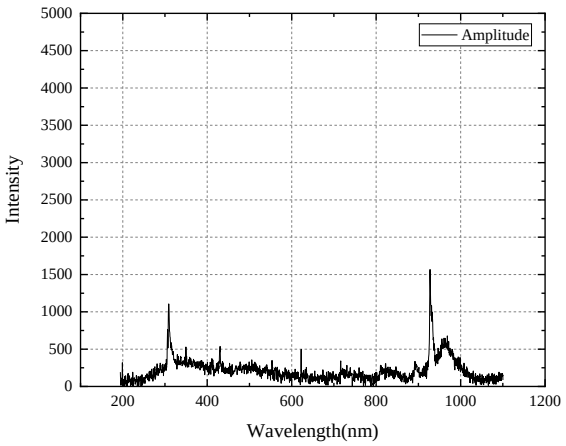

Medium duct(φ=0.77)

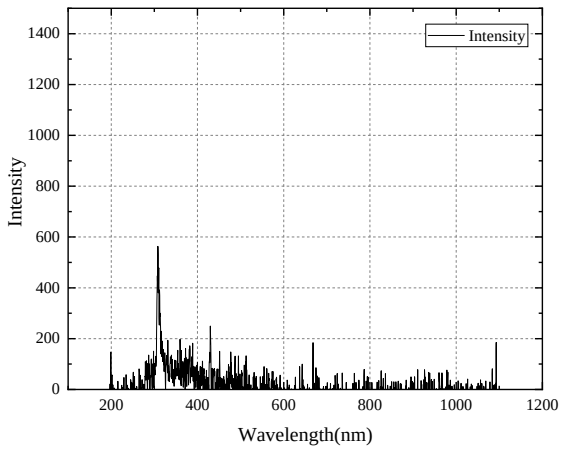

Small duct(φ=0.8)

Figure.77: Spectroscopic graph of different duct for 10LPM air at an equivalence ratio just higher oscillating flame

During Oscillating Flame

During the oscillating flame regime (Fig. 78), the intensity of the emitted light becomes lesser therefore here in this region when the spectroscopy carried out the graphs shows noise like data for spectroscopy. However, even in the noise like data little high amplitude is observed for 310nm and 431nm wavelength.

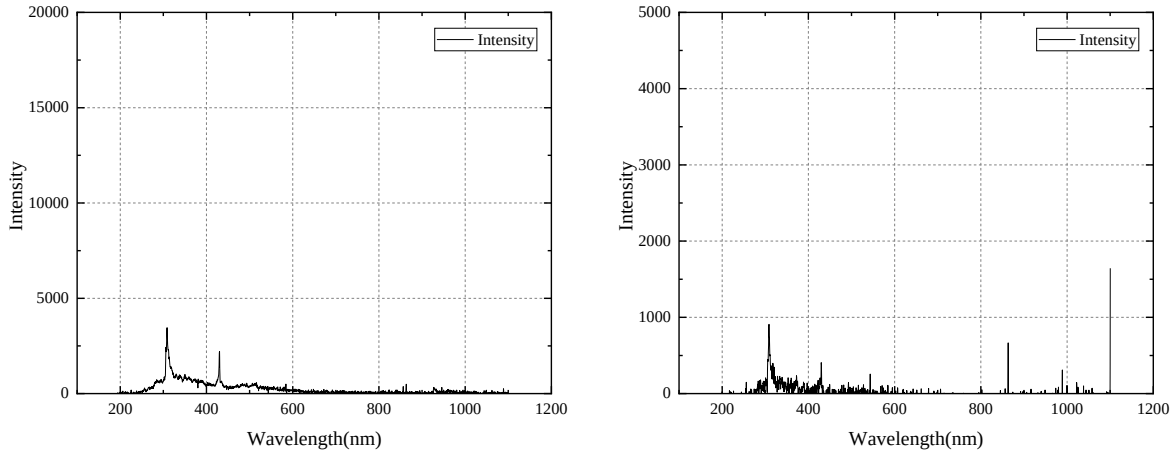

Big duct(φ=0.75) Medium duct(φ=0.75)

Figure 78: Spectroscopic graph of different duct for 10LPM air in oscillating flame zone equivalence ratio

Open+ duct flame zone

Initially when the flame transforms from the FREI zone to the open+duct flame zone the flame has bluish colour. The light emissions by this flame are 514nm, 430nm, 466nm, 588nm,561nm and 927nm (Fig. 78).

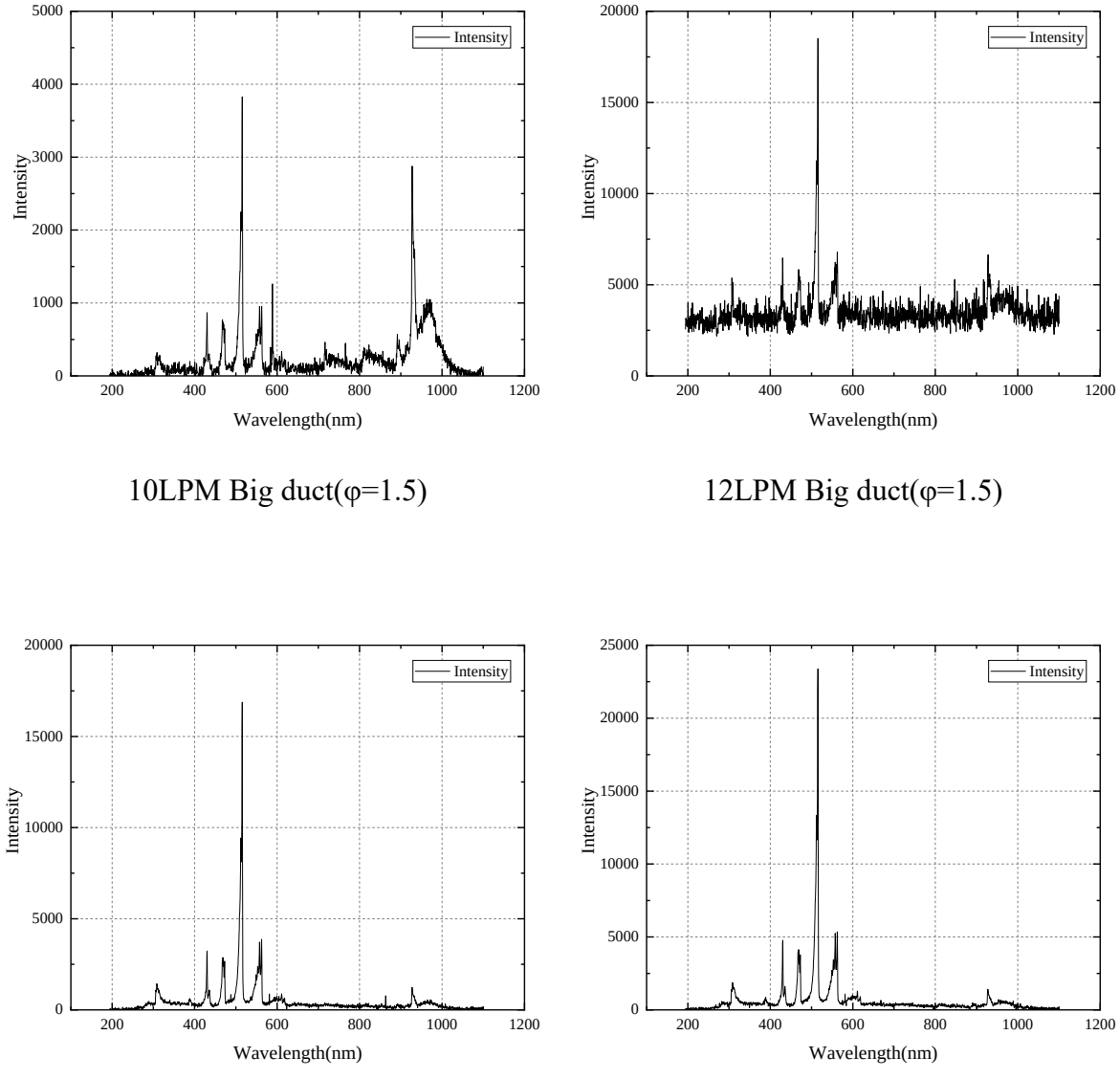

10LPM Big duct(φ=1.5) 12LPM Big duct(φ=1.5)

12LPM Medium duct(φ=1.5) 12LPM Small duct(φ=1.5)

Figure 79:Spectroscopic graph of different duct and different flow conditions at an equivalence ratio just after flame regime shifts from FREI to Open+duct flame zone

When the equivalence ratio is reduced to equivalence ratio of 1.3 then the spectroscopic data again changes and shows some particular peaks which is different from the result in equivalence ratio of 1.5. The flame starts to show a reddish colour in the flame therefore due to this phenomenon the spectroscopy result changes.

The peaks shown are 588nm,765nm and 930nm wavelength. For the 8 lpm when the flame moves form 1.4 equivalence ratio to 1.3 the intensity grows for the red colour that is seen clearly from the flame images provided before. From the spectroscopy data it is observed that all the 3 band of `wavelength has increased when equivalence ratio is changed.

Spectroscopic graph of different duct for 10LPM air for Open+duct flame zone has been shown in Fig. 80. Spectroscopic graph of different equivalence ratio for big duct for 12LPM air for Open+duct flame zone has been shown Fig. 81. Spectroscopic graph of different equivalence ratio for medium duct for 10LPM air for Open+duct flame zone has been shown in Fig. 82.

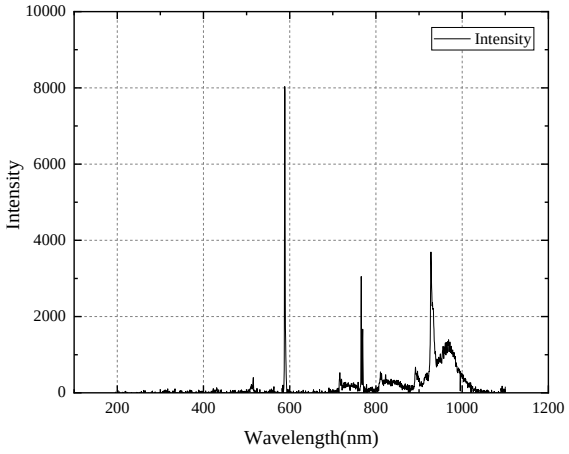

10LPM big duct(φ=1.4)

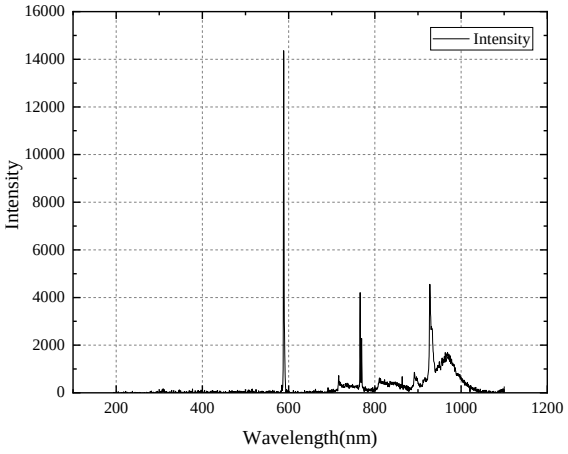

10LPM big duct(φ=1.3)

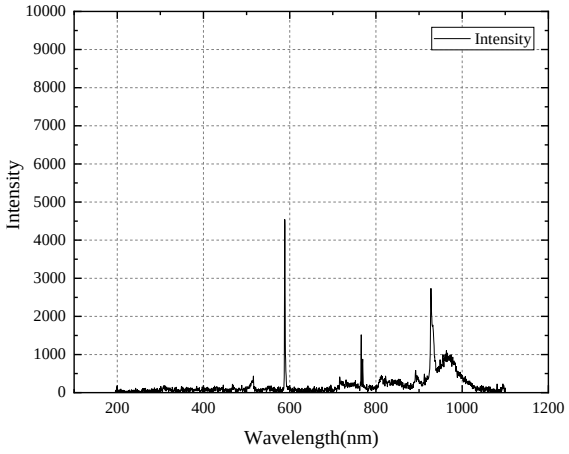

10LPM medium duct(φ=1.4)

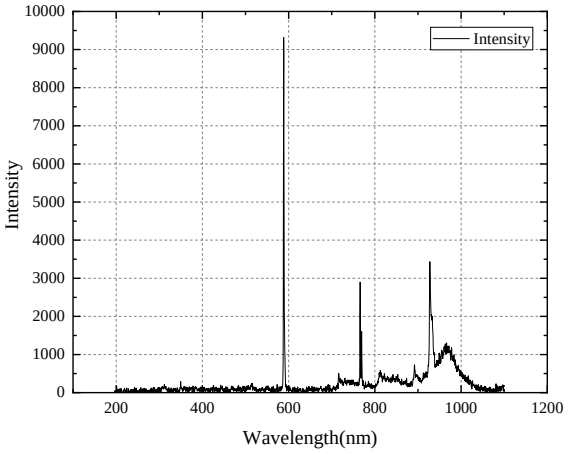

10LPM medium duct(φ=1.3)

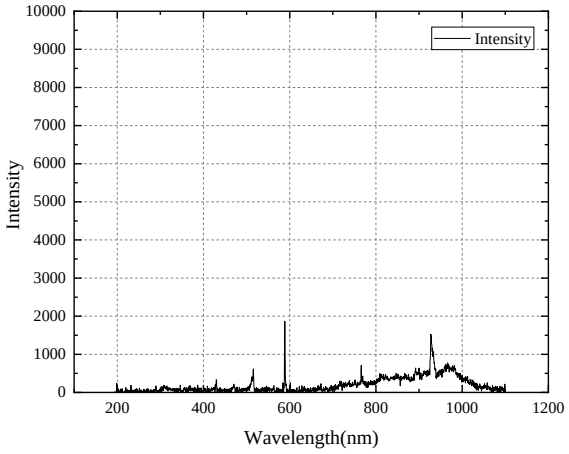

10LPM small duct(φ=1.4)

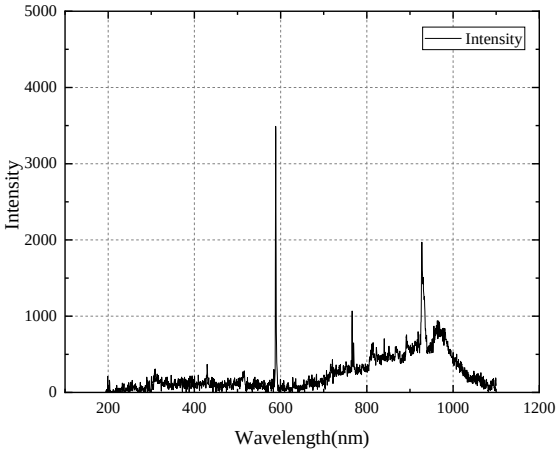

10LPM small duct(φ=1.3)

Figure 80: Spectroscopic graph of different duct for 10LPM air for Open+duct flame zone

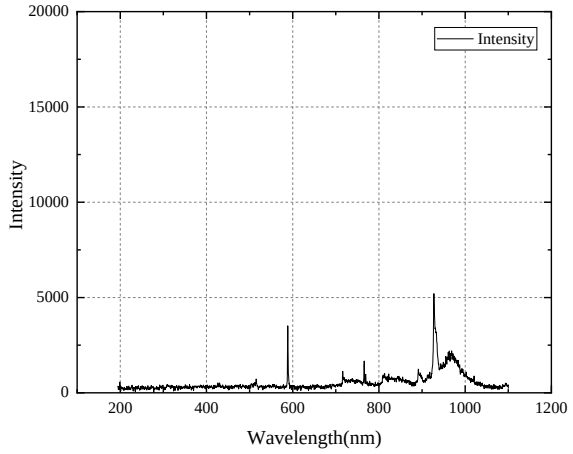

12LPM Big duct(φ=1.3)

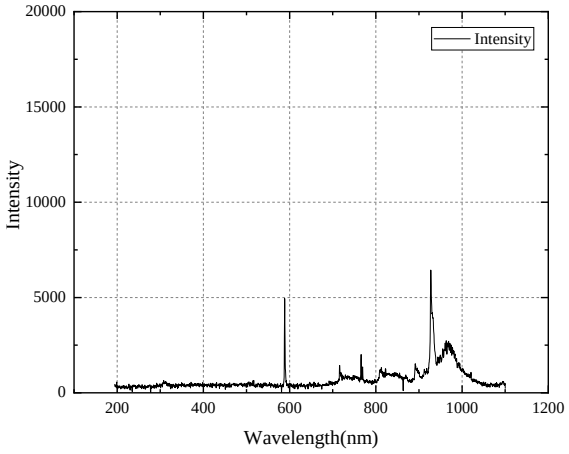

12LPM Big duct(φ=1.2)

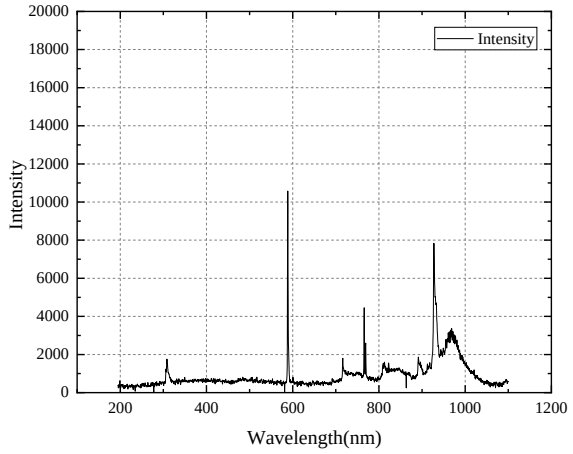

12LPM Big duct(φ=1.1)

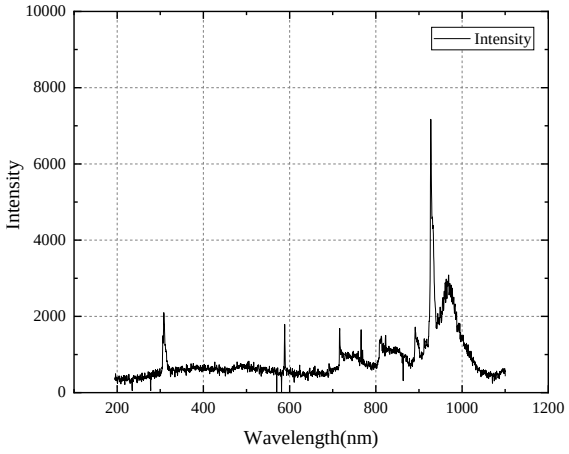

12LPM Big duct(φ=1.0)

Figure 81: Spectroscopic graph of different equivalence ratio for big duct for 12LPM air for Open+duct flame zone

For the 12 LPM (Fig. 81) flow rate initially the red colour starts to appears for an equivalence ratio of 1.3, after it when the equivalence ratio is lowered the red colour becomes more intense for φ=1.2 and it becomes maximum for the φ=1.1. However, after this when the flame is observed for the stoichiometry(φ=1.0) the red colour intensity started to disappear. The spectroscopic graph also shows the same thing observed from the flame images. For φ=1.3 the 588nm,765nm,930nm wavelength band's intensity is lower. For φ=1.2 all these wavelength band's intensity increases and becomes maximum for φ=1.1 and when the equivalence ratio

φ=1.0 is reached then again, these peaks stars to reduce and a new peak of 310nm stars to appear though in smaller intensity.

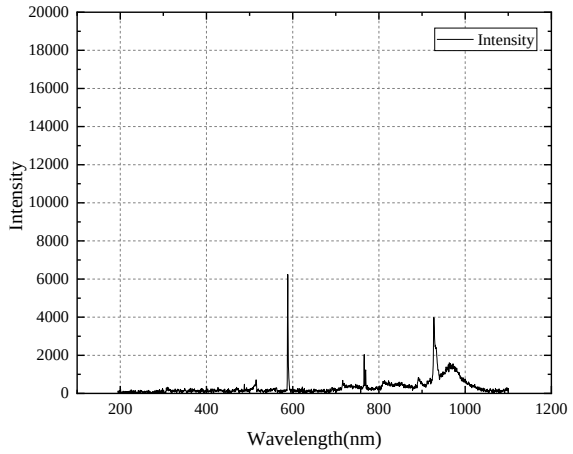

12LPM Medium duct(φ=1.3)

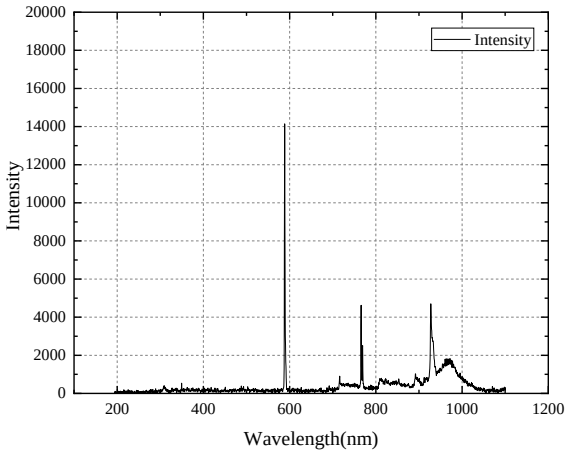

12LPM Medium duct(φ=1.2)

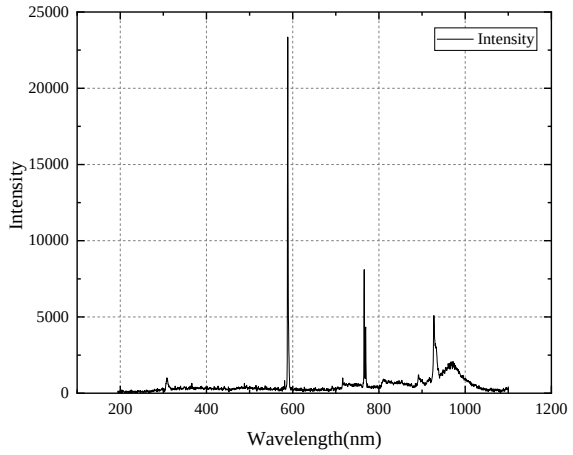

12LPM Medium duct(φ=1.1)

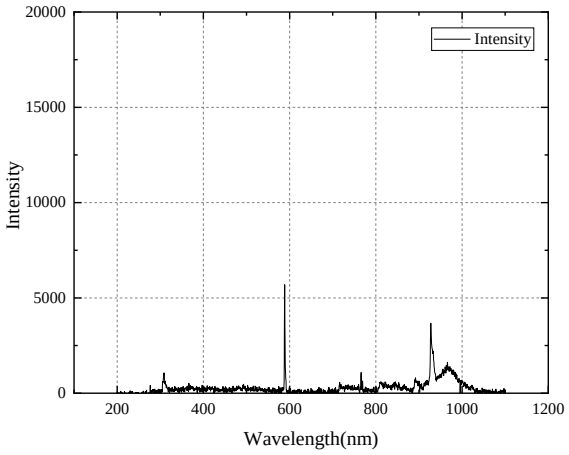

12LPM Medium duct(φ=1.0)

Figure 82: Spectroscopic graph of different equivalence ratio for medium duct for 10LPM air for Open+duct flame zone

For the medium duct also (Fig. 82), same observations are observed as for the big duct. The 3 peaks of 588nm,765nm and 930nm wavelength bands are there in spectroscopy. The reddish intensity appears for 1.3 and then it increases gets maximum for φ=1.1 and then starts to

disappear for equivalence ratio of 1. For the small duct also(Fig. 83), similar results are observed.

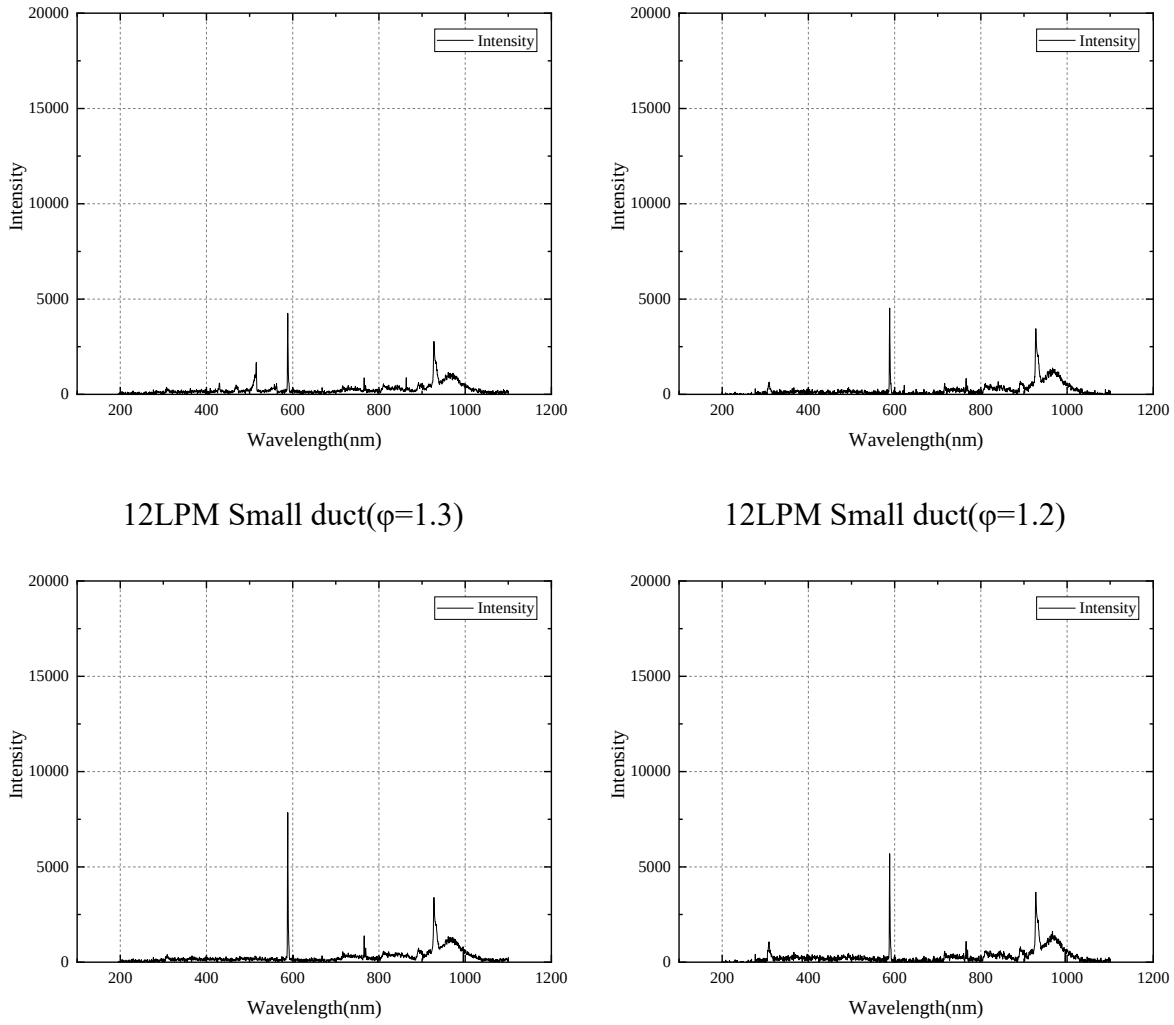

12LPM Small duct(φ=1.3) 12LPM Small duct(φ=1.2)

12LPM Small duct(φ=1.1) 12LPM Small duct(φ=1.0)

Figure 83: Spectroscopic graph of different equivalence ratio for small duct for 10LPM air for Open+duct flame zone

Table 3: Peak wavelength for different flame zone

EQUIVALENCE RATIO	FLAME ZONE	PEAK WAVELENGTH
1.3	Open+duct flame zone	588nm,765nm and 930nm
1.2	Open+duct flame zone	588nm,765nm and 930nm
1.1	Open+duct flame zone	588nm,765nm and 930nm
1.5	just after flame regime shifts from FREI to Open+duct flame zone	514nm, 430nm, 466nm, 588nm,561nm and 927nm.
0.8	just higher equivalence ratio to oscillating flame	308nm,431nm and 927nm

The 308 nm wavelength is associated with OH radical emission. The 431nm is due to the presence of CH radicals which is responsible for blue colour. 977nm wavelength is in IR zone and it is due to C_2 radicals' formation.

4.7 Maps of Flame Dynamics

There are several flame dynamics observed in the experiment for various flow conditions. The types of flame observed in the experiment is listed below

- Open flame zone
- FREI zone
- Open+duct flame
- Flashback zone
- Stable duct flame
- Oscillating flame
- Blowout

For big duct when the Reynold's no is 435 it is the lowest among the 3 different Reynold's no in which the experiment has been carried out. In this Reynold's no = 435 the flashback zone is widest which starts at equivalence ratio of 1.3 and goes onto 0.83 equivalence ratio. With the increasing Reynold's no the flashback zone become reduced and for 650 Reynold's no there is no flashback zone. This happens due to the higher flow velocity in the case of higher Reynold's no.

For higher Reynold's no the shift from the Open flame to FREI zone also starts later compared to the lower Reynold's no. Though the FREI zone starts at lower equivalence ratios for higher Reynold's no but the shift from the FREI zone to Open+Duct flame zone is occurring in similar equivalence ratios for all the cases (φ=1.4 to 1.5).

For the lowest Reynold's no the blowout also occur at lowest equivalence ratio while for other 2 Reynold's no the blowout occur at higher equivalence ratio. Like big duct also for medium and small duct the lowest Reynold's no is 504(8lpm) and 594(8lpm) respectively (Fig. 84).

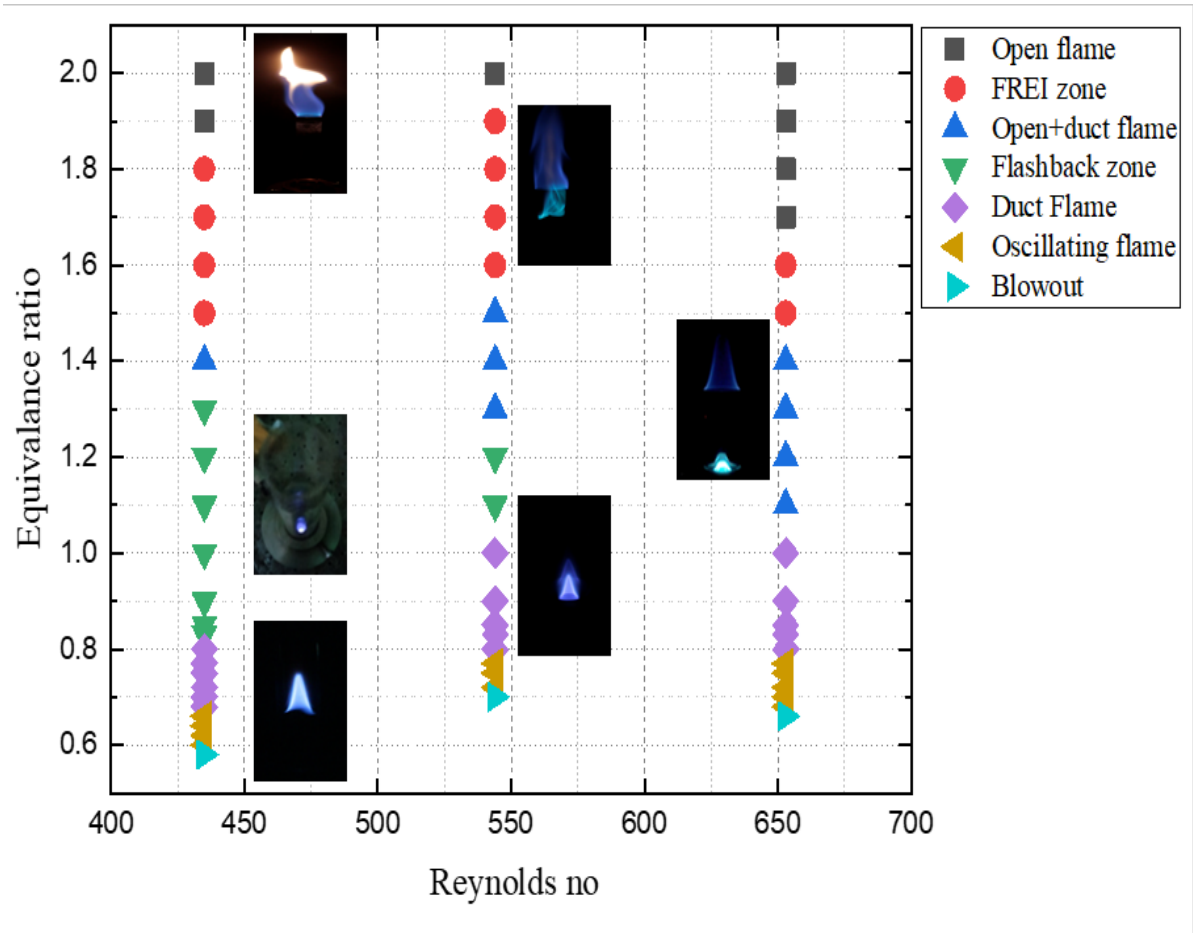

Figure 84: Flow regime map for big duct for different Reynold's no and equivalence ratio

Like big duct the flashback zone is widest for lower and medium ducts (Fig. 85) when the experiment is done for the lower Reynold's no. This s due to the reason that at lower Reynold's no the flow velocity also less therefore the lame speed can impact the flow speed for a larger extent of equivalence ratios.

For the small duct (Fig. 86) at a Reynold's no of 594 the open+duct flame is not there. Also, for small duct at Reynold's no 891 no flashback zone is observed due to the higher flow velocities. Also, when the duct diameter decreases then for the Reynold's no associated with 8LPM flow rate the stable duct flame zone is less wide compared to the other Reynold's no associated with higher flow rates.

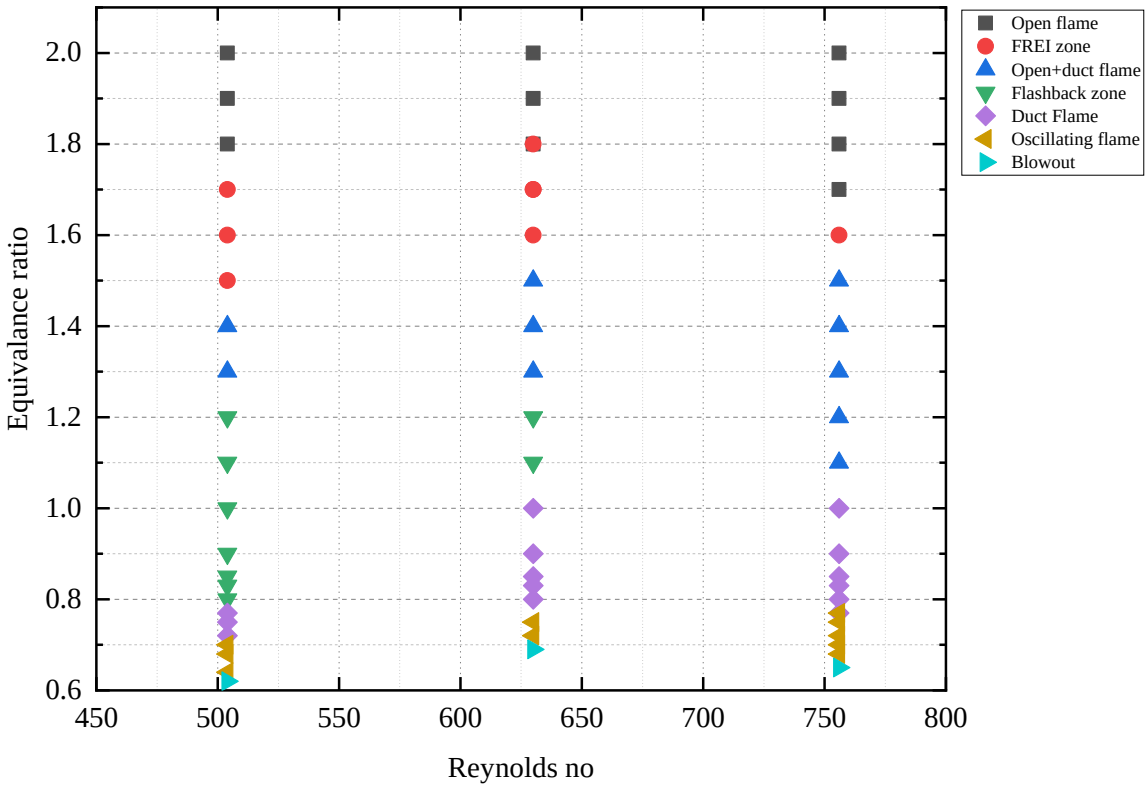

Figure 85: Flow regime map for medium duct for different Reynold's no and φ

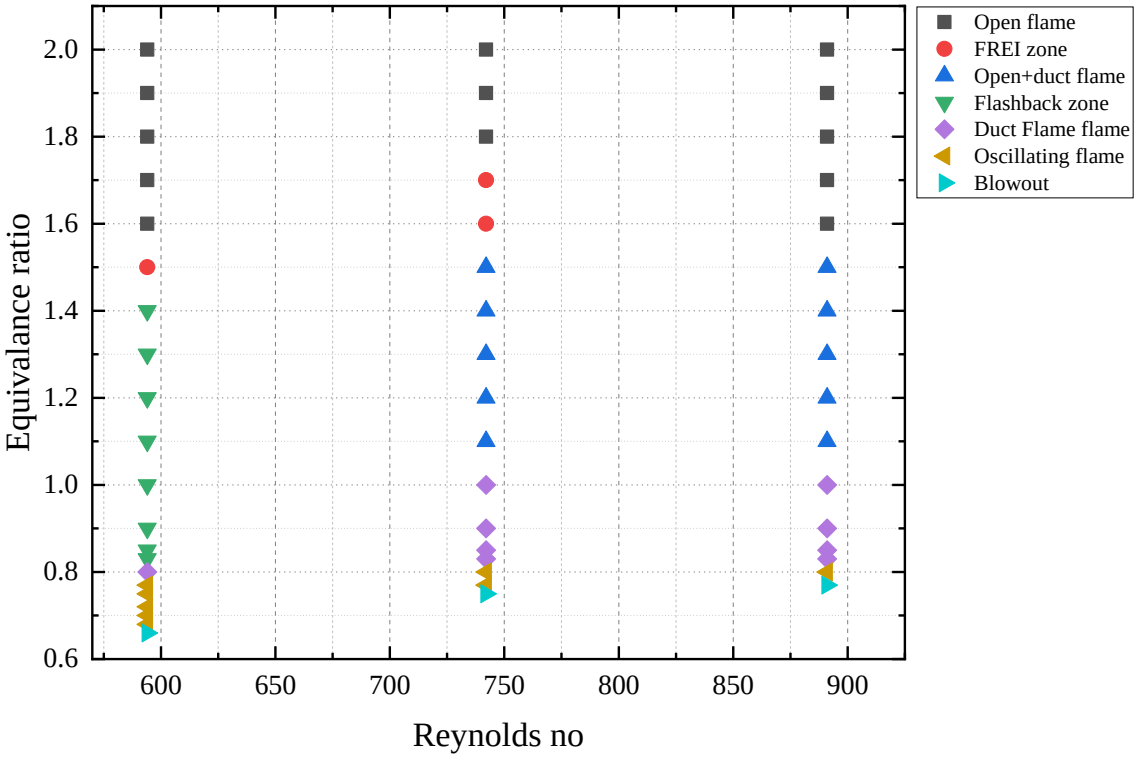

Figure 86: Flow regime map for small duct for different Reynold's no and φ

When the flow regime map is compared based on a single flow rate there are few observations. The flame regime maps for 10 (Fig. 87) 12LPM (Fig. 88) and 8LPM (Fig. 89) is shown. For the big duct the open flame to FREI zone shift happens quickly compared to other two ducts. Also, for the big duct the FREI zone is the wideset and for the small duct it is shortest. So basically, the order varies with duct diameter and due to the lower floe velocity of air fuel mixture for the big duct the shift from open flame to FREI occurs fastest. For medium duct it falls between the other ducts.

However, the shift from the FREI zone and shift from FREI zone to open + duct flame zone occurs at almost same equivalence ratio. But for the flashback zone it starts at higher equivalence ratio for big duct. The blowout occurs for the small duct at relatively higher equivalence ratio and then occurs for medium duct. Finally, the blowout occurs for highest equivalence ratio for the big duct

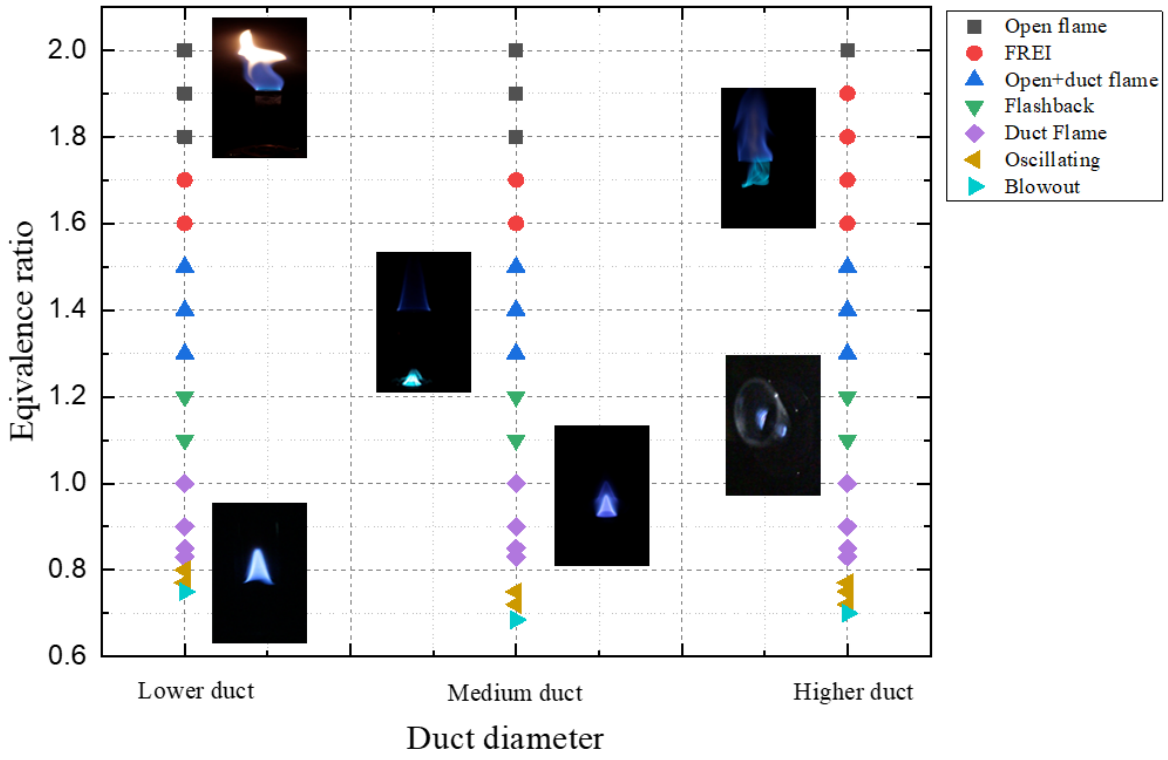

Figure 87: Flow regime map for 10 LPM constant air flow different diameter duct

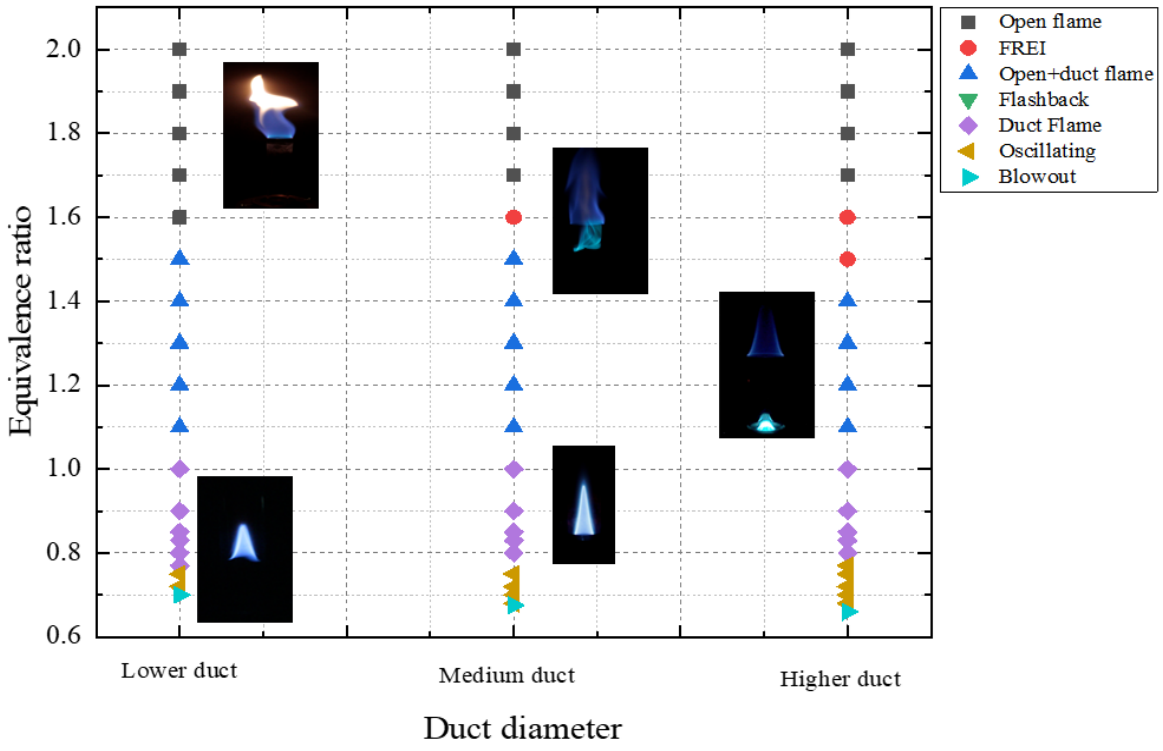

Figure 88: Flow regime map for 12 LPM constant air flow for different diameter duct

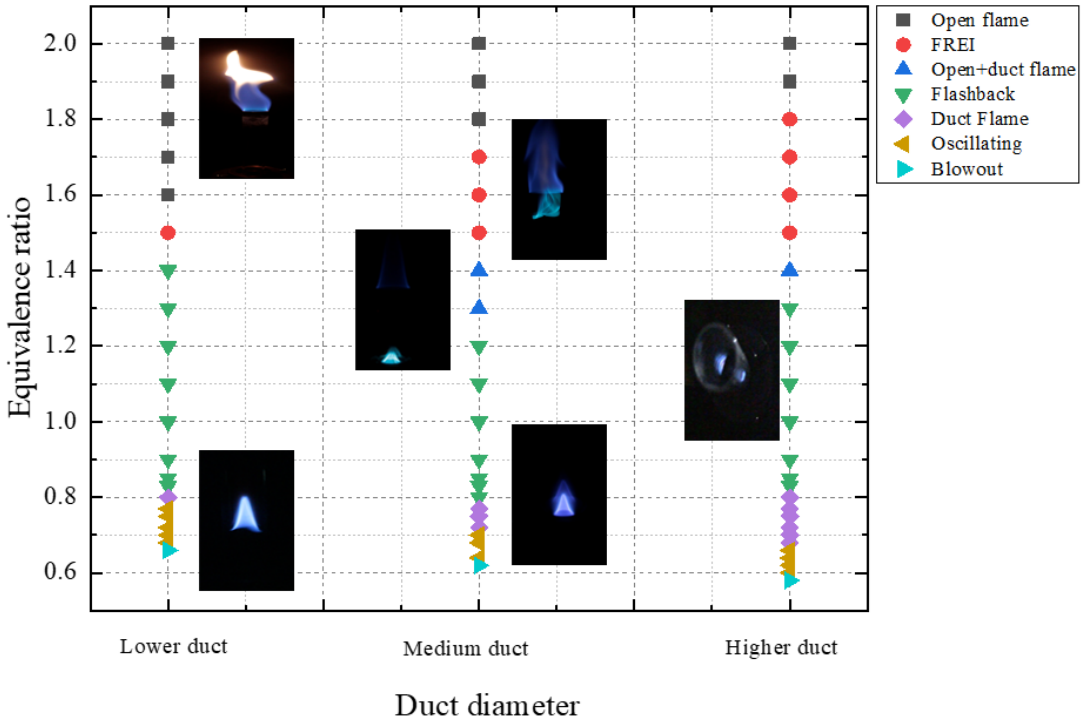

Figure 89: Flow regime map for 8 LPM constant air for different diameter duct

4.8 Flame Length

The length of the flame at different equivalence ratio for the 12LPM flow rate of air has been shown in the Fig. 90.for the big envelop. Here for the 1.5 and 1.6 due to the FREI zone present the open flame length cannot be obtained as for FREI flame position changes with time. Also as the duct flame is obtained from 1.4 equivalence ratio to LBO therefore the duct flame length has been calculated for 1.4 to LBO equivalence ratio.

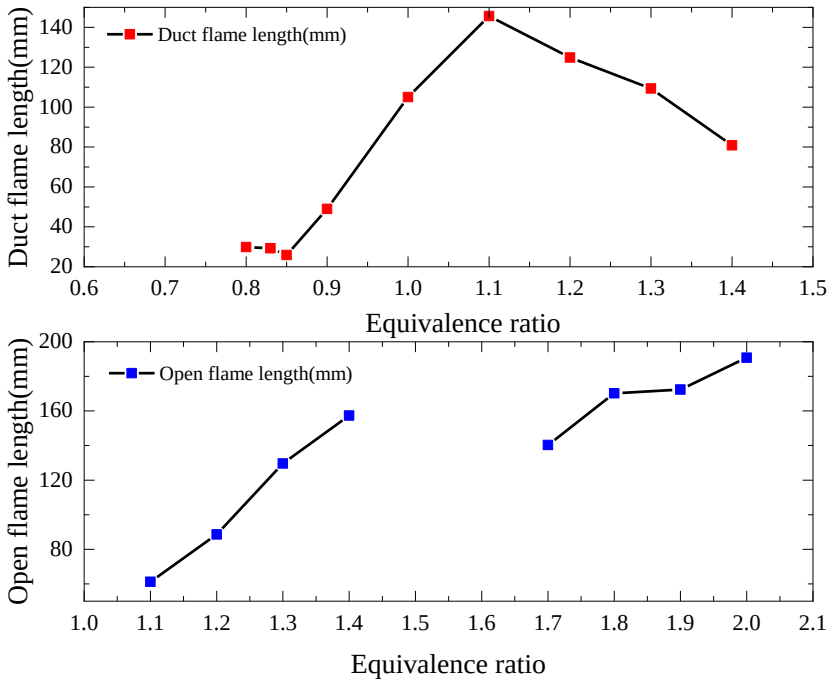

Figure 90: Duct and open flame length at different equivalence ratio for the 12LPM flow rate for the big duct.

So, for the open flame as the equivalence ratio is lower the flame length starts to decrease till the FREI zone starts. When FREI zone ends and both open flame and duct flame can ob observed together then initially the open flame length is maximum but with further decrase in equivalence ratio leads to the decrease of open flame length.

For the duct flame when it appears at φ=1.4 the flame length is 80.85 mm and then as the reddish colour starts to appears for lower equivalence ratios then flame length starts to increase. The duct flame length is maximum at 1.1 equivalence ratio. Then the flame starts to lose reddish colour and completely loses the reddish colour in 0.90 equivalence ratio. For equivalence ratio 1 there is little reddish colour is present. Therefore, the flame at equivalence ratio is lesser compared to 1.1 equivalence ratio and for the 0.9 the duct flame length is reduced significantly compared to equivalence ratio of 1.

As the equivalence ratio is further lowered the duct flame length is reduced however, when the flame reaches to a equivalence ratio when the oscillating flame zone is about to start the flame surface becomes stretched and the duct flame length increases. As shown in the figure the duct flame length is minimum at 0.85 equivalence ratio(25.9mm) and for 0.83(29.3mm) and 0.80(29.9mm) the duct flame length increases.

4.9 FREI Zone

FREI is very common phenomenon observed for meso scale combustor. When the temperature is too hot for autoignition the air fuel mixture auto ignites and moves upstream due to low temperature at the upstream flame is extinguished and then again ignition occurs at higher temperature where initially autoignition occurred. This is repeated periodically with time.

For the FREI flame the time vs position graph and frequency vs amplitude data has been obtained from the FREI flame video captured using digital camera. Figure shows the dynamics changes for FREI flame with time and the periodic behaviour it shows.

For the 8LPM flow rate the position and displacement plot has been given in theFig. 92. Here when equivalence ratio is lowered the periodicity in the position and time graph is increased. That means the frequency is increases for it. When the flame shift from the Open flame region to FREI zone the frequency of the flame is very low. The frequencies are listed below in Table-4

Table 4: Frequencies of FREI flame for different equivalence ratio for 8LPM

Φ=1.7 Higher duct	0.2 Hz
Φ=1.6 Higher duct	0.6 Hz
Φ=1.5 Higher duct	0.7Hz
Φ=1.6 Medium duct	0.6 Hz
Φ=1.5 Medium duct	0.9 Hz
Φ=1.5 Lower duct	0.4 Hz

The Fig. 91 gives a visual representation of the FREI flame which ignites and extinct repetitively with time and how the flame location is changing due to this behaviour of flame in the experiment carried out for mini combustor.

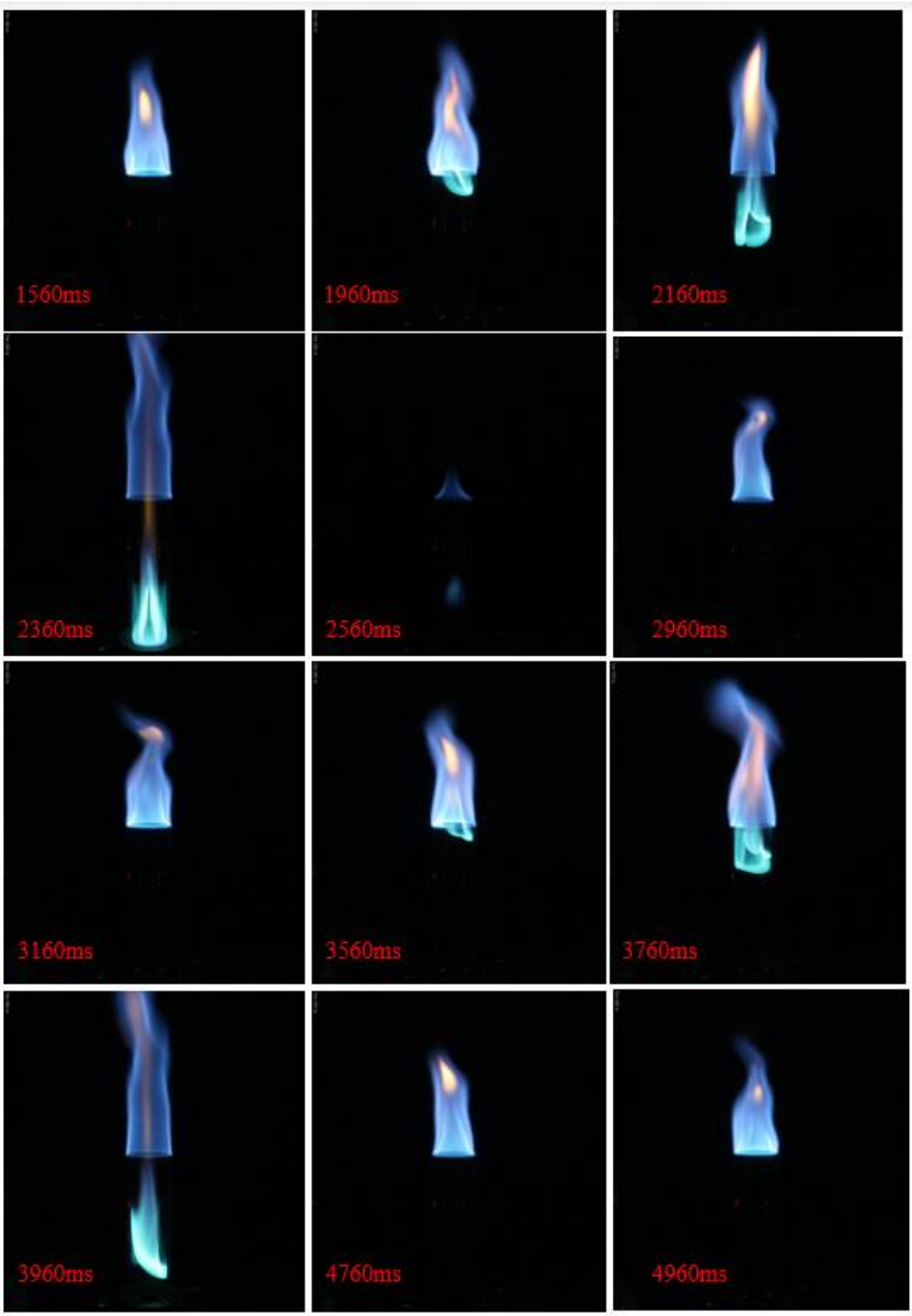

Figure 91: FREI flame visualization

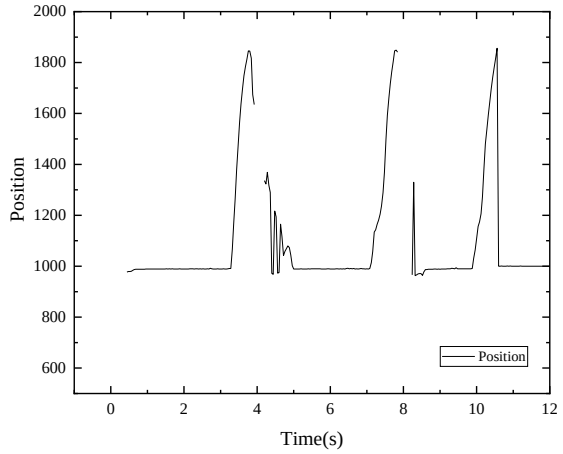

Φ=1.7 Higher duct

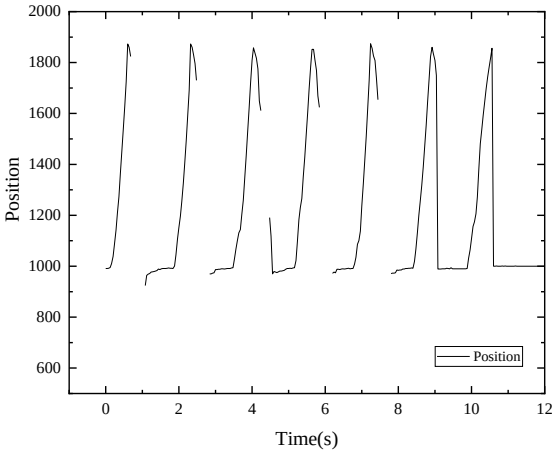

Φ=1.6 Higher duct

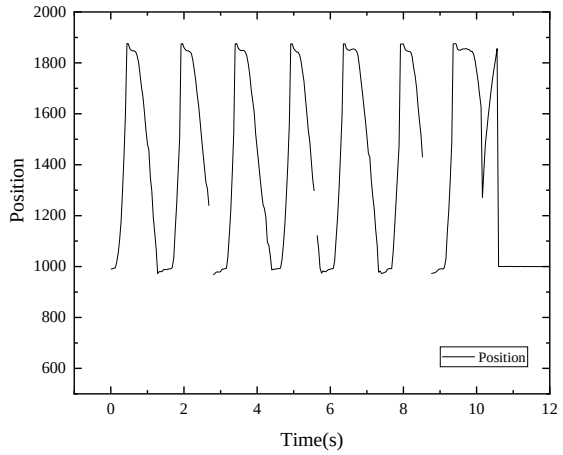

Φ=1.5 Higher duct

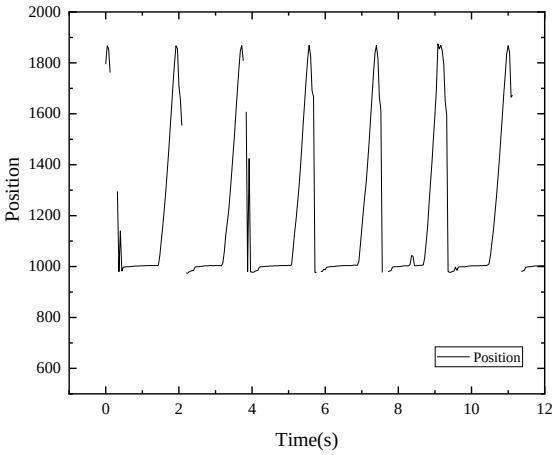

Φ=1.6 Medium duct

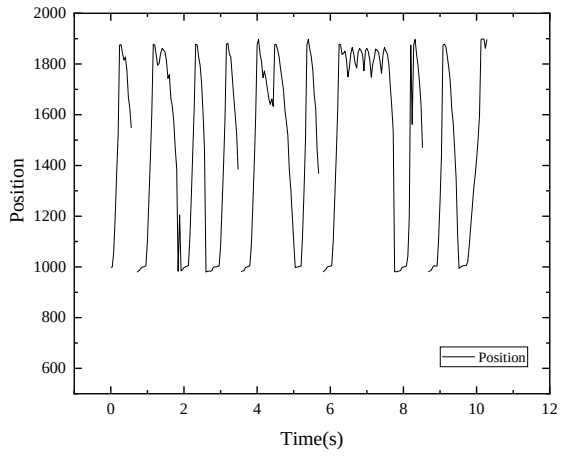

Φ=1.5 Medium duct

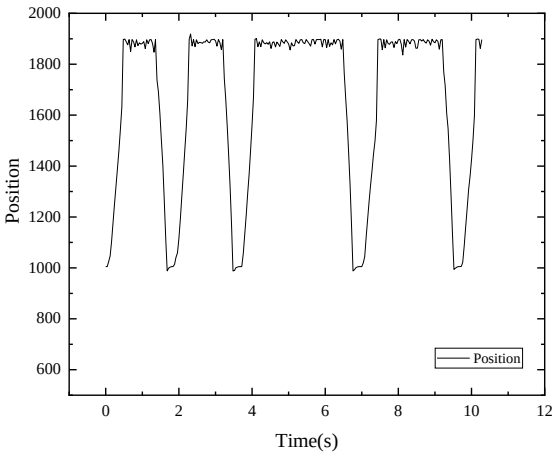

Φ=1.5 Lower duct

Figure 92: Position time graph for the base of the flame for FREI flames for different ducts and different equivalence ratio for 8LPM air flow

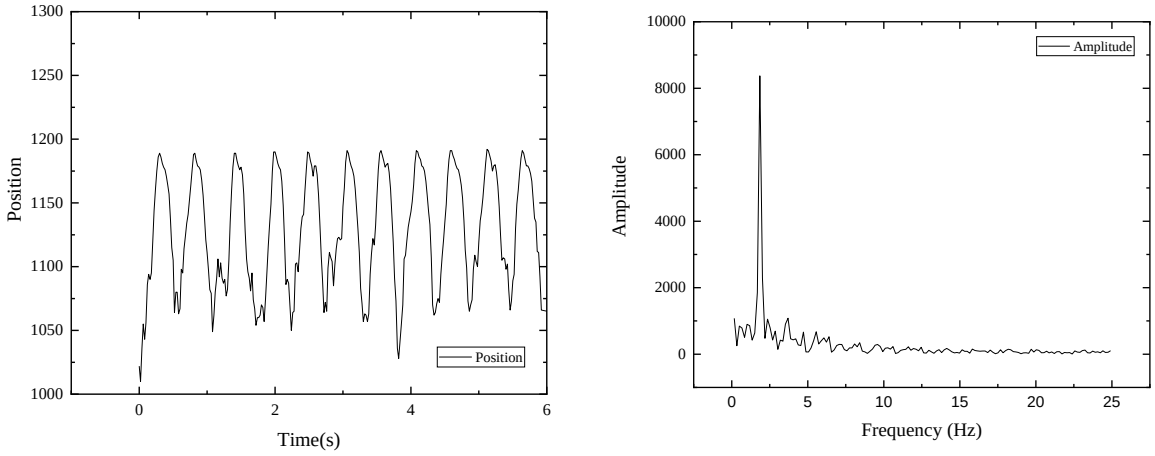

Φ=1.6 Higher duct

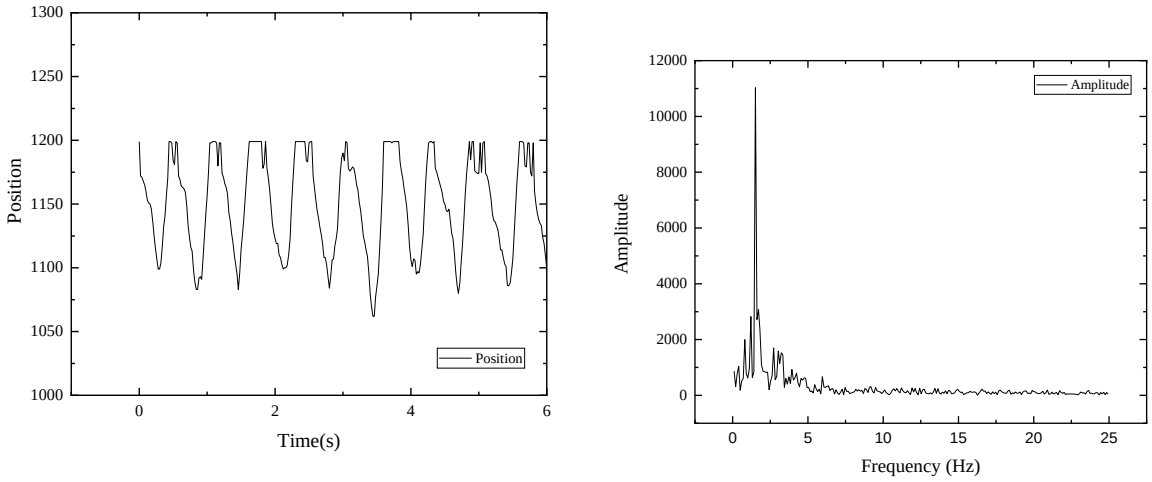

Φ=1.5 Higher duct

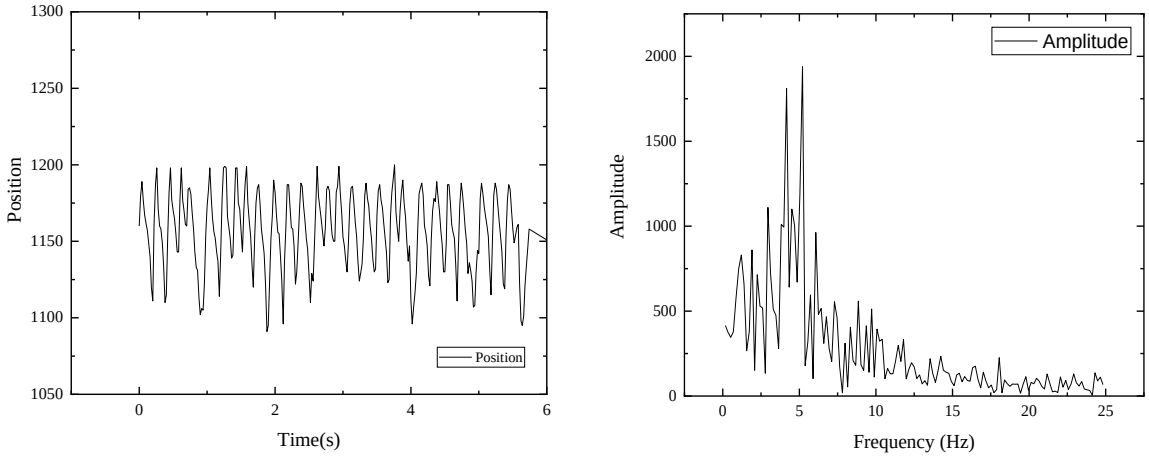

Φ=1.6 Medium duct

Figure 93: Position time graph and FFT graph for FREI flame for 12 LPM constant air flow.

From Fig. 93 for FREI flames for 12LPM flow rates it is observed that when the equivalence ratio lowered the frequency of the FREI increases (same observation like 8LPM) which could be beneficial in case of predicting the nature of the flame.

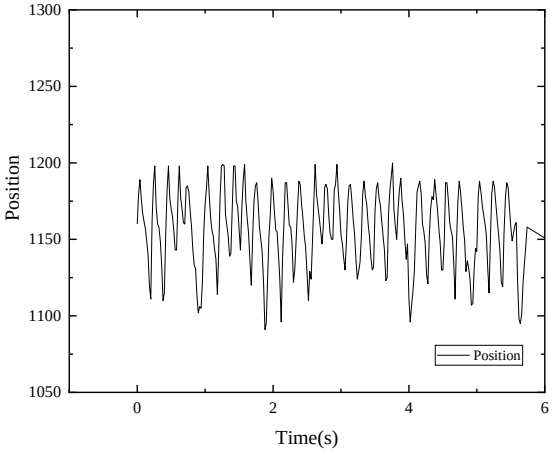

Φ=1.6 Medium duct (FREI)

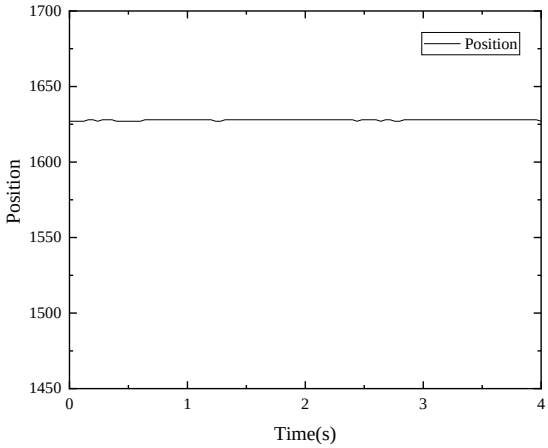

Φ=0.85 Medium duct (duct flame)

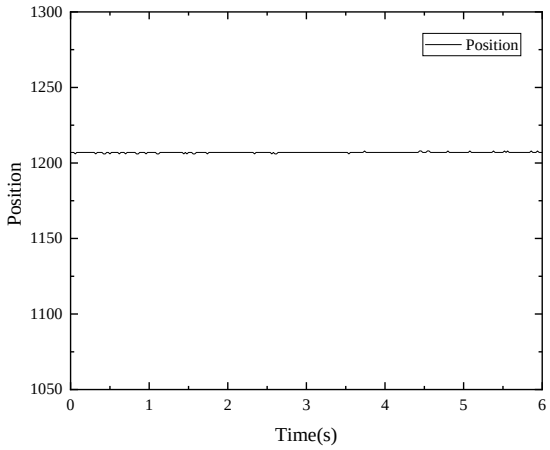

Φ=1.4 Big duct (open + duct flame)

Figure 94: Position time graph for FREI zone, duct flame, open + duct flame for 12 LPM constant air flow.

In the Fig. 94 a comparison between different flame regime is done to show how for the FREI zone the position for the flame changes with time and for duct flame or open + duct flame region the position of the flame doesn't change with time. Therefore, by obtaining the graph for position with time whether the flame is going through instability or not can be concluded.

CHAPTER 5: CONCLUSIONS:

The different flame behaviours for a mini combustor have been studied for premixed LPG flame. 3 different diameters of duct have been attached with the combustor to study it's effect on the flame behaviour of the combustor. Here the study has been conducted for three different air flow rates i.e., 8LPM, 10LPM and 12 LPM. Keeping the air flow rate constant fuel flow rate has been varied to obtain a wide range of equivalence ratio 2 to LBO and the flame characteristics have been observed for each equivalence ratio. The findings of the study are

- Different flame regimes of open flame, FREI zone, open + duct flame, flashback, duct flame, oscillating flame have been found out.
- When the flame speed is higher compared to the flow velocity of the air fuel mixture then the flashback zone is observed. The flashback zone is observed at equivalence ratio of 1.2 and 1.1 for 10 LPM air flow rate and for 8LPM flashback zone is observed from φ=1.3 to φ=0.85. Due to the higher flow velocity for 12LPM the flow velocity is not lesser than the flame speed therefore it does not show the flashback zone.
- A reddish flame is observed for different flow rates and different ducts for open + duct flames. The spectroscopic analysis shows that the peak wavelength bands present in this zone is 588nm,765nm and 930 nm.
- The blowout occurs at lower equivalence ratios for bigger duct than the medium duct blowout occurs and then at more increased equivalence ratio, at motr higher equivalence ratio for small duct and even higher equivalence ratio for
- When the flame is just about to go the oscillating flame the flamesspetrsopic analysis shows peaks at 308nm, 438nm and 930nm. The 438nm peak is of blue color due to the formation of CH radicals as intermediate radicals the LPG- air reaction. The 308nm is there due to OH radicals' formation. And 930nm is present due to the C_2 radicals.

- The flame surface is appearing to be stretched and the length of the flame increases when the flame length is observed for duct flame at an equivalence ratio just before oscillating flame regime.
- The FFT of the oscillating flame regime shows with decreasing value of equivalence ratio the flame becomes more chaotic therefore more frequency peaks of higher amplitude are observed for FFT when oscillating flame is just about to blowout compared to the equivalence ratio when the oscillating flame regime started.

REFERENCES

[1] H. Ritchie, P. Rosado, and M. Roser, “Energy Production and Consumption,” OurWorldInData.org, 2020. [Online]. Available: https://ourworldindata.org/energy-production-consumption. [Accessed: 29-May-2024].

[2] K. Aruga, M. M. Islam, and A. Jannat, “Effects of COVID-19 on Indian Energy Consumption,” Sustainability, vol. 2020, 2020.

[3] IEA, “Covid-19 impact on electricity,” IEA, Paris, 2021. [Online]. Available: https://www.iea.org/reports/covid-19-impact-on-electricity. [Accessed: 29-May-2024].

[4] U.S. Energy Information Administration, “Energy Institute - Statistical Review of World Energy 2023,” 2023.

[5] BP, “BP Energy Outlook country and regional insights - India,” 2018. [Online]. Available: https://www.bp.com/content/dam/bp/en/corporate/pdf/energy-economics/energy-outlook/bp-energy-outlook-2018-country-insight-india.pdf. [Accessed: 30-Jun-2018].

[6] U.S. Energy Information Administration, “EIA Energy Outlook 2019 with projections to 2050,” 2019. [Online]. Available: https://www.eia.gov/outlooks/aeo/pdf/aeo2019.pdf. [Accessed: 29-May-2024].

[7] M. S. Whittingham, “History, Evolution, and Future Status of Energy Storage,” 2023.

[8] K. H. LaCommare and J. H. Eto, “Understanding the Cost of Power Interruptions to U.S. Electricity Consumers,” 2004. [Online]. Available: http://certs.lbl.gov/pdf/55718.pdf. [Accessed: 29-May-2024].

[9] Grand View Research, “Battery Market Share, Size & Trend Analysis Report by Product (Lead Acid, Li-ion, Nickel Metal Hydride, Ni-Cd) By Application (Automotive, Industrial, Portable), By Region, and Segment Forecasts 2020-2027,” 2023.

[10] International Energy Agency, “Global EV Outlook 2019,” International Energy Agency, Paris, France, 2019.

[11] Grand View Research, “Battery Market Size, Share & Trends Analysis Report By Product (Lead Acid, Li-ion, Nickel Metal Hydride, Ni-Cd), By Application, By End-use, By Region, And Segment Forecasts, 2023 - 2030,” 2023.

[12] S. Fletcher, *Bottled Lightning: Superbatteries, Electric Cars, and the New Lithium Economy*. New York: Hill and Wang, 2011.

[13] K. Kang, Y. S. Meng, J. Breger, C. P. Grey, and G. Ceder, “Electrodes with high power and high capacity for rechargeable lithium batteries,” *Science*, vol. 311, no. 5763, pp. 977-980, 2006.

[14] R. Srinivasan, I. M. Hsing, P. E. Berger, K. F. Jensen, S. L. Firebaugh, M. A. Schmidt, et al., “Micromachined reactors for catalytic partial oxidation reactions,” *AIChE Journal*, vol. 43, no. 11, pp. 3059-3069, 1997.

[15] R. A. Yetter, V. Yang, M. H. Wu, Y. Wang, D. Milius, I. A. Aksay, et al., “Combustion issues and approaches for chemical microthrusters,” in *Advancements in Energetic Materials and Chemical Propulsion*, K. K. Kuo and J. de Dios Rivera, Eds., Begell House, 2007.

[16] A. Tang, Y. Xu, C. Shan, J. Pan, and Y. Liu, “A comparative study on combustion characteristics of methane, propane and hydrogen fuels in a micro-combustor,” *International Journal of Hydrogen Energy*, vol. 40, no. 46, pp. 16587-16596, Dec. 2015. [Online]. Available: https://doi.org/10.1016/j.ijhydene.2015.09.101. [Accessed: 29-May-2024].

[17] C. T. Cloney, R. C. Ripley, M. J. Pegg, and P. R. Amyotte, “Laminar combustion regimes for hybrid mixtures of coal dust with methane gas below the gas lower flammability limit,” *Combustion and Flame*, vol. 198, pp. 14-23, Dec. 2018. [Online]. Available: https://doi.org/10.1016/j.combustflame.2018.09.004. [Accessed: 29-May-2024].

[18] N. S. Kaisare and D. G. Vlachos, “A review on microcombustion: Fundamentals, devices and applications,” *Progress in Energy and Combustion Science*, vol. 38, no. 3, pp. 321-359, 2012. [Online]. Available: https://doi.org/10.1016/j.pecs.2012.01.001. [Accessed: 29-May-2024].

[19] A. C. Fernandez-Pello, “Micropower generation using combustion: issues and approaches,” *Proceedings of the Combustion Institute*, vol. 29, pp. 883-899, 2002.

[20] R. A. Yetter, V. Yang, M. H. Wu, Y. Wang, D. Milius, I. A. Aksay, et al., “Combustion issues and approaches for chemical microthrusters,” in *Advancements in Energetic Materials and Chemical Propulsion*, K. K. Kuo and J. de Dios Rivera, Eds., Begell House, 2007.

[21] R. Srinivasan, I. M. Hsing, P. E. Berger, K. F. Jensen, S. L. Firebaugh, M. A. Schmidt, et al., “Micromachined reactors for catalytic partial oxidation reactions,” *AIChE Journal*, vol. 43, no. 11, pp. 3059-3069, 1997.

[22] M. H. Wu, R. A. Yetter, and V. Yang, “Development and characterization of ceramic micro chemical propulsion and combustion systems,” in *46th AIAA Aerospace Sciences Meeting and Exhibit*, 2008, AIAA-2008-966.

[23] K. Zhang, S. Chou, and S. Ang, “MEMS-Based solid propellant microthruster design, simulation, fabrication, and testing,” *Journal of Microelectromechanical Systems*, vol. 13, no. 2, pp. 165-175, 2004.

[24] A. London, A. Ayon, A. Epstein, S. Spearing, T. Harrison, Y. Peles, et al., “Microfabrication of a high pressure bipropellant rocket engine,” *Sensors and Actuators A: Physical*, vol. 92, no. 1-3, pp. 351-357, 2001.

[25] D. Lewis, S. Janson, R. Cohen, and E. Antonsson, “Digital micropropulsion,” *Sensors and Actuators A: Physical*, vol. 80, no. 2, pp. 143-154, 2000.

[26] A. Mehra, X. Zhang, A. A. Ayon, I. A. Waitz, M. A. Schmidt, and C. M. Spadaccini, “A six-wafer combustion system for a silicon micro gas turbine engine,” *Journal of Microelectromechanical Systems*, vol. 9, pp. 517-527, 2000.

[27] A. H. Epstein, S. D. Senturia, O. Al-Midani, G. Anathasuresh, A. Ayon, K. Breuer, et al., “Micro-heat engines, gas turbines, and rocket engines – the MIT microengine project,” in *28th Fluid Dynamics Conference*, 1997, AIAA-1997-1773.

[28] H. Davy, “Some researches on flame,” *Philosophical Transactions of the Royal Society of London*, pp. 45-76, 1817.

[29] C. M. Miesse, R. I. Masel, C. D. Jensen, M. A. Shannon, and M. Short, “Submillimeter-scale combustion,” *AIChE Journal*, vol. 50, no. 12, pp. 3206-3214, 2004.

[30] Q. Peng, et al., “Effects of porosity and multilayers of porous medium on the hydrogen-fueled combustion and microthermophotovoltaic,” *Renewable Energy*, vol. 174, pp. 391-

402, Aug. 2021. [Online]. Available: https://doi.org/10.1016/j.renene.2021.04.108.

[31] Q. Lu, J. Pan, S. Hu, A. Tang, and X. Shao, "Hetero-/homogeneous combustion of premixed hydrogen-oxygen mixture in a micro-reactor with catalyst segmentation," *Int. J. Hydrogen Energy*, vol. 41, no. 28, pp. 12387–12396, Jul. 2016, doi: 10.1016/j.ijhydene.2016.06.043.

[32] A. C. Fernandez-Pello, "Micropower generation using combustion," *Issues and Approaches*, 2002.

[33] D. C. Walther and J. Ahn, "Advances and challenges in the development of power-generation systems at small scales," *Prog. Energy Combust. Sci.*, vol. 37, no. 5, pp. 583–610, Sep. 2011, doi: 10.1016/j.pecs.2010.12.002.

[34] C. Zhou, A. Tang, T. Cai, D. Zhao, and Q. Huang, "Numerical study on flame shape transition and structure characteristic of premixed CH_4/H_2-air in the micro-planar combustor," *Chem. Eng. Process. - Process Intensif.*, vol. 166, Sep. 2021, doi: 10.1016/j.cep.2021.108460.

[35] T. Cai, A. Tang, D. Zhao, C. Zhou, and Q. Huang, "Flame dynamics and stability of premixed methane/air in micro-planar quartz combustors," *Energy*, vol. 193, Feb. 2020, doi: 10.1016/j.energy.2019.116767.

[36] Z. Cao et al., "Experimental study of flame evolution, frequency and oscillation characteristics of steam diluted micro-mixing hydrogen flame," *Fuel*, vol. 301, Oct. 2021, doi: 10.1016/j.fuel.2021.121078.

[37] M. Malushte and S. Kumar, "Flame dynamics in a stepped microcombustor for non-adiabatic wall conditions," *Therm. Sci. Eng. Prog.*, vol. 13, Oct. 2019, doi: 10.1016/j.tsep.2019.100394.

[38] J. Wan and X. Cheng, "Numerical investigation of the local extinction and re-ignition mechanisms of premixed flame in a micro combustor with a flame holder and preheating channels," *Fuel*, vol. 264, Mar. 2020, doi: 10.1016/j.fuel.2019.116837.

[39] A. Alipoor and K. Mazaheri, "Combustion characteristics and flame bifurcation in repetitive extinction-ignition dynamics for premixed hydrogen-air combustion in a heated micro channel," *Energy*, vol. 109, pp. 650–663, 2016, doi: 10.1016/j.energy.2016.05.042.

[40] E. K. Quaye, J. Pan, Q. Lu, Y. Zhang, Y. Wang, and A. A. Alubokin, "Study on combustion characteristics of premixed methane-oxygen in a cylindrical porous media combustor," *Chem. Eng. Process. - Process Intensif.*, vol. 159, Feb. 2021, doi: 10.1016/j.cep.2020.108207.

[41] K. Maruta, T. Kataoka, N. I. Kim, S. Minaev, and R. Fursenko, "Characteristics of combustion in a narrow channel with a temperature gradient," *Proc. Combust. Inst.*, vol. 30, pp. 2429–2436, 2005.

[42] G. Zarabian Ghaeini, M. P. Ghofrani Maab, S. M. Bathaei et al., "Effect of hydrogen concentration on the stabilization of premixed ammonia/hydrogen flames in a heated micro-combustor: numerical investigation," *J. Braz. Soc. Mech. Sci. Eng.*, vol. 45, p. 290, 2023, doi: 10.1007/s40430-023-04222-w.

[43] G. Cinieri, Z. A. Shah, G. Marseglia, and M. G. De Giorgi, "Toward Zero Carbon Emissions: Investigating the Combustion Performance of Shaped Microcombustors Using H_2/Air and NH_3/Air Mixtures," *Aerospace*, vol. 11, p. 12, 2024, doi: 10.3390/aerospace11010012.

[44] A. Di Stazio et al., "Combustion in micro-channels with a controlled temperature gradient," *Exp. Therm. Fluid Sci.*, 2015, doi: 10.1016/j.expthermflusci.2015.09.020.

[45] D. G. Norton and D. G. Vlachos, "Combustion characteristics and flame stability at the microscale: a CFD study of premixed methane/air mixtures," *Chem. Eng. Sci.*, vol. 58, no. 21, pp. 4871–4882, 2003, doi: 10.1016/j.ces.2002.12.005.

[46] C. H. Sai, "The Asymmetric Behavior of Steady Laminar Flame Propagation in Ducts," *Combust. Sci. Technol.*, vol. 180, no. 3, pp. 533–545, 2008, doi: 10.1080/00102200701807177.

[47] S. Cai, W. Yang, and J. Wan, "Combustion and thermal performances of methane-air premixed flame in a novel preheated micro combustor with a flame holder," *Int. J. Therm. Sci.*, vol. 197, p. 108813, 2024.

[48] F. Fruzza, R. Lamioni, A. Mariotti, M. V. Salvetti, and C. Galletti, "Flashback propensity due to hydrogen blending in natural gas: Sensitivity to operating and geometrical parameters," *Fuel*, vol. 362, p. 130838, 2024.

[49] S. Cai, W. Yang, and J. Wan, "Combustion and thermal performances of methane-air premixed flame in a novel preheated micro combustor with a flame holder," *Int. J. Therm. Sci.*, vol. 197, p. 108813, 2024.

[50] F. H. Vance, Y. Shoshin, J. A. van Oijen, and L. P. H. de Goey, "Effect of Lewis number on premixed laminar lean-limit flames stabilized on a bluff body," *Proc. Combust. Inst.*, 2018, doi: 10.1016/j.proci.2018.07.072.

[51] F. H. Vance, Y. Shoshin, L. P. H. de Goey, and J. A. van Oijen, "An investigation into flashback and blow-off for premixed flames stabilized without a recirculation vortex," *Combust. Flame*, vol. 235, p. 111690, 2022, doi: 10.1016/j.combustflame.2021.111690.

[52] J. Wan and H. Zhao, "Experimental study on blow-off limit of a preheated and flame holder-stabilized laminar premixed flame," *Chem. Eng. Sci.*, vol. 223, p. 115754, 2020, doi: 10.1016/j.ces.2020.115754.

[53] K. Maruta, T. Kataoka, N. I. Kim, S. Minaev, and R. Fursenko, "Characteristics of combustion in a narrow channel with a temperature gradient," *Proc. Combust. Inst.*, vol. 30, no. 2, pp. 2429–2436, 2005.

[54] F. Richecoeur and D. C. Kyritsis, "Experimental study of flame stabilization in low Reynolds and Dean number flows in curved mesoscale ducts," *Proc. Combust. Inst.*, vol. 30, no. 2, pp. 2419–2427, 2005.

[55] C. J. Evans and D. C. Kyritsis, "Operational regimes of rich methane and propane/oxygen flames in mesoscale non-adiabatic ducts," *Proc. Combust. Inst.*, vol. 32, no. 2, pp. 3107–3114, 2009.

[56] S. Minaev, K. Maruta, and R. Fursenko, "Nonlinear dynamics of flame in a narrow channel with a temperature gradient," *Combust. Theory Model.*, vol. 11, no. 2, pp. 187–203, 2007.

[57] D. G. Norton and D. G. Vlachos, "Combustion characteristics and flame stability at the microscale: a CFD study of premixed methane/air mixtures," *Chem. Eng. Sci.*, vol.

58, no. 21, pp. 4871–4882, 2003.

[58] T. L. Jackson, J. Buckmaster, Z. Lu, D. C. Kyritsis, and L. Massa, "Flames in narrow circular tubes," *Proc. Combust. Inst.*, vol. 31, no. 1, pp. 955–962, 2007.

[59] G. Pizza, C. E. Frouzakis, J. Mantzaras, A. G. Tomboulides, and K. Boulouchos, "Dynamics of premixed hydrogen/air flames in microchannels," *Combust. Flame*, vol. 152, no. 3, pp. 433–450, 2008.

[60] G. Pizza, C. E. Frouzakis, J. Mantzaras, A. G. Tomboulides, and K. Boulouchos, "Dynamics of premixed hydrogen/air flames in mesoscale channels," *Combust. Flame*, vol. 155, no. 1-2, pp. 2–20, 2008.

[61] Y. Fan, Y. Suzuki, and N. Kasagi, "Experimental study of micro-scale premixed flame in quartz channels," *Proc. Combust. Inst.*, vol. 32, no. 2, pp. 3083–3090, 2009.

[62] A. Alipoor and K. Mazaheri, "Combustion characteristics and flame bifurcation in repetitive extinction-ignition dynamics for premixed hydrogen-air combustion in a heated micro channel," *Energy*, vol. 109, pp. 650–663, 2016.

[63] V. N. Gamezo and E. S. Oran, "Flame acceleration in narrow tubes: Applications for micropropulsion in low-gravity environments," *43rd AIAA Aerospace Sciences Meeting and Exhibit*, AIAA-2005-0540, 2005.

[64] A. Alipoor and K. Mazaheri, "Maps of flame dynamics for premixed lean hydrogen-air combustion in a heated microchannel," *Energy*, 2019, doi: 10.1016/j.energy.2019.116852.

[65] H. Nakamura et al., "Bifurcations and negative propagation speeds of methane/air premixed flames with repetitive extinction and ignition in a heated microchannel," *Combust. Flame*, vol. 159, pp. 1631–1643, 2012.

[66] Y. Tsuboi, T. Yokomori, and K. Maruta, "Lower limit of weak flame in a heated channel," *Proc. Combust. Inst.*, vol. 32, pp. 3075–3081, 2009.

[67] E. Miyata et al., "Direct numerical simulation of micro combustion in a narrow circular channel with a detailed kinetic mechanism," *Proc. Combust. Inst.*, vol. 35, pp. 3421–3427, 2015.

[68] A. Yamamoto et al., "Stabilized three-stage oxidation of gaseous n-heptane/air mixture in a micro flow reactor with a controlled temperature profile," *Proc. Combust. Inst.*, vol. 33, pp. 3259–3266, 2011.

[69] B. Xu and Y. Ju, "Experimental study of spinning combustion in a mesoscale divergent channel," *Proc. Combust. Inst.*, vol. 31, no. 2, pp. 3285–3292, 2007.

[70] G. Pizza, C. E. Frouzakis, J. Mantzaras, A. G. Tomboulides, and K. Boulouchos, "Three-dimensional simulations of premixed hydrogen/air flames in micro tubes," *Journal of Fluid Mechanics*, vol. 658, pp. 463-491, 2010.

[71] A. A. Deshpande and S. Kumar, "On the formation of spinning flames and combustion completeness for premixed fuel-air mixtures in stepped tube microcombustors," *Applied Thermal Engineering*, vol. 51, no. 1-2, pp. 91-101, 2013. doi:10.1016/j.applthermaleng.2012

[72] V. Nayagam and F. A. Williams, "Rotating spiral edge flames in von Karman swirling flows," *Physical Review Letters*, vol. 84, no. 3, p. 479, 2000.

[73] H. G. Pearlman and P. D. Ronney, "Self-organized spiral and circular waves in premixed gas flames," *Journal of Chemical Physics*, vol. 101, no. 3, p. 2632, 1994.

[74] K. Robbins, M. Gorman, J. Bowers, and R. Brockman, "Spiral dynamics of pulsating methane-oxygen flames on a circular burner," *Chaos*, vol. 14, p. 467, 2004.

[75] A. Fan, S. Minaev, S. Kumar, W. Liu, and K. Maruta, "Regime diagrams and characteristics of flame patterns in radial microchannels with temperature gradients," *Combustion and Flame*, vol. 153, no. 3, pp. 479-489, 2008.

[76] A. Fan et al., "Experimental study on flame pattern formation and combustion completeness in a radial microchannel," *Journal of Micromechanics and Microengineering*, vol. 17, no. 12, pp. 2398-2406, 2007.

[77] S. Kumar, K. Maruta, S. Minaev, and R. Fursenko, "Appearance of target pattern and spiral flames in radial microchannels with CH_4-air mixtures," *Physics of Fluids*, vol. 20, p. 024101, 2008.

[78] G. Pizza, C. E. Frouzakis, J. Mantzaras, A. G. Tomboulides, and K. Boulouchos, "Dynamics of premixed hydrogen/air flames in microchannels," *Combustion and Flame*, 2008.

[79] G. Pizza, C. E. Frouzakis, J. Mantzaras, A. G. Tomboulides, and K. Boulouchos, "Dynamics of premixed hydrogen/air flames in mesoscale channels," *Combustion and Flame*, 2008.

[80] S. Kumar, K. Maruta, and S. Minaev, "Pattern formation of flames in radial microchannels with lean methane-air mixtures," *Physical Review E*, vol. 75, p. 016208, 2007.

[81] A. Fan et al., "Experimental and numerical investigations of flame pattern formations in a radial microchannel," *Proceedings of the Combustion Institute*, vol. 32, no. 2, pp. 3059-3066, 2009.

[82] S. Minaev, E. Sereshchenko, R. Fursenko, A. Fan, and K. Maruta, "Splitting flames in a narrow channel with a temperature gradient in the walls," *Combustion, Explosion, and Shock Waves*, vol. 45, no. 2, pp. 119-125, 2009.

[83] A. Fan et al., "Dynamic behavior of splitting flames in a heated channel," *Combustion, Explosion, and Shock Waves*, vol. 45, no. 3, pp. 245-250, 2009.